

REDOX AND RELATED PROPERTIES OF MICROSOMAL
CYTOCHROME P-450


by

Michael R. Waterman, B.A.


A THESIS

Presented to the Department of Biochemistry
and the Graduate Division of
The University of Oregon Medical School
in partial fulfillment of
the requirements for the degree of
Doctor of Philosophy
June 1969

APPROVED:



Professor in Charge of Thesis



Chairman, Graduate Council

Financial support through a National Institutes of Health pre-doctoral fellowship and through grants from the United States Public Health Service is gratefully acknowledged.

For his guidance and personal instruction during the course of this research I am very indebted to Professor H. S. Mason. His stimulation is greatly appreciated.

I am greatly indebted to Dr. Y. Miyake for the insight provided during the years 1965 through 1967.

The assistance of Dr. T. E. King and Dr. F. C. Yong of Oregon State University in carrying out the ORD experiments is acknowledged.

Dedication

To My Wife

and

Parents

TABLE OF CONTENTS

	Page
I. INTRODUCTION	1
1. Statement of Problem	1
2. Discovery of Redox Active Hemoproteins	3
3. Microsomal Electron Transport	21
A. Components of Microsomal Electron Transport	21
B. Microsomal Electron Transport and Mixed- Function Oxidation	32
4. Redox Potential Studies of Cytochromes	44
A. Methods for Determining the Redox Potentials of Cytochromes	44
B. Summary of Cytochrome Redox Potentials . . .	52
C. Evaluation of Potential Data	68
II. EXPERIMENTAL	80
1. Materials	80
A. Chemicals	80
B. Oxidation-Reduction Dyestuffs	83
C. Microsomes	86
2. Equipment	97
3. Procedures	99
A. Quantitative ESR	99
B. Redox Potential Determination	101

	Page
C. Stoichiometry of Cytochrome P-450 Reduction	132
D. Spin State Conversion	135
E. Optical Rotatory Dispersion of Cytochrome P-450	136
III. RESULTS	138
1. Redox Potential Determination	139
2. Stoichiometry of Cytochrome P-450 Reduction . . .	155
3. Spin State Conversion	161
4. Optical Rotatory Dispersion	176
IV. DISCUSSION	179
1. Redox Potential Determination	179
2. Stoichiometry of Cytochrome P-450 Reduction . . .	192
3. Spin State Conversion	196
4. Optical Rotatory Dispersion	199
5. Integration of Results	202
V. SUMMARY	204
REFERENCES	205

LIST OF FIGURES

	Page
1. THE PROSTHETIC GROUP OF FERRIC HEME PROTEINS	8
2. THE FIRST SCHEMATIC REPRESENTATION OF THE RESPIRATORY CHAIN (1925)	13
3. LOCATION OF CYTOCHROMES IN THE RESPIRATORY CHAIN	13
4. WARBURG'S FORMULATION OF THE RESPIRATORY CHAIN	17
5. PROPOSED REACTION SEQUENCE FOR CYTOCHROME b_5 REDUCTASE	27
6. REDOX COMPONENTS OF LIVER MICROSOMES	34
7. EFFECT OF HEXOBARBITAL ON RAT LIVER MICROSOME DIFFERENCE SPECTRUM	38
8. EFFECT OF ANILINE ON RAT LIVER MICROSOME DIFFERENCE SPECTRUM	38
9. OXIDATION-REDUCTION INDICATORS	51
10. APPARATUS USED FOR OXIDATION-REDUCTION POTENTIAL DETERMINATION OF HORSERADISH PEROXIDASE	65
11. ABSORPTION SPECTRA OF INDIGO SULFONATES	88
12. ABSORPTION SPECTRUM OF PHENOSAFRANINE	90
13. ABSORPTION SPECTRA OF VIOLOGEN DYESTUFFS	92
14. SCHEMATIC REPRESENTATION OF RABBIT LIVER MICROSOME PREPARATION	96

	Page
15. ANAEROBIC ESR TUBE USED IN REDOX POTENTIAL DETERMINATION OF MICROSOMAL Fe_x	104
16. 50% REDUCED INDIGOTETRASULFONATE OBTAINED WITH THE INITIAL ANAEROBIC TECHNIQUE	107
17. ESR TUBE HOLDER FOR CARY SCATTERED TRANSMISSION ATTACHMENT	110
18. CLOSED SYSTEM USED FOR ANAEROBIC TITRATIONS	113
19. LOSS OF PHENOSAFRANINE UPON REDUCTION WITH PALLADIUM ASBESTOS	116
20. REDUCTION OF MICROSOMAL Fe_x BY HYDROGEN-REDUCED METHYL VIOLOGEN	119
21. BOIS-POLTORATSKY ANAEROBIC APPARATUS	123
22. BEER'S LAW RELATIONSHIP FOR SOLUTIONS IN CYLINDRICAL ESR TUBES	131
23. EFFECT OF REDUCED INDIGOTETRASULFONATE ON MICROSOMAL Fe_x	144
24. EFFECT OF REDUCED INDIGODISULFONATE ON MICROSOMAL Fe_x	146
25. INDICATION OF MICROSOMAL Fe_x REDUCTION BY REDUCED PHENOSAFRANINE	148
26. PROOF THAT REDUCTION OF MICROSOMAL Fe_x BY REDUCED PHENOSAFRANINE DOES NOT OCCUR	150
27. REDOX TITRATION CURVE OBTAINED FOR MICROSOMAL Fe_x	152
28. NADPH TITRATION CURVE OF CYTOCHROME P-450 IN THE PRESENCE OF CO	157
29. TYPICAL ESR SPECTRUM OF LOW SPIN MICROSOMAL Fe_x	165

	Page
30. TYPICAL ESR SPECTRUM OF HIGH SPIN MICROSOMAL Fe_x	165
31. EFFECT OF pH ON THE $g = 2.25$ COMPONENT OF THE LOW SPIN MICROSOMAL Fe_x ESR SPECTRUM	167
32. EFFECT OF pH ON THE $g = 6.1$ COMPONENT OF THE HIGH SPIN MICROSOMAL Fe_x ESR SPECTRUM	169
33. pH EFFECT ON HIGH AND LOW SPIN MICROSOMAL Fe_x - 5 MINUTE SAMPLES	171
34. pH EFFECT ON HIGH AND LOW SPIN MICROSOMAL Fe_x - 1 HOUR SAMPLES	173
35. PCMS EFFECT ON $g = 2.06$ ESR SIGNAL IN ACID TREATED MICROSOMES	175
36. OPTICAL ROTATORY DISPERSION CURVES OF CYTOCHROME P-450	178
37. THE PROPOSED LIGAND SYSTEM OF MICROSOMAL Fe_x AND THE RELATIONSHIP BETWEEN MICROSOMAL Fe_x AND CYTOCHROME P-450	189

LIST OF TABLES

	Page
1. SOME MICROSOMAL MIXED-FUNCTION OXIDASES	23
2. COMPOUNDS GIVING TYPE I AND TYPE II SPECTRAL CHANGES IN RAT LIVER MICROSOMES	40
3. COMPILATION OF CYTOCHROME REDOX POTENTIALS	55
4. PORPHYRINS AND THEIR SIDE CHAINS	73
5. INFLUENCE OF SIDE CHAINS ON IRON-PORPHYRIN REDOX POTENTIALS	76
6. MAXIMUM PER CENT REDUCTION OF MICROSOMAL Fe ^x BY REDUCED METHYL VIOLOGEN IN VARIOUS MICROSOMAL PREPARATIONS	154
7. RESULTS OF NADPH TITRATION OF CYTOCHROME P-450 IN THE PRESENCE OF CO	159

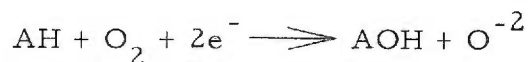
LIST OF ABBREVIATIONS

NADH:	Reduced nicotinamide adenine dinucleotide (DPNH).
NAD:	Oxidized nicotinamide adenine dinucleotide (DPN).
NADPH:	Reduced nicotinamide adenine dinucleotide phosphate (TPNH).
NADP:	Oxidized nicotinamide adenine dinucleotide phosphate (TPN).
ATP:	Adenosine triphosphate.
ADP:	Adenosine diphosphate.
FMN:	Riboflavin phosphate; flavin mononucleotide.
FAD:	Isoalloxazine-adenine dinucleotide; flavin adenine dinucleotide.
FADH ₂ :	Reduced flavin adenine dinucleotide.
ESR:	Electron spin resonance; electron paramagnetic resonance.
ORD:	Optical rotatory dispersion.
Neotetrazolium:	p, p' - diphenylene-bis(3, 5-diphenyl) tetrazolium phosphate.

I. INTRODUCTION

1. Statement of Problem

The various classes of respiratory reactions which involve molecular oxygen include external mixed-function oxidation (1):



From the equation it is seen that mixed-function oxidations require substrate, molecular oxygen, and two reducing equivalents.

In the liver the reaction of reducing equivalents with oxygen and substrate takes place within a highly organized membranous structure (2, 3), the endoplasmic reticulum. The reducing equivalents used in the endoplasmic reticular mixed-function oxidations are brought into reaction with substrate and oxygen by an electron transport system. The terminal electron acceptor in this system also is a microsomal mixed-function oxidase and therefore represents an intersection between electron transport and mixed-function oxidation.

In microsomes, this component has been spectrophotometrically identified as a hemoprotein, cytochrome P-450 (4), and by ESR as a low spin hemoprotein, "microsomal Fe_x " (5). Cytochrome P-450-dependent mixed-function oxidations are involved in metabolism of steroids (6, 7), lipids (8, 9), drugs (10, 11, 12), and carcinogens (13, 14), and are therefore of fundamental metabolic importance. Knowledge of the physical and chemical properties of this

hemoprotein is of great importance in leading to a complete understanding of the manner in which electron transport and mixed-function oxidation interact, and of the mechanisms by which mixed-function oxidation reactions proceed.

The purpose of this thesis is to examine some of the properties of cytochrome P-450 as a basis for explaining its function and mechanism of action. While its spectral and electron spin resonance properties are already well known, its redox properties are unknown. These properties have now been investigated along with its optical rotatory dispersion, its change of spin state of the iron upon treatment with acid, and the stoichiometry of its reduction.

The results of these investigations are reported herein. An attempt is made to coordinate these results with existing knowledge of components of liver endoplasmic reticular mixed-function oxidations. It will be shown that these results expand our knowledge of this hemoprotein and therefore our knowledge of microsomal mixed-function oxidations in general.

2. Discovery of Redox Active Hemoproteins

The field of oxidation-reduction as a major branch of biochemistry began with the work of the French chemist Antoine Lavoisier (1743-1794). In 1784 he showed that when sugar burned, it combined with air to give carbon dioxide and water which weighed more than the original sugar. In 1777 he had concluded that combustion was the combination of Joseph Priestley's "dephlogisticated air" with a combustible substance. In 1778, Lavoisier named the dephlogisticated air "oxygen", meaning "acidifying principle", because combination of this principle with phosphorous and other elements, such as sulfur, gave acids. He said "it (oxygen) is the constituent principle of acidity and is common to all acids" (15). Lavoisier called the product formed by addition of oxygen an "oxide". The process of combining a combustible substance with oxygen became known as "oxidation" (15).

General chemistry texts sometimes define oxidation as the loss of one or more electrons and reduction as the gain of one or more electrons (16). This definition is not adequate to explain all the experimental observations concerning biological oxidation. In general, reactions in which a molecule combines with oxygen or hydroxyl, or loses hydrogens or electrons, are called oxidations because all these processes involve the loss of electrons from an orbital of an atom or

molecule (the group being oxidized). "Since oxidation implies simultaneous reduction, oxidation-reduction is the transfer of oxygen, hydroxyl, hydrogen, or electrons" (17).

The association of proton transfer with electron transfer in biological oxidation-reduction is derived from the work of Wieland and Warburg. Heinrich Wieland observed that many biological oxidations did not appear to involve molecular oxygen. In 1912, he stated that the fundamental process in biological oxidation-reduction was activation of hydrogen (18). He arrived at this hypothesis by observing that bacteria were able to oxidize alcohol to acetic acid in the absence of oxygen, if a hydrogen acceptor such as methylene blue was present. For this reason a large number of cases of oxidation became known as dehydrogenations, with the substrate being dehydrogenated (oxidized) while the hydrogen acceptor was reduced (19). This theory was further advanced by the advent of the Thunberg technique (20), which consists of studying the effect of the addition of substrate on the reduction of methylene blue by tissues washed free from substrate. The reaction was carried out in the absence of oxygen in a "Thunberg tube". From this work Thunberg was able to identify a number of enzymes (dehydrogenases) which were involved in oxidation-reduction, such as succinic dehydrogenase (21), and the term "hydrogen transport" was substituted for "oxidation-reduction" (22). With the advent of deuterium as a tracer, it has been shown

just how highly specific hydrogen transport can be during biological oxidation-reduction (23). For example, Westheimer et al. have demonstrated that during reduction of NAD by dideuteroethanol, catalyzed by alcohol dehydrogenase, a deuterium atom is transferred stoichiometrically and stereochemically from the ethanol to the NAD (23, 24).

Otto Warburg, on the other hand, observed that many biological compounds such as cytochrome c oxidase ("Atmungsferment"), had a very high affinity for oxygen and that metal binding compounds such as cyanide could inhibit the consumption of oxygen by cells. For these reasons he stated that the fundamental process in respiration was activation of molecular oxygen (25). A. Szent-Gyorgyi resolved the conflict by observing that both activation of substrate hydrogen atoms and activation of oxygen were involved in intracellular oxidations. He demonstrated that aerobic oxidation of succinate by tissues was inhibited by cyanide but oxidation of succinate in the presence of methylene blue was not so affected (26).

The term "electron transport" is now used in descriptions of biological oxidation-reduction and this term is frequently used synonymously with "hydrogen transport". For example, in mitochondrial respiratory systems oxygen is reduced by transfer of electrons through an electron transport system. These electrons originate from reduced pyridine nucleotide (NADH) and they are transferred to

oxygen which is reduced to water. The net result is the transfer of four reducing equivalents from two molecules of NADH to one molecule of oxygen, giving two moles of water. The reducing equivalent may be a hydride ion (H^-), a hydrogen atom ($\text{H}\cdot$), a free electron and a proton ($\text{e}^- + \text{H}^+$), or any of these associated with the other atoms or groups in the transfer process. The nature of the reducing equivalent in the above reaction is not known and the cytochrome sequence is called an electron transport chain, although a hydrogen nucleus may accompany an electron (17).

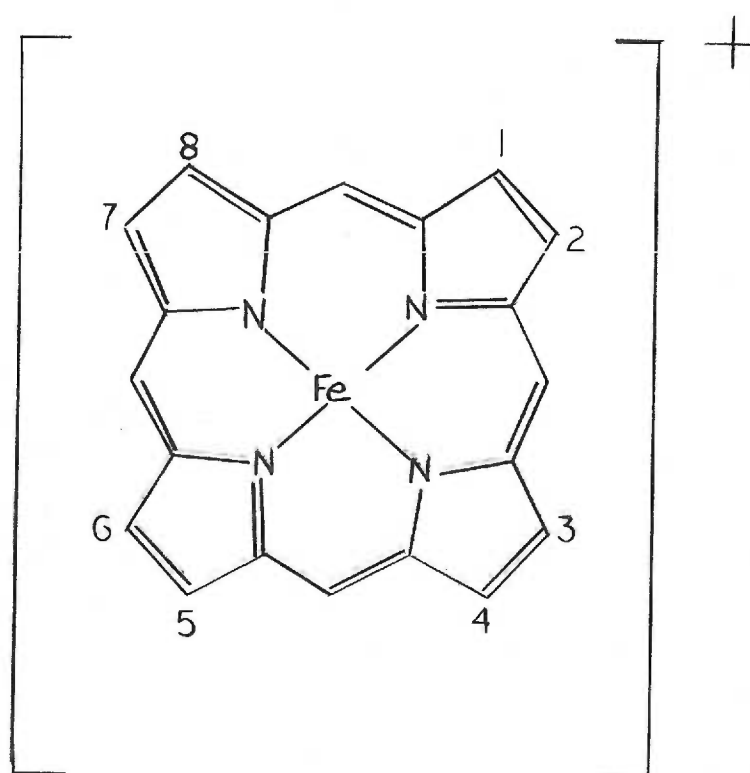
Among biological compounds which undergo oxidation-reduction during electron transport are hemoproteins called "cytochromes". In current usage, "cytochrome" refers to hemoproteins which act in electron transport in a ferrous-ferric cycle (27). As the name implies, hemoproteins are proteins containing heme as a prosthetic group. The heme group is shown in Fig. 1. It consists of a proporphyrin ring with an iron atom in the center. Differences between heme proteins may arise from a number of sources. The iron atom in heme has six possible coordination positions, four of which are bound to pyrrole nitrogen atoms. Two are at right angles to the plane of the porphyrin ring and are available for other binding (28). In hemoglobin, heme is bound to protein through a histidine group at coordination position 5 (29). The fifth and sixth positions on iron-porphyrin complexes are those below and above the plane of the heme molecule

FIG. 1

THE PROSTHETIC GROUP OF FERRIC HEME PROTEINS

The numbers represent points of attachment of side chains onto the porphyrin ring. These side chains determine the different types of heme groups as seen in Table 3.

According to Falk (28)



and correspond to positions 1 and 6 in octahedral complexes in general coordination chemistry (30). In cytochrome c, one ligand to the iron is an imidazole side chain of a histidyl residue while the other ligand to the iron is possibly a methionyl residue (31). Also in cytochrome c there is linkage between two cysteine-SH groups of the protein and two vinyl side chains on the porphyrin ring by two covalent thioether bonds. A heme peptide chain can be isolated from cytochrome c which contains the heme group attached by thioether linkages (32). A further variation in heme proteins is due to differences in the side chains of the porphyrin ring (see Table 4). These side chains are not only involved in linkage between heme and protein, but also affect electronic structure at the iron atom (28).

C. A. MacMunn first observed the cytochromes in 1884 using a microspectroscope and called them "myohaematin" (found in muscles) and "histohaematin" (found in other tissues) (33).

Thus from echinoderms to man throughout the animal kingdom, we find in various tissues and organs a class of pigments whose spectra show a most remarkable resemblance to each other; they are allied to hemochromogen, the bands of which are sometimes closely imitated by the histohaematin. They are probably simpler in constitution than hemochromogen prepared from vertebrate blood, at least they do not yield all its decomposition products; their bands are intensified by alkalis and enfeebled by acids, intensified by reducing agent, and enfeebled by oxidizing agents; they accordingly appear to be capable of oxidation and reduction and are therefore respiratory. If this view be correct, and I have every reason to believe that it is, we may consider that the histohaematin are of use in enabling the tissues in which they occur to take up the oxygen from the circulating blood and hold it in the

Thirty-five years later David Keilin rediscovered the compounds of MacMunn and named them "cytochromes", meaning "cellular pigment". He used a live wax moth (Galleria mellonella) and was able to observe, with a microspectroscope, cytochrome bands at 604.5 m μ , 565.7 m μ , 549.5 m μ , and 520 m μ , which appeared as the moth struggled. These wavelengths represent the positions of maximum absorption and he named these bands a, b, c, and d respectively. Keilin observed that the intensity of the bands increased as the moth struggled and that the bands appeared in a nitrogen atmosphere and disappeared in an air atmosphere. For these reasons he identified cytochrome as a respiratory catalyst. He also claimed that the cytochrome bands were due to three separate components by showing that in a yeast suspension band c disappeared more rapidly than the other bands in air, while band b seemed to become more intense and remained for some time along with bands a and d. At this point he gave the first representation of the respiratory chain as seen in Fig. 2 (34).

In 1929, Keilin proposed that cytochrome components c and a were oxidized by indophenol oxidase, an insoluble oxidase which catalyzes the oxidative synthesis of indophenol from α -naphthol, dimethyl-p-phenylene-diamine, and oxygen. He showed that inhibitors of indophenoloxidase activity such as KCN and CO also inhibited oxygen uptake in cells. At the same time he proposed that the

FIG. 2

THE FIRST SCHEMATIC REPRESENTATION OF THE RESPIRATORY CHAIN (1925)

R in this diagram represents oxidized substances in cells.

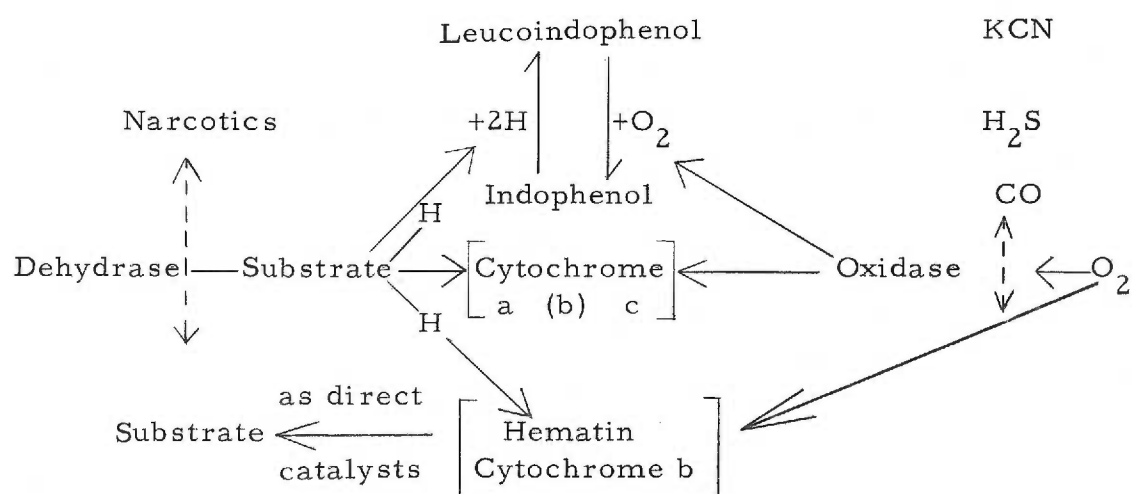
According to Keilin (34)

FIG. 3

LOCATION OF CYTOCHROMES IN THE RESPIRATORY CHAIN

Note that the autoxidizability of cytochrome b is indicated.

According to Keilin (35)



cytochromes were reduced by dehydrogenating enzymes or "dehydrases", because "dehydrase" inhibitors such as ethyl urethane or elevated temperature inhibited reduction of the oxidized cytochromes. Keilin reformulated the respiratory chain to accommodate this new information concerning the nature of the cytochrome oxidase and cytochrome reductase (Fig. 3) (35). The nature of the oxidase was still under debate. Warburg identified the oxidase with "Atmungsferment" (cytochrome c oxidase) because of the effect of CO on respiration (25).

MacMunn was aware that the compounds he was dealing with were hematin in nature from their spectroscopic properties. Anson and Mirsky in 1925, suggested that the cytochromes contained heme combined with nitrogenous compounds because their examination of various hemochromogen compounds showed that the spectral properties of hemochromogens depended on the nitrogenous compounds (36). Conant showed that the hemoglobin-methemoglobin system was truly a reversible oxidation-reduction system by studying the equilibrium of these two compounds in the presence of oxidized and reduced dye-stuffs (37). A reversible oxidation-reduction system is one which follows the same path (titration curve) upon addition of oxidizing or reducing equivalents. This means that the same equilibrium positions are obtained by titration in either direction. Conant also demonstrated that the combination of hemoglobin with molecular oxygen

left the iron in the ferrous state. Potentiometric titration of oxyhemoglobin with oxidizing or reducing agents gave the same titration curve as did titration of hemoglobin in a nitrogen atmosphere. For this reason he suggested that the combination of hemoglobin with oxygen was a process of oxygenation rather than oxidation. He also theorized that the respiratory pigments, the cytochromes, are capable of undergoing oxidation by molecular oxygen (37). The distinction between oxygenation and oxidation was thus made clear. With this information available Keilin realized that he was really looking at three different cytochromes represented by three different hemochromogen compounds and that the spectral differences between the cytochromes were, as Anson and Mirsky had suggested (36), due to the different nitrogen compounds involved. In the case of the cytochromes the different nitrogen compounds were their protein moieties. Keilin also showed that the cytochromes did not all contain protoporphyrin IX (38). Protoporphyrin has three different types of side chains (see Table 4) which give rise to fifteen possible isomers. Protoporphyrin IX is the naturally occurring isomer (39).

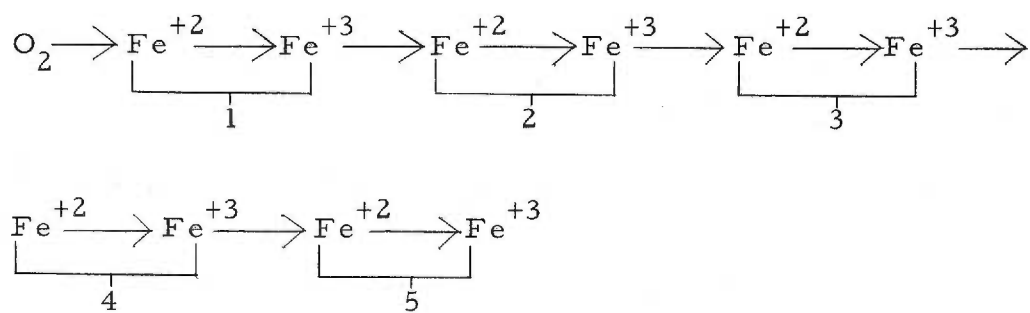
Warburg, in 1933, formulated the respiratory chain, as depicted in Fig. 4. He included a cytochrome sequence which was in general accord with Szent-Gyorgyi's idea that biological oxidations involve only small differences of redox potential in each reaction even though the potentials were not known at that time (27).

FIG. 4

WARBURG'S FORMULATION OF THE RESPIRATORY CHAIN (1933)

This figure shows the sequential action of the respiratory chain cytochromes. Numbers 3, 4, and 5 represent the cytochromes, while Number 1 is the oxidase and Number 2 is an intermediary iron enzyme.

According to Warburg (25)



In 1938, Ball arranged the cytochromes a, b, and c, correctly by determining their redox potentials as will be discussed later (40) and in 1940 Okunuki identified cytochrome c₁ and claimed it was intermediate in potential between c and b (27).

Keilin and Hartree, in 1939, discovered cytochrome a₃ in a heart muscle preparation. They identified it as the terminal component of the respiratory chain because it was autoxidizable and combined with respiratory inhibitors. They were convinced of the hematin nature of the oxidase from its spectral characteristics and from the fact that it combined with cyanide, azide, and CO, all of which were known to combine with hemoproteins (41).

Since the discovery of the classical cytochrome chain in mammalian tissues, many different electron transport systems involving cytochromes have been found in bacteria (42) and plants (43). For this reason it has become necessary to establish precise criteria by which newly discovered cytochromes may be classified and their properties thereby related to those of known cytochromes.

The classification of the cytochromes is based on the nature of the prosthetic group. The International Union of Biochemistry has recently recommended that cytochromes be divided into four major groups which should not be sub-classified (44):

1. Cytochromes a: Cytochromes in which the heme prosthetic group contains a formyl side-chain.

2. Cytochromes b: Cytochromes with protoheme as prosthetic group.
3. Cytochromes c: Cytochromes with covalent linkages between the heme side-chains and protein. This group includes all cytochromes with prosthetic groups linked in this way. To date, only thioether linkages are known, and the prosthetic groups can be termed "substituted mesohemes".
4. Cytochromes d: Cytochromes with dihydroporphyrin (chlorin)-iron as prosthetic group.

The nature of the prosthetic group has considerable influence on the positions of the α -absorption band of the spectra of reduced cytochromes (32). One of the practical tests, adopted by the International Union of Biochemistry, as a criterion in determining the type of cytochrome is the position of the α -band of the pyridine ferro-hemochrome (formerly hemochromogen) (44):

a-type: 580 m μ to 590 m μ .

b-type: 556 m μ to 558 m μ .

c-type: 549 m μ to 551 m μ .

d-type: 600 m μ to 620 m μ .

The α -band is one of the three major absorption bands of heme proteins, these bands being particularly intense and sharp in the reduced state. The α - and β -bands are characteristic of the porphyrin side chains and the extra ligands on the heme iron (28). The β -band is

found in the region of 500 to 540 m μ . The Soret (or γ -band) is the most intense of the absorption bands and is found in the region of 400 to 440 m μ . This band is also characteristic of metal free porphyrins, however, its placement must also be influenced by porphyrin side chains and extra ligands on the iron (28).

Another band is found at wavelengths shorter than those of Soret bands. This is the δ -band. It is found, for example, at 314 m μ (ferrocytochrome c) and at 362 m μ (oxyhemoglobin) (45). Recently Urry has reported on the contribution of the heme chromophore at even shorter wavelengths in the ultraviolet and has labeled an absorption maximum at 277 m μ found with the heme undecapeptide of cytochrome c as the ϵ -hemochromogen band (46).

The a, b, and c bands described by Keilin represent the α -bands of the cytochromes a, b, and c, while the d band described by Keilin is the fused β -bands of cytochromes b and c.

3. Microsomal Electron Transport

A. Components of Microsomal Electron Transport

Cellular structure is characterized by a predominance of double membranes as seen by electron microscopy (47). The extensive system of these membranes found in cytoplasm is known as the endoplasmic reticulum. It is isolated by differential centrifugation as double membraned vesicles called "microsomes" (2). Among the activities localized in liver microsomes are many mixed-function oxidase reactions, active in lipid and steroid metabolism, and also in the metabolism of xenobiotic¹ compounds (Table 1). Mixed-function oxidations require reducing equivalents and involve microsomal redox components.

Strittmatter and Ball reported, in 1952, that the major intrinsic pigment in liver microsomes was a hemochromogen resembling, yet distinct from, the cytochromes a, b, and c, first described by Keilin (48). They found that this pigment, in microsomes, could be rapidly reduced by NADH and that the pigment could reduce cytochrome c, although cytochrome c is not found in the microsomes. Pappenheimer and Williams named this compound "cytochrome

¹"Xenobiotic" is derived from the Greek, Xenos and bios, meaning stranger to life, and refers to chemicals which are foreign to the metabolic network (49).

TABLE 1

SOME MICROSOMAL MIXED-FUNCTION OXIDASES

According to Mason et al. (49)

Metabolism of lipids and xenobiotic compounds		Metabolism of steroids	
Enzyme	Donor	Enzyme	Donor
Fatty acid hydroxylase	TPNH	Testosterone-2- β -hydroxylase	TPNH
Fatty alcohol oxidase	TPNH/ THBP*	Estriol-2-hydroxylase	TPNH
Polyenoic acid dehydrogenase	TPNH or DPNH	Androstenedione-6- β -hydroxylase	TPNH
Phenol- <u>o</u> -hydroxylase	TPNH	Testosterone-6- β -hydroxylase	TPNH
Nonspecific hydroxylase	TPNH	Estradiol-6- β -hydroxylase	TPNH
Polycyclic hydrocarbon hydroxylase	TPNH	3- β -Hydroxycholeonic hydroxylase	TPNH
Drug oxidative demethylase deethylase	TPNH	Testosterone-7- α -hydroxylase	TPNH
Drug <u>N</u> -hydroxylase	TPNH	Estrone-10- β -hydroxylase	TPNH
<u>N</u> -oxidase	TPNH	Dehydroepiandrosterone-16- α - hydroxylase	TPNH
<u>N</u> -oxide dearyase	TPNH	Estradiol-16- α -hydroxylase	TPNH
Carcinogen hydroxylase	TPNH	Squalene synthetase	TPNH
Deiodinase	TPNH	Squalene cyclizing enzyme	TPNH, DPNH
		17-Hydroxycorticosterone-11- β - hydroxylase	TPNH
		Steroid C-21-hydroxylase	TPNH

*THBP = Tetrahydrobiopterin

\underline{b}_5 '' (50).

In 1956, Strittmatter and Velick isolated cytochrome \underline{b}_5 from rabbit liver microsomes by pancreatic lipase digestion and ammonium sulfate precipitation. No flavin or non-heme iron was found with the cytochrome and neither NADPH or NADH would reduce it. When soluble reductases from microsomes were added, cytochrome \underline{b}_5 was rapidly and completely reduced. It was not rapidly autoxidizable. The standard redox potential at pH 7.0 was found to be -0.02v. and the stoichiometry showed that the cytochrome behaved as a univalent electron donor and acceptor (51). They also found that a NADH-cytochrome \underline{b}_5 reductase could be released from microsomes by digestion with snake venom (phospholipase). This reductase was found to be a flavoprotein, molecular weight 40,000, with one mole of FAD per mole of enzyme (52).

Garfinkel isolated another reductase in 1957, from pig liver microsomes. It contained FMN and catalyzed reduction of cytochrome \underline{c} by NADH (53). This protein is known as NADH-''cytochrome \underline{c} '' reductase, although, no cytochrome \underline{c} is found in carefully prepared microsomes. At the present time the natural substrate for this reductase is unknown.

Strittmatter purified both cytochrome \underline{b}_5 and NADH-cytochrome \underline{b}_5 reductase as homogeneous, low molecular weight proteins (54, 55). He determined the amino acid composition of cytochrome \underline{b}_5 and

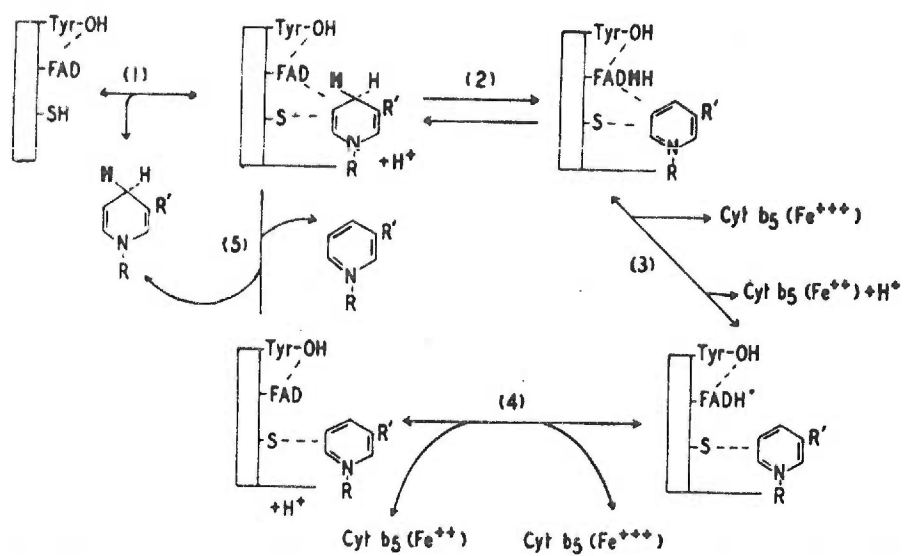
demonstrated that the protoheme could be removed from the protein and then added back with full restoration of physical and chemical properties (56). Strittmatter also studied the reduction of cytochrome b_5 by its NADH reductase, and arrived at a reaction mechanism for NADH-cytochrome b_5 reductase (Fig. 5) by examining the reactions of the apo-reductase with FAD and pyridine nucleotide derivatives. He observed that iodination of a tyrosine hydroxyl blocked flavin interaction with the apo-reductase and that reduced pyridine nucleotide could be displaced from the apo-enzyme by one equivalent of p-mercuribenzoate, indicating that a single sulfhydryl group is involved in the interaction of the nucleotide with the enzyme. Sulfhydryl reagents did not displace the NADH in the holoenzyme indicating that a stable complex is formed between flavin and NADH and a stable complex between the reduced flavin ($FADH_2$) and NAD is formed. The latter was detected spectrophotometrically (57). Recently Sato has suggested that cytochrome b_5 is involved in fatty acid desaturation (58). However, at this time the nature of the electron acceptor from cytochrome b_5 remains a mystery and function of this electron transport system remains uncertain.

In 1958, Klingenberg observed a carbon monoxide-binding pigment in rat liver microsomes (as a reduced-CO minus reduced

FIG. 5

PROPOSED REACTION SEQUENCE FOR CYTOCHROME b_5
REDUCTASE

According to Strittmatter (57)



difference spectrum²). He demonstrated by pyridine ferroheme-chrome determinations that the total heme content of the microsomes was more than twice that of cytochrome b₅ content (59). Garfinkel observed the CO-binding pigment in pig liver microsomes at about the same time and suggested that because of its complexing properties with carbon monoxide and cyanide this pigment contained some sort of metal ion. He suggested, however, that the pigment was not a heme protein because no peaks were found spectrophotometrically in the region of 500 to 600 mμ in the reduced-CO minus reduced difference spectrum (60).

Horecker had purified a NADPH-cytochrome c reductase in 1950 from whole pig liver acetone powder and had demonstrated that the activity was associated with particles, although the nature of the particles was not then known (61). Williams et al., in 1959, observed that rat liver microsomes catalyzed the reduction of neotetrazolium by NADPH (62). They also observed that cytochrome c inhibited the microsomal reduction of neotetrazolium by NADPH. They were able to isolate a soluble flavoprotein from the microsomes by lipase treatment and ammonium sulfate fractionation. It contained two moles of FAD per mole of enzyme, was substantially iron free,

²This expression means that the absorption difference between a sample treated with reducing agent and carbon monoxide and a sample treated with only reducing agent was measured.

and had a molecular weight of 68,000 (63). Phillips and Langdon independently purified the enzyme in the same year by trypsin solubilization (64). This enzyme can reduce one- and two-electron acceptors but reacts very slowly with oxygen. Kamin et al., observed that the oxidation states of the flavin are the same during catalysis of reduction of either one- or two-electron acceptors, and demonstrated a mechanism hitherto undescribed for flavin catalysis: alternation of the flavin between the fully reduced (FADH_2) form and the half-reduced, semiquinoid (FADH) form (65).

In 1962, Sato and Omura studied the CO-binding pigment of rabbit liver microsomes and suggested that it was a hemoprotein based on the spectral evidence that it combined with CO, NO, and ethyl isocyanide in the reduced state. They named the pigment cytochrome P-450 (4). The pigment showed no α - or β -band in the reduced-CO minus reduced difference spectrum; however, upon treatment of microsomes with snake venom or deoxycholate cytochrome P-450 was converted into cytochrome P-420, a form which gave a characteristic hemoprotein reduced-CO minus reduced difference spectrum. The ethyl isocyanide difference spectrum of liver microsomes also indicated the hemoprotein nature of cytochrome P-450 (64). It was known that cytochrome b_5 had no affinity for ethyl isocyanide even after snake venom treatment and Omura and Sato demonstrated a competition between CO and ethyl isocyanide for dithionite-reduced

microsomes. For this reason it was concluded that the microsomal CO- and ethyl isocyanide-binding pigments were the same (64).

Omura and Sato also demonstrated that there was more protoheme in liver microsomes than could be accounted for by cytochrome b_5 , a fact which had been previously noted (59, 60). Omura and Sato concluded from the above information that cytochrome P-450 was a hemoprotein (66). Further evidence for the hemoprotein nature of cytochrome P-450 was demonstrated by Cooper et al. who showed that the CO bound to cytochrome P-450 in liver microsomes was photodissociable (67). In microsomes, cytochrome P-450 could be reduced by NADH and NADPH only under anaerobic conditions, indicating that the pigment was autoxidizable (66).

Hashimoto et al., in 1962, reported the ESR spectrum of rabbit liver microsomes (5). The signal was identified as that of a low spin heme protein because of the three anisotropic g -values³ centered around $g = 2$ (68). Purified cytochrome b_5 gave no absorption under these conditions, although recently a broad, weak ESR signal has been obtained from purified cytochrome b_5 , indicating that the cytochrome is low spin (69). The concentration of the microsomal heme protein (see Experimental) was found to be equal to the difference

³The g -value is a measure of the spin magnetic moment and the orbital magnetic moment contributions to the total angular momentum of an electron (see Experimental).

between the pyridine ferrohemochrome and cytochrome b_5 determinations (5). The microsomal ESR signal could be reduced by NADPH or NADH under anaerobic conditions, while addition of oxygen caused the reappearance of the original signal. This hemoprotein was named microsomal Fe_x , indicating a microsomal iron protein, probably a low spin heme protein, but unidentified at that time (5).

In 1964, Omura and Sato isolated the degradation product of cytochrome P-450, cytochrome P-420, and showed that its spectral properties were characteristic of those of a b -type cytochrome. The pyridine ferrohemochrome of cytochrome P-420 had spectral properties very similar to those of the b -type cytochromes (70). The b -type cytochromes contain iron protoporphyrin IX as the prosthetic group (17). Protoporphyrin IX as seen in Table 4 has 4 methyl, 2 vinyl, and 2 propionic acid side chains on the porphyrin ring. The redox potential of cytochrome P-420 was found to be -0.02v. at pH 7.0 (70).

Recently a soluble form of cytochrome P-450 has been isolated from two sources. Katagiri et al., have isolated a soluble cytochrome P-450-like protein from Pseudomonas putida which contains protoporphyrin IX (71). Appleby has isolated a cytochrome P-450-like hemoprotein from Rhizobium japonicum which also contains protoporphyrin IX and has a molecular weight of about 50,000. Appleby has predicted that the Rhizobium cytochrome P-450 contains two

protoheme molecules at the active site because of the ethyl isocyanide difference spectrum (72).

Lu and Coon have recently isolated a "soluble" cytochrome P-450-containing fraction from rabbit liver microsomes which when combined with two other soluble fractions, one containing no protein (phospholipid) and one containing NADPH cytochrome c reductase, will catalyze the ω -hydroxylation of laurate (73). Whether cytochrome P-450 is the only heme protein present in the "soluble" fraction is not reported. Lu and Coon claim the cytochrome P-450-containing fraction to be soluble, but because it was obtained by using sodium deoxycholate and must still contain this reagent, it may only be optically clarified.

From the above information, a scheme can be drawn depicting the components of microsomal electron transport and their relationship to one another (Fig. 6).

B. Microsomal Electron Transport and Mixed-Function Oxidation

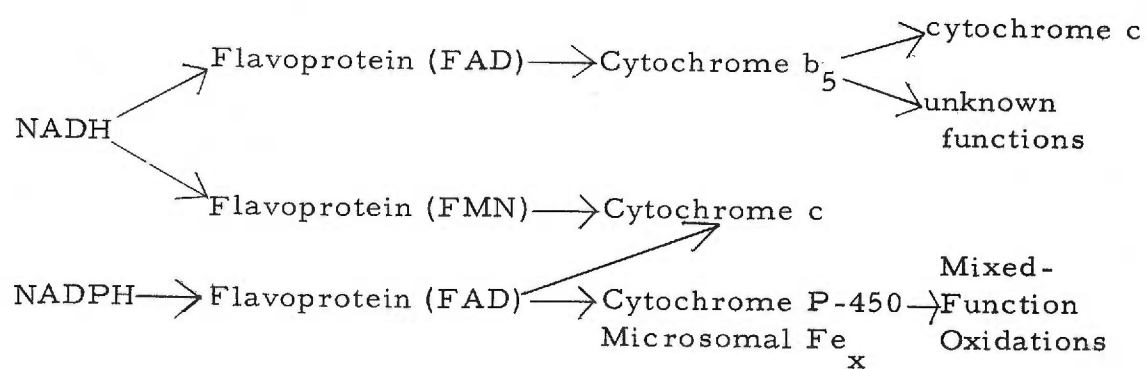
It has been shown that rat liver microsomal mixed-function oxidation activities associated with drug hydroxylations, such as hexobarbital oxidation, show an adaptive increase when drugs such as phenobarbital are administered to rabbits (74). Upon treatment of rabbits with phenobarbital the hexobarbital hydroxylation activity

FIG. 6

REDOX COMPONENTS OF LIVER MICROSOMES

It should be noted that cytochrome c is not endogenous to liver microsomes.

After Mason et al. (49)



increases. It returns to a normal level when phenobarbital treatment is stopped. Orrenius and Ernster showed that the adaptive increase in rats of the capacity to oxidatively demethylate aminopyrine was accompanied by increase in the microsomal CO-binding hemoprotein, cytochrome P-450, and NADPH-cytochrome c reductase activity in liver microsomes (75). More recently direct evidence has been found for the participation of cytochrome P-450 in adrenal cortical microsomal mixed-function oxidation reactions. Estabrook et al., demonstrated that the 21-hydroxylation of 17-hydroxyprogesterone in adrenal cortical microsomes was CO sensitive, and that the photochemical action spectrum for the light reversal of the CO-inhibition of this reaction shows a maximum at 450 m μ (76). The same photochemical action spectrum for the reversal of CO-inhibition has been shown for the oxidative demethylation of codeine, the oxidative demethylation of monomethylaminopyrine, and the aromatic ring hydroxylation of acetanilide in rat liver microsomes (67), and for the hydroxylation of acetanilide and coumarin in rat and rabbit liver microsomes (77). Gillette has summarized liver microsomal drug hydroxylations which are inhibited by CO, although the photochemical action spectrum has not been determined for most of these reactions (78). Cytochrome P-450 is now generally recognized as a participant in a number of microsomal mixed-function oxidations.

Estabrook and his coworkers demonstrated that inhibition of

21-hydroxylation of 17-hydroxyprogesterone is a function of the CO/O₂ ratio, i. e. there is a competition of CO and O₂ for a common reactive site (76). It has also been shown by using ¹⁸O₂ that atmospheric oxygen is incorporated into the products of microsomal hydroxylations (79). Cytochrome P-450 therefore acts as an oxygen-activating enzyme. The manner in which this occurs is still obscure. Cytochrome P-450 meets the requirements for a mixed-function oxidase: it is a terminal acceptor of electrons and acts as an oxygen activating site.

Drugs such as hexobarbital produce a change in the oxidized difference spectrum of rat liver microsomes (Type I - see Table 2). The difference spectrum is obtained by using oxidized microsomes in both cuvettes and substrate only in the sample cuvette. The spectral change is represented by a trough at 419 mμ and a peak at 385 mμ (Fig. 7). Substrates containing nitrogenous bases, such as aniline, produce another type of change (Type II - see Table 2) in the difference spectrum, represented by a peak at 430 mμ and a trough at 393 mμ (Fig. 8) (80). These changes occur in the oxidized state of cytochrome P-450. Imai and Sato have reported only very small spectral changes caused by addition of aniline to reduced microsomes (81). These changes have been attributed to the formation of an enzyme-substrate complex between cytochrome P-450 and substrate (80). Any inference that cytochrome P-450 reacts directly with

FIG. 7

EFFECT OF HEXOBARBITAL ON RAT LIVER MICROSOME
DIFFERENCE SPECTRUM (Type I Spectral Change)

Microsome sample was diluted equally in two cuvettes and a baseline was recorded. Varying amounts of hexobarbital were added to the sample cuvette to give the following concentration: (a) 0.083 mM; (b) 0.33 mM; (c) 0.66 mM; (d) 4.7 mM.

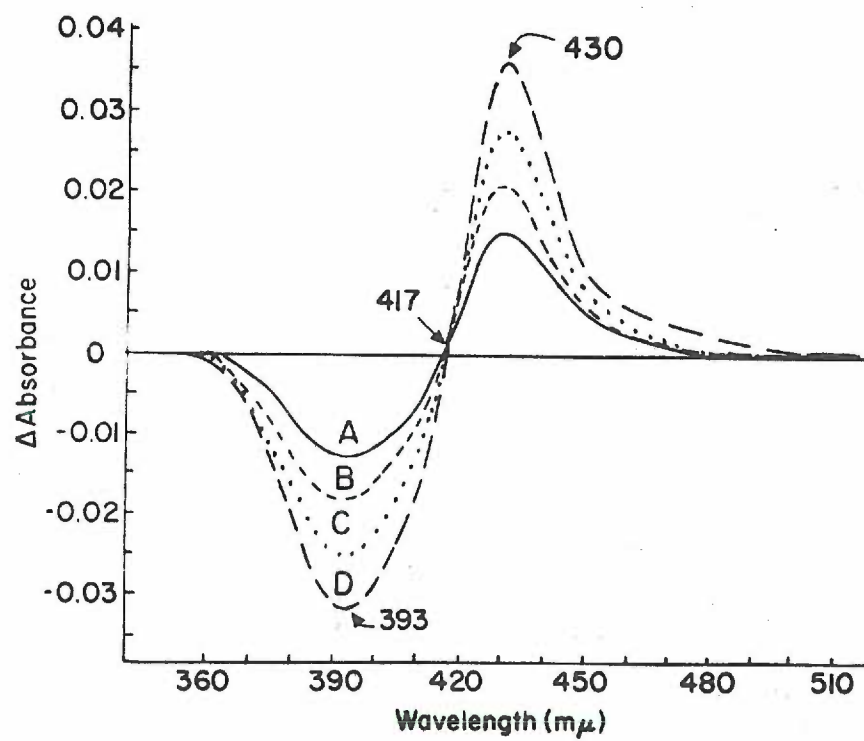
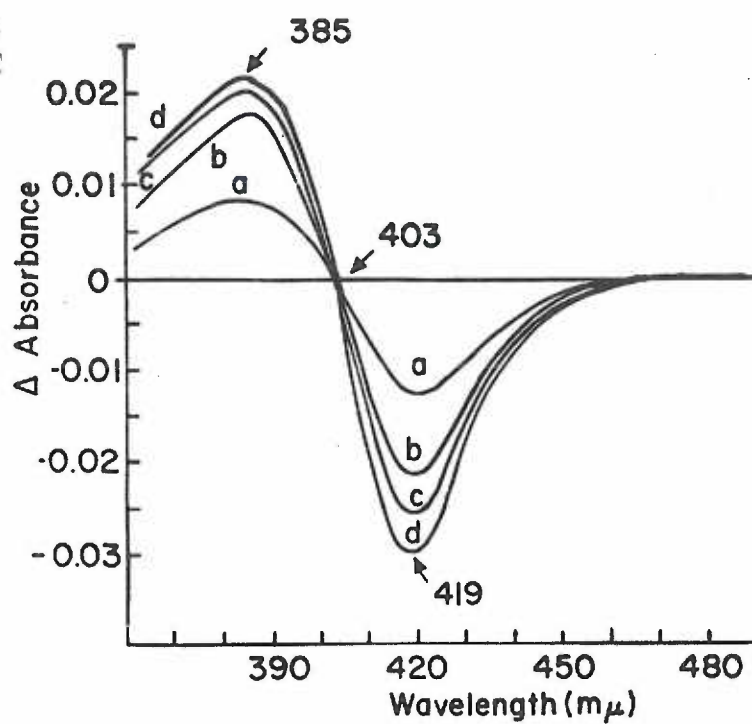
According to Estabrook et al. (80)

FIG. 8

EFFECT OF ANILINE ON RAT LIVER MICROSOME DIFFERENCE
SPECTRUM (Type II Spectral Change)

Microsome sample was diluted equally in two cuvettes and a baseline was recorded. Varying amounts of aniline were added to the sample cuvette to give the following concentration: (a) 0.27 mM; (b) 0.54 mM; (c) 1.2 mM; (d) 2.5 mM.

According to Estabrook et al. (80)



TYPE I COMPOUNDS

Aminopyrine (4-dimethylamino-2,3-dimethyl-1-phenyl-3-pyazolin-5-one)

Phenobarbital (5-ethyl-5-phenylbarbituric acid)

Amobarbital (5-ethyl-5-isoamylbarbituric acid)

Hexobarbital (5-(1-cyclohexen-1-yl)-1,5-dimethylbarbituric acid)

SKF 525-A (2-diethylaminoethyl 2,2-diphenylvalerate HCl)

DDT (dichlorodiphenyltrichloroethane)

N,N-Dimethylaniline

Testosterone

Imipramine (N-(γ -dimethylaminopropyl) iminodibenzyl hydrochloride)

β -Estradiol

Ethylmorphine

TYPE II COMPOUNDS

Nicotine

Aniline

Nicotinamide

Pyridine

p-Aminophenol

DPEA (2,4-dichloro-6-phenylphenoxyethylamine HBr)

oxygen and substrate remains to be proven. Orrenius and Ernster showed that ^{14}C -labeled aniline and phenobarbital are bound to rat liver microsomes in about the same concentrations as the microsomal cytochrome P-450 present. These substrates are not bound to microsomes from other tissues, such as skeletal muscle, devoid of cytochrome P-450. The binding of substrates is not changed in reduced microsomes, although the extent of substrate binding in the presence of dithionite is greatly diminished by CO. For these reasons they suggest that cytochrome P-450 is involved in binding of the substrate to be hydroxylated (82).

What is the relationship of the ESR-detectable hemoprotein, microsomal Fe_x , to cytochrome P-450? Cytochrome P-450 is observed spectrophotometrically from the reduced-CO minus reduced difference spectrum, while microsomal Fe_x is observed by ESR in the oxidized form. The total heme content of microsomes is equal to the cytochrome b_5 content plus the cytochrome P-450 content as determined spectrally (4). It is also equal to the cytochrome b_5 content plus the microsomal Fe_x content as determined from ESR measurements (5). Sulfhydryl reagents, such as p-chloromercuribenzoate (PCMB) and p-chloromercuriphenylsulfonate (PCMS), convert cytochrome P-450 to cytochrome P-420 and also convert microsomal Fe_x from the low spin form to the high spin form (86). Both cytochrome P-450 and reduced microsomal Fe_x are affected by

CO (4, 5). Recently a cytochrome P-450 particle has been prepared which contains only small amounts of other heme components. The ESR-detectable microsomal Fe_x in this particle is also equal to the cytochrome P-450 content (87). Murakami and Mason have discussed the relationship between cytochrome P-450 and microsomal Fe_x and have described microsomal Fe_x as an integral part of the cytochrome P-450 complex on the basis of comparison of ESR and spectral data (86).

While liver and adrenal microsomes (88, 89) from all sources examined contain the same electron transport system, an interesting exception is found in adrenal cortical mitochondria. Here, a system is found which carries out 11 β -hydroxylation of steroids. Again, cytochrome P-450 is found to be the terminal oxidase, but a non-heme iron protein named "adrenodoxin" is found to transfer electrons from flavoprotein to cytochrome P-450. Both adrenodoxin reductase (flavoprotein) and adrenodoxin are required for 11 β -hydroxylase activity of steroids (90). No similar non-heme iron protein can be detected in rabbit liver microsomes. Miyake et al. examined liver microsomes at liquid helium temperatures with ESR looking for the typical non-heme iron protein signal at $g = 1.94$ in the reduced state and were not able to observe the presence of adrenodoxin (91). As Palmer and Sands have pointed out, some non-heme iron proteins can be observed only under these conditions (92). Kimura has tried to

isolate an adrenodoxin-like non-heme iron protein from liver microsomes with no success (93).

4. Redox Potential Studies of Cytochromes

A. Methods for Determining the Redox Potentials of Cytochromes

For the general reversible chemical process:



the equilibrium constant, K , is equal to the ratio of the activities of the products to the activities of the reactants (17).

$$K = \frac{a_C \cdot a_D}{a_A \cdot a_B}$$

If the components of the system under consideration are at their equilibrium concentrations (activities), the free energy change resulting from the transfer of reactants to products is zero. If, however, the reactants and products are at non-equilibrium concentrations the transfer of reactants to products is accompanied by a definite free energy change. The standard free energy change (ΔF°) of a reaction is equal to:

$$\Delta F^\circ = -RT \ln K = -RT \ln \frac{[C][D]}{[A][B]}$$

where R is the gas constant, T is the absolute temperature, and $[A]$, $[B]$ etc, are equilibrium concentrations (94). If the activities of the initial reactants are not in the standard state (1 molal concentration in solution) the free energy change of the reaction is related to the

standard free energy change by the following equation:

$$\Delta F = \Delta F^\circ + RT \ln \frac{[C][D]}{[A][B]}$$

If the reversible system being studied is an electrical cell, the electromotive force of the cell with respect to a standard cell is E volts. The process taking place in the cell is accompanied by the passage of n faradays (nF coulombs)⁴. The work done by the system is equal to nFE volt-coulombs or joules. In a reversible cell the work is equal to the change of free energy accompanying the cell reaction:

$$\Delta F = -nFE = \Delta F^\circ + \frac{RT}{nF} \ln \frac{[C][D]}{[A][B]}$$

$$E = E_o + \frac{RT}{nF} \ln \frac{[C][D]}{[A][B]}$$

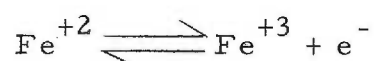
E_o is the standard state electromotive force with respect to the standard hydrogen electrode (94).

If an inert electrode is placed in a solution containing the oxidized and reduced forms of a given solution the electrode is called an oxidation-reduction electrode. The electrode potential recorded is actually the EMF of the cell with respect to the opposing cell. The EMF is called the oxidation-reduction potential as it is measured

⁴The faraday is the quantity of electricity required to liberate one equivalent of any substance and is equal to 96,500 coulombs. The coulomb is the unit of charge or the quantity of electricity passing when one ampere flows for one second (94).

against some standard electrode (94). Biological oxidation-reduction potentials are measured against the hydrogen electrode (17), defined as having a potential of zero.

Peters in 1898 examined the potential difference of the ferrous-ferric system as measured against a calomel half-cell:



He found that the potential difference of the system was a function of the ratio of the concentrations of the ferrous and ferric ions (22).

From this observation Bredig and Luther developed the Peters equation (more popularly known as the Nernst equation):

$$E = E'_0 + \frac{RT}{nF} \ln \frac{[\text{oxidized}]}{[\text{reduced}]}$$

E is the potential at any given point (the measured potential referred to the standard hydrogen electrode); E'_0 is the standard redox potential at a specified pH and is a constant, R is the gas constant (8.315 joules per degree); T is the absolute temperature; F is the Faraday (96,487 coulombs); and n is the valence change taking place in the system (number of equivalents). The natural log function is a ratio of the concentrations of the oxidized and reduced species.

There are a number of approaches which can be used for the determination of the redox potential of a hemoprotein. The use of a potentiometric (electrode) method has been successful in the case of pure hemoproteins, of which the work of Harbury with peroxidase

(95), Coolidge with cytochrome c (96), and Wurmser with cytochrome c (97), are examples. The method is straightforward, consisting of titrating the hemoprotein with a suitable reducing agent and measuring the potential at each equilibrium point using an electrode while monitoring the reduction of the hemoprotein spectrophotometrically. In this type of measurement a big concern is that no autoxidation takes place in the system, i. e. that the equilibrium condition is established and maintained throughout the period of measurement. The redox potential is calculated using the Peters equation. The E'_O should be the same for each ratio of oxidized and reduced cytochrome.

When no pure preparation of hemoprotein is available, the potentiometric technique becomes undesirable. The electrode is then measuring the potential of the total system rather than that of any particular component. In the case of microsomes or mitochondria which contain many redox components, it is not feasible to use the potentiometric method for the potential determination of one of the components. In these cases, a dyestuff technique can be successfully employed. This technique utilizes a dyestuff of known redox potential in place of the electrode. By adding a known ratio of oxidized and reduced dye or by titrating an oxidized or a reduced dyestuff, one can determine the redox potential of any given component. In this type of measurement it is possible to determine the

concentration of the oxidized or reduced dyestuff as well as the cytochrome, spectrophotometrically. Instead of measuring the potential at each equilibrium point potentiometrically, the concentration of either oxidized or reduced dyestuff is measured spectrophotometrically. From this information and the total dyestuff concentration, the ratio of oxidized and reduced forms of the dyestuff can be calculated. Peters equation is then used to calculate the potential using the known E'_O of the dyestuff. The calculated potential at each equilibrium point becomes the E in another Peters equation. In the second Peters equation the measured ratio of oxidized and reduced cytochrome at each equilibrium point is used and the E'_O , the standard redox potential of the cytochrome, is the unknown. Therefore, from a combination of two Peters equations the E'_O of one species (cytochrome) can be determined without using potentiometric techniques if the E'_O of the other species (dyestuff) is known. As in the potentiometric method, anaerobic techniques must also be employed with the dyestuff method. In this case the dyestuff also may be autoxidizable. One further precaution must be taken with the dyestuff technique. It is important that the overlap of the absorption of the dye with the absorption of the cytochrome is minimal.

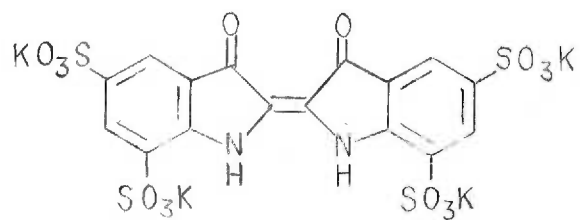
Clark has given a rather complete list of dyestuffs which are reversible oxidation-reduction indicators. Among the most commonly used of these dyes, and their E'_O 's at pH 7.0, are:

FIG. 9

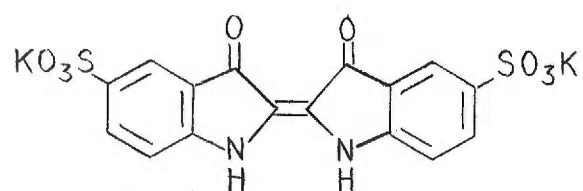
OXIDATION-REDUCTION INDICATORS
(All are two-electron acceptors)

- (A) Indigotetrasulfonate
- (B) Indigodisulfonate
- (C) Methylene blue
- (D) Phenosafranine
- (E) 2,6-dichlorophenolindophenol

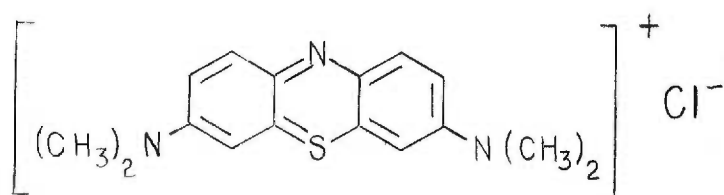
A



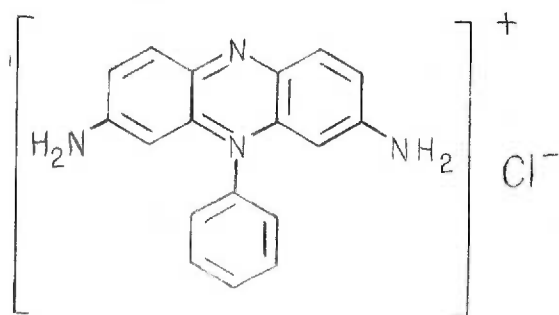
B



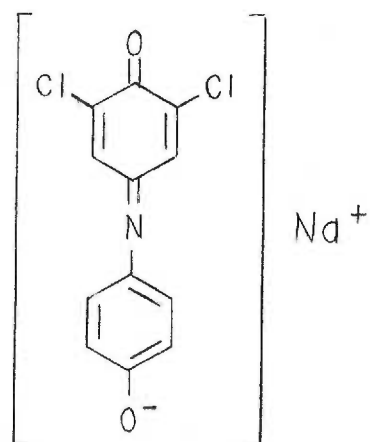
C



D



E



B. Summary of Cytochrome Redox Potentials

The first reported redox potential for a cytochrome was given by Coolidge in 1932 (96). He used the potentiometric method to measure the potential of an impure cytochrome c isolated from yeast and reported an E'_o of +0.260v. at pH 7.0. Green, also using standard potentiometric techniques, reported a value of +0.127v. from pH 4.59 to pH 7.14 for impure yeast cytochrome c (98). After a technique for purification of cytochrome c was worked out, Wurmser, using a potentiometric method, obtained a value of +0.254v. from pH 5.0 to pH 8.0 for liver cytochrome c (97), while Stotz, Sidwell, and Hogness obtained a value of +0.262v. from pH 5.0 to pH 8.0 for beef heart cytochrome c using the dyestuff technique (99).

At this same time Ball had been able to estimate the potentials of three cytochromes in a crude heart muscle extract as pointed out earlier. This determination was extremely important, because it allowed Ball to arrange the cytochromes in the respiratory chain according to their redox potentials. Ball obtained the redox information by observing the intensity of the completely reduced cytochrome bands, then poisoning the potentials by adding definite ratios of oxidized and reduced forms of dyestuffs and measuring changes in the intensities of the cytochrome bands. He obtained the following values: -0.04v. for cytochrome b, +0.27v. for cytochrome c, and +0.29v. for cytochrome a, all at pH 7.4 (40).

Since this initial work, the redox potentials of many cytochromes have been determined. While it is not possible to discuss each separate determination, the most interesting and pertinent results will be discussed in detail. A compilation of redox potential determinations of cytochromes is found in Table 3, including the source of the material and technique used.

A classical redox study of a hemoprotein was the work of Harbury on horseradish peroxidase (95). Peroxidase proved to be a very interesting and difficult hemoprotein as far as redox properties were concerned. Because horseradish peroxidase was known to be highly autoxidizable, extreme care had to be taken to assure anaerobic conditions. Harbury assembled a titration apparatus (Fig. 10) which permitted collection of spectrophotometric and potentiometric data throughout the course of titration. He was able to carry out both oxidative and reductive titrations, measuring the potential of his system after each addition potentiometrically and measuring the peroxidase concentration spectrophotometrically. With his design, Harbury was able to move the mixture from the electrode to the spectrophotometric cell using helium gas as a driving force. This is a classical experiment in terms of apparatus design and exactness of titration curves. The potential of purified horseradish peroxidase is -0.271v. at pH 7.0.

One extremely interesting aspect of the redox behavior of

TABLE 3
COMPILATION OF CYTOCHROME REDOX POTENTIALS

Cytochrome	Source	Potential	Conditions	Technique	Reference
c	yeast	+0.260v.	pH 7.0, impure prep.	potentiometric	96
c	heart muscle	+0.27v.	pH 7.4, muscle extract	dyestuff	40
c	heart	+0.247v.	pH 6.8, pure preparation	dyestuff	100
c	yeast	+0.127v.	pH 4.59 to 7.14 yeast extract	potentiometric	98
c	beef heart	+0.262v.	pH 5.0 to 8.0	dyestuff	99
c	heart muscle	+0.255v.	pH 6.4, 25°C pure prep.	potentiometric	101
c	beef heart	+0.254v.	pH 1.75 to 7.8, pure prep.	potentiometric	102
c	liver	+0.253v	pH 5.0 to 8.0, pure prep.	potentiometric	97
c	beef heart	+0.251v.	pH 6.73 to 7.55, pure prep.	dyestuff	103
c	yeast	+0.123v.	pH 7.0, yeast extract	dyestuff	104

Cytochrome	Source	Potential	Conditions	Technique	Reference
c	<u>Rhodospirillum rubrum</u>	+0.33v.	pH 7.0, pure preparation	dyestuff	105
c	<u>Pseudomonas stutzeri</u>	+0.24v.	?	?	106
c	Unidentified pseudomonad	+0.26v.	pH 7.0, pure preparation	dyestuff	107
c	<u>Rhodopseudomonas palustris</u>	+0.35v.	?	?	108
c	<u>Rhodomicrobium vannieli</u>	+0.30v.	?	?	109
c	<u>Micrococcus</u> sp.	+0.25v.	?	?	106
c	<u>Micrococcus</u> sp.	+0.18v.	?	?	106
c	<u>Micrococcus</u> sp.	+0.11v.	?	?	106
c	<u>Porphyra teneru</u> (algae)	+0.34v.	pH 7.0, pure preparation	dyestuff	108

Cytochrome	Source	Potential	Conditions	Technique	Reference
c	<u>Grateloupia</u> sp. (algae)	+0.30v.	pH 7.0, pure preparation	dyestuff	108
c	<u>Undaria</u> <u>pinnatifida</u> (algae)	+0.34v.	pH 7.0, pure preparation	dyestuff	108
c	<u>Ulva</u> sp. (algae)	+0.30v.	pH 7.0, pure preparation	dyestuff	108
c	<u>Monostroma</u> <u>nitidum</u> (algae)	+0.31v.	pH 7.0, pure preparation	dyestuff	108
c	<u>Tolypothrix</u> <u>tenuis</u> (algae)	+0.30v.	pH 7.0, pure preparation	dyestuff	108
c	<u>Endarachne</u> <u>binghamiae</u> (algae)	+0.35v.	?	?	106
c	<u>Navicula</u> <u>pelliculosa</u> (algae)	+0.34v.	?	?	106
c	<u>Euglena</u> <u>gracilis</u>	+0.37v.	?	?	106
c	<u>Tetrahymena</u> <u>pyriformis</u> (protozoa)	+0.23v.	?	?	106

Cytochrome	Source	Potential	Conditions	Technique	Reference
c ₁	beef heart	+0.223v.	pH 6.73 to 7.55, pure prep.	dyestuff	103
c ₁	Unidentified Pseudomonad	+0.20v.	pH 7.0, pure preparation	dyestuff	107
c (c ₂ ?)	<u>Chromatium</u>	+0.01v.	pH 7.0, pure preparation	dyestuff	109
c ₃	<u>Desulphovibrio desulphuricans</u>	-0.14v. to -0.25v.	pH 7.0, cell free extract	dyestuff	110
c ₃	<u>Desulphovibrio desulphuricans</u>	-0.205v.	30°C, pure preparation	potentiometric	111
c ₄	<u>Azotobacter vinelandii</u>	+0.30v.	pH 6.0 to 7.5, pure prep.	dyestuff	112
c ₅	<u>Azotobacter vinelandii</u>	+0.32v.	pH 6.0 to 7.5	dyestuff	112
c type	<u>Pseudomonas aeruginosa</u>	+0.30v.	pH 7.0, pure preparation	dyestuff	113
cyt-550 (c type)	<u>Rhodospirillum capsulatus</u>	+0.32v.	pH 7.0, pure preparation	dyestuff	114
cyt-552 (c type)	<u>Rhodospirillum palustris</u>	+0.30v.	pH 7.0, pure preparation	dyestuff	114

Cytochrome	Source	Potential	Conditions	Technique	Reference
cyt-550 (c type)	<u>Rhodospirillum rubrum</u>	+0.33v.	pH 7.0, pure preparation	dyestuff	114
cyt-550 (c type)	<u>Micrococcus denitrificans</u> (anaerobic)	+0.25v.	pH 7.0, pure preparation	dyestuff	114
cyt-550 (c type)	<u>Micrococcus denitrificans</u> (aerobic)	+0.24v.	pH 7.0, pure preparation	dyestuff	114
cyt-552, 548 (c type)	<u>Micrococcus</u> sp.	+0.223v.	pH 7.2, pure preparation	dyestuff	115
cyt-554(I) (c type)	<u>Micrococcus</u> sp.	+0.113v.	pH 7.0, 25°C pure prep.	dyestuff	116
cyt-554(II) (c type)	<u>Micrococcus</u> sp.	+0.18v.	pH 7.0, 25°C	dyestuff	116
cyt-551 (c type)	<u>Micrococcus</u> sp.	+0.249v.	pH 7.0, 25°C pure prep.	dyestuff	116
cyt-552 (c type)	<u>Pseudomonas denitrificans</u>	+0.32v.	pH 7.0, pure preparation	dyestuff	114
cyt-551 (c type?)	<u>Pseudomonas aeruginosa</u>	+0.250v.	pH 7.0, pure preparation	dyestuff	117

Cytochrome	Source	Potential	Conditions	Technique	Reference
cyt-552 (c type)	<u>Escherichia coli</u>	-0.20v.	pH 7.0, pure preparation	dyestuff	118
cyt-553 (c-type)	<u>Chlorobium thiosulfatophilum</u>	+0.098v.	pH 7.0, pure preparation	dyestuff	119
cyt-553 (c type)	<u>Chlorobium thiosulfatophilum</u>	+0.163v.	pH 7.0, pure preparation	potentiometric	120
cyt-554 (c type)	<u>Chlorobium thiosulfatophilum</u>	+0.140v.	pH 7.0, pure preparation	potentiometric	120
cyt-549 (c type)	<u>Anacystis nidulans</u> (algae)	-0.26v.	pH 7.0, pure preparation	dyestuff	121
cyt-553 (c type)	<u>Petalonia</u> sp. (algae)	+0.35v.	pH 7.0, pure preparation	?	122
cyt-554.5 (c type)	<u>Codium latum</u> (algae)	+0.38v.	pH 7.0, pure preparation	?	122
cyt-552 (c type)	<u>Euglena gracilis</u>	+0.36v.	pH 6.2 to 7.7 pure prep.	dyestuff	123
? (c type?)	Bacteria	+0.280v.	pH 7.0	potentiometric	124
b	Heart muscle	-0.04v.	pH 7.4, muscle extract	dyestuff	40

Cytochrome	Source	Potential	Conditions	Technique	Reference
b	Heart muscle	+0.077v.	pH 7.0, 25°C Keilin-Hartree particles	dyestuff	125
b	Beef heart	-0.34v.	pH 7.0, pure preparation	dyestuff	126
b	Heart muscle	-0.05v.	?	potentiometric	127
b	Wheat roots	+0.14v. to +0.17v.	?	?	22
b ₁	<u>Escherichia</u> <u>coli</u>	-0.34v.	pH 7.0, crystalline	dyestuff	128
b ₁	<u>Escherichia</u> <u>coli</u>	-0.01v. to -0.016v.	pH 7.0, crude preparation	dyestuff	128
b ₃	pea leaves	+0.04v.	pH 7.0	?	22
b ₅	Pig liver	-0.014v.	pH 6.5, pure preparation	dyestuff	129
b ₅	Rabbit liver	+0.02v.	pH 7.0, pure preparation	dyestuff	51
b ₅	Dog liver	-0.13v.	pH 7.5, crude liver prep.	dyestuff	130

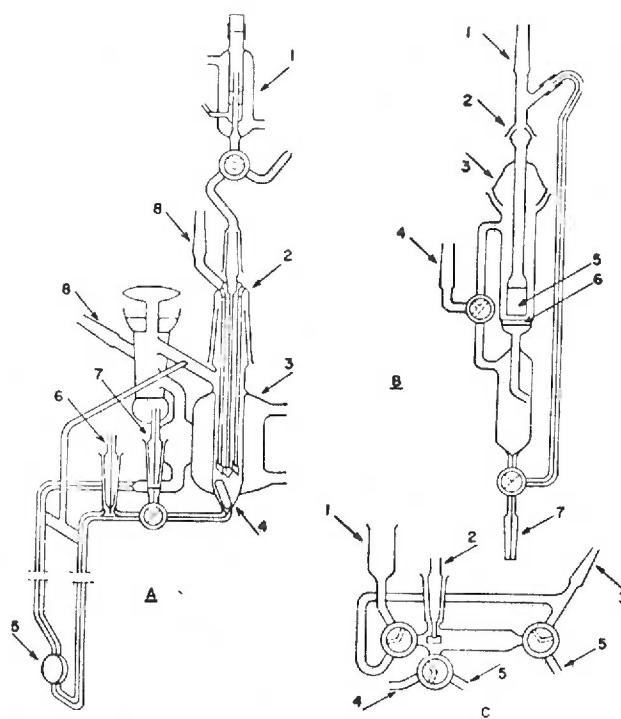
Cytochrome	Source	Potential	Conditions	Technique	Reference
b_5	Rat liver	-0.12v.	pH 7.0, microsomes	dyestuff	48
b_5	Beef liver	-0.14v.	pH 7.0, microsomes	dyestuff	131
b_5	Beef liver	+0.01v.	pH 7.0, lipase treatment of microsomes	dyestuff	131
b_5	Beef liver	-0.12v.	pH 7.0, micro-somal lipid added back to lipase treated microsomes	dyestuff	131
b_6	barley chloroplasts	-0.07v.	pH 7.0, in chloroplasts	dyestuff	132
b_7	spadix of <u>Arum maculatum</u>	-0.03v.	pH 7.0	?	22
a	Heart muscle	+0.29v.	pH 7.4, muscle extract	dyestuff	40
a	Beef heart	+0.26v.	pH 8.0, in cytochrome oxidase prep.	dyestuff	133

Cytochrome	Source	Potential	Conditions	Technique	Reference
cytochrome oxidase	Beef heart	+0.285v.	pH 7.4	dyestuff	135
o	<u>Vitreoscilla</u>	+0.10v. (Fraction I) -0.09v. (Fraction II)	pH 7.0, both purified fractions	dyestuff	136
f	<u>Petroselinum sativum</u> (parsley)	+0.365v.	pH 6.0 to 7.7, pure prep.	dyestuff	137
cyt-554 (f type?)	<u>Anacystis nidulans</u> (algae)	+0.35v.	pH 7.0, pure preparation	dyestuff	121
Cytochrome P-420	Rabbit liver	-0.020v.	pH 7.0, partially pure prep.	dyestuff	70
cyt-554 (? type)	<u>Pseudomonas aeruginosa</u>	+0.225v.	pH 7.0, pure preparation	dyestuff	117
?	<u>Chromatium</u>	-0.040v.	pH 7.0, pure preparation	dyestuff	138
RHP	<u>Rhodospirillum rubrum</u>	-0.008v.	pH 7.0, pure preparation	dyestuff	139
RHP	<u>Chromatium</u>	-0.005v.	pH 7.0, pure preparation	dyestuff	109

FIG. 10

APPARATUS USED FOR OXIDATION-REDUCTION POTENTIAL
DETERMINATION OF HORSERADISH PEROXIDASE

According to Harbury (95)



A, apparatus for oxidation-reduction titrations; (1), water-jacketed calomel half cell; (2), electrode assembly, consisting of two gold-plated platinum electrodes and a saturated potassium chloride salt bridge suspended from the outer member of a 24/40 standard taper joint; (3), water-jacketed electrode vessel, 16 mm. inside diameter; (4), Pyrex-sheathed bar driven magnetically; (5), fused absorption cell for spectrophotometry; (6), connection to modified Rheberg microburette, 10/30 standard taper joint; (7), connection to vessel used in reduction with hydrogen and a platinized asbestos catalyst (B) or to vessel for deaeration of solutions (not shown), capillary 10/30 standard taper joint; (8), connection to gas supply or exit trap, 10/30 standard taper joint. B, accessory for reduction of solutions with hydrogen in the presence of a platinized asbestos catalyst; (1), entrance for gas, 10/30 standard taper joint; (2), 12/5 ball and socket joint; (3), 35/20 ball and socket joint; (4), to vacuum pump or to exit trap, 10/30 standard taper joint; (5) extra coarse fritted glass cylinder; (6), ultrafine fritted glass plate; (7), 10/30 capillary standard taper, inserted in A, 7. C, hydrogen electrode vessel of Clark (11), modified; (1), entrance for the sample; (2), electrode, inserted via 10/30 standard taper joint; (3), gas inlet, 10/30 standard taper joint; (4), saturated potassium chloride salt bridge; (5), exit for liquid and gas.

cytochromes is the difference found between purified and naturally-occurring forms. This is especially true for membrane-bound cytochromes, of which cytochrome b is the best example. The potential in crude heart muscle of cytochrome b is -0.04v. at pH 7.4 (40), although recently a value as high as $+0.077\text{v.}$ at pH 7.0 has been reported for cytochrome b in a particle system (125). The potential of 60-fold purified cytochrome b has also been determined. This preparation could not be reduced by mitochondrial dehydrogenases; its redox potential as determined by the dyestuff technique was found to be -0.340v. at pH 7.0. Upon addition of mitochondrial structural protein the potential was raised to near zero (126). This demonstrates clearly that the potential of a cytochrome in its natural environment and in a purified state can be vastly different, indicating that changes in ligands or heme geometry have taken place.

The redox work on hemoproteins most pertinent to the experiments described in this thesis, is the previous work carried out on microsomes and microsomal components. In 1951, Yoshikawa showed that cytochrome b₅ (called cytochrome b' by Yoshikawa) in a dog liver preparation had an E'_0 of -0.13v. at pH 7.5 (130). These results were obtained by placing the enzyme preparation and an oxidation-reduction dyestuff together in a test tube, layering the mixture with liquid paraffin to prevent oxygen from diffusing in, and adding sodium dithionite dropwise until the absorption band of reduced

cytochrome b_5 appeared. The color of the dye mixture was then compared with standard mixtures of oxidized and reduced dye. This procedure was carried out with a number of redox dyestuffs to obtain the potential. In 1952, Strittmatter and Ball used much the same technique on a preparation of rat liver microsomes. They obtained an E'_0 of -0.12v. at pH 7.0 for the same pigment (48). Pappenheimer and Williams subsequently named this pigment cytochrome b_5 (50). In 1956, Strittmatter and Velick isolated cytochrome b_5 from rabbit liver microsomes, and found that it had a standard redox potential of $+0.02\text{v.}$ at 7.0 using a dyestuff technique under anaerobic conditions (51). They also showed that the stoichiometry of the reduction of cytochrome b_5 indicated that it was a one electron donor and acceptor. Raw et al., in 1958, determined the E'_0 of a partially purified cytochrome preparation from pig liver using the dyestuff technique and found -0.014v. at pH 6.5 (129). Kawai et al., in 1962, resolved the discrepancy in potential between the microsomal bound and purified cytochrome b_5 by showing that the E'_0 is -0.14v. at pH 7.0 in beef liver microsomes, but becomes $+0.01\text{v.}$ at pH 7.0 upon lipase treatment of the microsomes. Lipase treatment disrupts the microsomes, releasing cytochrome b_5 from its lipoprotein environment. Addition of microsomal lipid lowers the potential back to -0.12v. at pH 7.0 (131). This demonstrates that the potential of cytochrome b_5 is also dependent on its environment. Note that the

Etioporphyrin	$C_{22}H_{18}N_4$	4 CH_3 (methyl)	4 C_2H_5 (ethyl)		4 M, 4 E
Mesoporphyrin	$C_{24}H_{20}O_4N_4$	4 CH_3	2 C_2H_5 (ethyl)	2 $CH_2CH_2CO_2H$ (propionic acid)	4 M, 2 E, 2 P
Protoporphyrin	$C_{34}H_{26}O_4N_4$	4 CH_3	2 $CH = CH_2$ (vinyl)	2 $CH_2CH_2CO_2H$	4 M, 2 V, 2 P
Deuteroporphyrin	$C_{30}H_{20}O_4N_4$	4 CH_3	2 H	2 $CH_2CH_2CO_2H$	4 M, 2 H, 2 P
Hematoporphyrin	$C_{34}H_{26}O_4N_4$	4 CH_3	2 $CH(OH)CH_3$ (hydroxyethyl)	2 $CH_2CH_2CO_2H$	4 M, 2 EOH, 2 P
Coproporphyrin	$C_{36}H_{28}O_4N_4$	4 CH_3	—	4 $CH_2CH_2CO_2H$	4 M, 4 P
Uroporphyrin	$C_{40}H_{30}O_6N_4$	—	—	$\begin{cases} 4 CH_2CH_2CO_2H \\ 4 CH_2CO_2H \text{ (acetic acid)} \end{cases}$	4 AC, 4 P

becomes stabilized and more positive redox potentials will be found. The inductive effect of porphyrin side chains is important because the porphyrin ring is highly conjugated (Fig. 1). The inductive properties of the side chains are easily transmitted throughout this highly resonant system to the central iron atom. As seen in Falk's book, the potentials of protoporphyrin and hematoporphyrin are higher than those of the other iron porphyrins with less strong electron attracting side chains (Table 5) (28).

Falk and Perrin have pointed out that while the porphyrin side chains of cytochromes c (mesoporphyrin), b (protoporphyrin), and a (heme a) increase in electron-attracting power in that order, there is no correlation in increasing redox potential (30). From this it seems clear that there are other factors which control the redox potentials of heme proteins. The factors which must be examined are the protein moieties, and for those heme proteins which occur in a highly organized membrane (such as cytochrome P-450), the membrane structure. But effects of the protein moieties are specific for each hemoprotein and it is extremely difficult to find any general pattern which can be applied to model systems as a test.

Iron porphyrin complexes bind two ligands out of the heme plane, one above and one below, assuming octahedral symmetry. When considering the influence on redox potentials of addition of one or two extra ligands onto an iron porphyrin, whether these ligands

TABLE 5

INFLUENCE OF SIDE CHAINS ON IRON-PORPHYRIN REDOX
POTENTIALS

According to Falk (28)

Ferro- porphyrin	Side-chains at positions			pK_3 of porphyrin methyl ester (cf. Table 2, p. 28)	E^0 (mV) of complexes*		
	2	4	8		(Pyridine) ₂ pH 9.6	(γ -Picoline) ₂ pH 9.6	(CN ⁻) ₂ pH 9.6
Meso-	C ₂ H ₅	C ₂ H ₅		5.8	-63		-229
Copro-	CH ₂ CH ₂ COOCH ₃	CH ₂ CH ₂ COOCH ₃		5.5	-36		-247
Aetio-		all alkyl			-29		
Haemato-	CHOHCH ₃	CHOHCH ₃			+4		
Proto-	CH=CH ₂	CH=CH ₂		4.8	+15	-99	-200
Chlorocruoro-	CHO	CH=CH ₃		3.7	+137	-33	-183
Haem <i>a</i>	CHOHCH ₂ R	CH=CHR	CHO	3.4***	+246	-10	-113
					+288		

arise from the protein moiety of a hemoprotein or from other sources, one must consider the effect that these ligands have on the electronic structure of the iron porphyrin chelate.

A transition metal, such as iron, has five 3d orbitals, designated the $d_{x^2-y^2}$, d_z^2 , d_{xy} , d_{xz} , and d_{yz} orbitals. The $d_{x^2-y^2}$ orbital has the probability distribution of its electron density in porphyrins pointing toward the four pyrrole nitrogen atoms while the electron density of the d_z^2 orbital lies perpendicular to the plane of the porphyrin ring. The electron density of the d_{xy} orbital also lies in the plane of the porphyrin, while the electron density of the d_{xz} orbital lies between the x and z axes and that of the d_{yz} orbital lies between the y and z axes. The $d_{x^2-y^2}$ and d_z^2 orbitals may form coordinate or σ (sigma) bonds if they are not already filled with metal electrons. Sigma bonds have their greatest electron density along the internuclear axis between the iron atom and the ligand. The d_{yz} , d_{xy} , and d_{xz} orbitals may overlap with vacant π (pi) orbitals of the ligand atom if they are occupied by metal electrons (28). The electron density of pi bonds lies in some other direction than that of the internuclear axis. Ferric iron has five 3d electrons which can be arranged in two different ways when an octahedral complex is formed. The electrons may be all unpaired in the presence of so-called weak field ligands, giving rise to a high spin complex. In the case of ferric iron one unpaired electron is found in each of the

above iron orbitals. A weak field ligand causes a small energy difference to exist between the sigma bonding and pi bonding orbitals of the iron. Because this splitting is small the electrons distribute themselves in all of the 3d orbitals (143). If the ligand is of the strong field type, the electrons are forced to pair up as much as possible in the pi bonding orbitals and a low spin complex is formed. In the case of ferric iron two electron pairs are found in two pi bonding orbitals, the fifth 3d electron being in the other pi bonding orbital (143). A strong field ligand causes a large splitting between energy levels of the sigma and pi bonding orbitals. Pi bonding orbitals are of lower energy than sigma bonding orbitals and the iron 3d electrons are forced to pair up in them (144). From a purely electrostatic standpoint, an anion such as fluoride which has a high electronegativity will favor the more oxidized form of a hemoprotein and the potential will be lower than if water were the ligand. But fluoride is a weak field ligand which tends to give a high spin hemoprotein, and for this reason it will not lower the potential as much as a strong field ligand will; that is, one which has a strong electron donating power. So while electrostatic effects are important, it is more important to consider the electron donating power of the ligand attached to the iron porphyrin chelate. The greater the electron donating power of the ligand, the lower the potential of the chelate (28). On the other hand, electron attracting substituents would raise

the E'_O .

The standard redox potential of hemoproteins fall into the physiological range because of the electrostatic effect of pyrrole nitrogen atoms and the highly conjugated porphyrin system. The difference in potential between heme proteins can be understood in terms of two factors. The first is the effect of the different side chains on the porphyrin ring. While the inductive effect of these side chains is significant, it may be overshadowed in heme proteins by the addition of two more ligands to the fifth and sixth coordination positions of the iron. The electron donating ability of these ligands from the protein moiety or from other sources can have a great effect on the redox potential of a heme protein.

As the structure of more hemoproteins becomes known it will be possible to correlate redox information with structure and function. However, at this time, we can obtain some ideas from redox potential information as to the nature of the heme linkage in a cytochrome and also as to the function and mechanism of the redox reaction in which the cytochrome is involved.

II. EXPERIMENTAL

1. Materials

A. Chemicals

All water used was quartz distilled and deionized by passage through a Barnstead standard mixed-bed ion exchange column; it had a conductance of 1 to 2 μ mho.

All buffers were prepared according to Gomori (145). Sodium phosphate buffer salts (reagent grade) were obtained from Merck & Co., Inc., as was sodium citrate (reagent grade). Potassium chloride (reagent grade) was obtained from the J. T. Baker Chemical Co.. Sucrose (reagent grade) was obtained from Allied Chemical Co.. Potassium chromate (reagent grade) was obtained from Matheson Coleman, & Bell Inc..

NADPH (95-99% purity) and FMN (commercial grade) were obtained from Sigma Chemical Company. Catalase (20,000 EU/mg.) was obtained from Calbiochem Corp., while glucose oxidase (30,000 glucose oxidase units/gm.) was obtained from Nutritional Biochemicals Corporation.

Sodium phenobarbital was obtained from The Vitarine Co., Inc..

Prepurified nitrogen (less than 8 ppm O₂) and prepurified

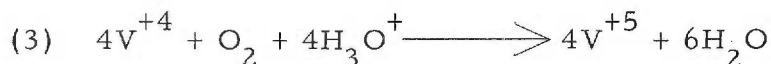
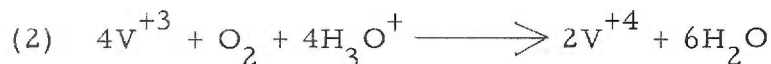
hydrogen (less than 10 ppm O_2) were obtained from Industrial Air Products. Carbon monoxide (99.5% min.) was obtained from Matheson Co., Inc..

Platinum asbestos was prepared by dissolving one gram of chloroplatinic acid in 15 ml. of water and then adding 2 ml. of formalin to this mixture. Nine grams of acid washed asbestos were ground into a fine powder with a mortar and pestle. The asbestos and the chloroplatinic acid solution were mixed together and stirred well. Seven ml. of 20% NaOH was added drop-wise to the asbestos mixture with mixing while the asbestos was cooled in ice. The mixture was kept at room temperature for 12 hours and then washed with 50 ml. 2.5% HCl. The platinum asbestos was then washed with H_2O , dried, and finely ground with a mortar and pestle (146).

Grease used for lubrication of all ground joints and stopcocks in anaerobic experiments was Lubriseal, distributed by Arthur H. Thomas Company. This grease is easily removed by carbon tetrachloride.

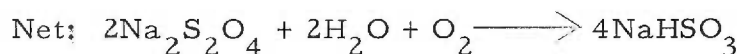
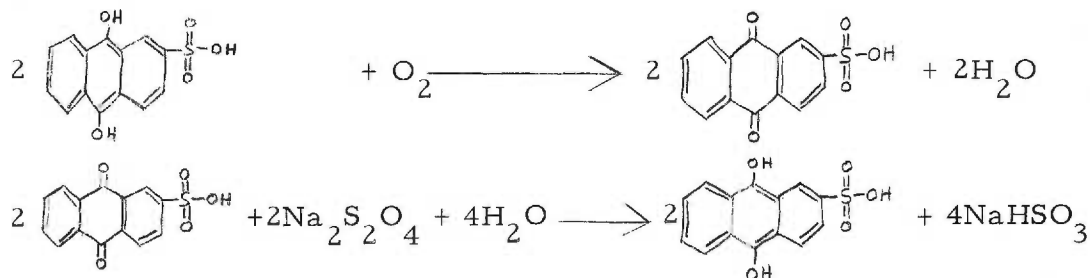
Vanadyl sulfate (purified) was obtained from Fisher Scientific Company and mossy zinc (reagent grade) was obtained from Matheson, Coleman and Bell. Two hundred and fifty ml. of a 0.1M solution of vanadyl sulfate was placed over 100 grams of amalgamated zinc in each gas bottle. The amalgamated zinc was prepared by mixing 100 grams of mossy zinc with 150 ml. water, 10 ml. concentrated

HCl, and 10 grams mercuric chloride for 5 minutes and then washing the amalgamated zinc with water (147). A solution of vanadous sulfate over amalgamated zinc is an excellent oxygen scavenger:



Note that in this system both the vanadic (V^{+3}) and the vanadite (V^{+4}) ions serve as oxygen scavengers (147).

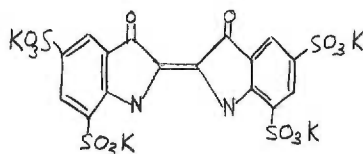
Anthraquinone-2-sulfonic acid (sodium salt, research grade) was obtained from Aldrich Chemical Company. Fieser's reagent was prepared by adding 20 grams KOH to 100 ml. H_2O . Two grams of sodium anthraquinone-2-sulfonate and 15 grams of sodium hyposulfite ($\text{Na}_2\text{S}_2\text{O}_4 \cdot 2\text{H}_2\text{O}$) were then added to the warm KOH solution. The mixture was stirred and was ready to use when cool (148). Fieser's reagent is also a good oxygen scavenger and was used to remove oxygen from carbon monoxide because carbon monoxide chelates with vanadyl sulfate.



As can be seen from the equations the system is limited by the amount of sodium dithionite present (148). As with all gas scrubbers, efficiency of this system is a function of the rate at which the gas passes through the reagent.

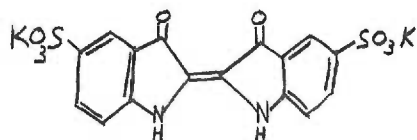
B. Oxidation-Reduction Dyestuffs

Indigotetrasulfonic acid (potassium salt, 95-99% pure):



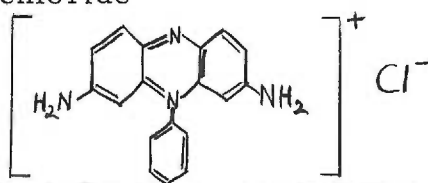
was obtained from K & K Laboratories, Inc.. The E'_O of indigotetrasulfonate is -0.46v. at pH 7.0 (149). The shape of the absorption curve of the K & K dyestuff fit very well the reported curve (150), however, the reported absorption maximum for indigotetrasulfonate is 590 m μ while the K & K dyestuff had its maximum absorption at 600 m μ (Fig. 11). The reported extinction coefficient of indigotetrasulfonate is $8.6 \times 10^2 \text{ M}^{-1} \text{ cm}^{-1}$ at 590 m μ when dissolved in water (150). The extinction coefficient at 600 m μ of the K & K dyestuff was found to be $1.1 \times 10^3 \text{ M}^{-1} \text{ cm}^{-1}$ when dissolved in 0.1 M phosphate buffer, pH 7.0. Indigotetrasulfonate is blue in the oxidized form and colorless in the reduced form. It is a two-equivalent redox indicator..

Indigodisulfonic acid (sodium salt, 94% pure):



was obtained from National Aniline Corporation. The E'_O of indigodisulfonate is -0.125v. at pH 7.0 (149). The shape of the absorption curve of the National Aniline dyestuff fit very well the reported curve (150). However, the reported absorption maximum for indigodisulfonate is $608\text{ m}\mu$ while the National Aniline dyestuff had its maximum absorption at $615\text{ m}\mu$ (Fig. 11). The reported extinction coefficient of indigodisulfonate at $608\text{ m}\mu$ is $1.28 \times 10^3\text{ M}^{-1}\text{ cm}^{-1}$ when dissolved in water (150). The extinction coefficient of the National Aniline indigodisulfonate was found to be $1.20 \times 10^3\text{ M}^{-1}\text{ cm}^{-1}$ at $615\text{ m}\mu$ when dissolved in 0.1 M phosphate buffer pH 7.0. Indigodisulfonate is blue in the oxidized state and colorless in the reduced state. It is a two-equivalent redox indicator.

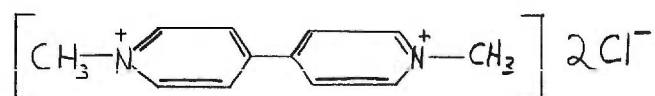
Phenosafranine chloride



was obtained from British Drug Houses (BDH) Ltd.. It has an E'_O of -0.267v. at pH 7.0 according to the suppliers. The reported E'_O for phenosafranine is -0.252v. at pH 7.0 (151). The shape of the absorption curve of the BDH phenosafranine fit the reported curve (152). The reported absorption maximum for phenosafranine lies between $517\text{ m}\mu$ and $525\text{ m}\mu$ (152, 153, 154). The absorption maximum

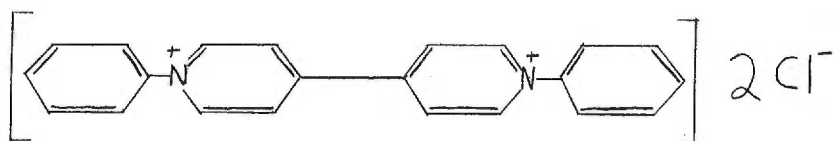
of the BDH phenosafranine is found to be 520 m μ (Fig. 12). The reported extinction coefficient for phenosafranine in water between 520 m μ and 522 m μ is $3.8 \times 10^4 \text{ M}^{-1} \text{ cm}^{-1}$ (152). The extinction coefficient of the BDH phenosafranine at 520 m μ was found to be $3.6 \times 10^4 \text{ M}^{-1} \text{ cm}^{-1}$ in 0.1 M phosphate buffer at pH 7.0. Phenosafranine is red in the oxidized form and colorless in the reduced form. It is a two-equivalent redox indicator.

Methyl viologen dichloride:



was obtained from Mann Research Laboratories, lot # S3534, and had an E'_0 of -0.440v. at pH 7.0 according to the suppliers. The reported E'_0 for methyl viologen is -0.440v. at pH 7.0 (155). The shape of the absorption curve of the Mann methyl viologen fit very well the reported curve (156). The reported absorption maxima for methyl viologen are 601 m μ and 570 m μ although the solvent is not given (156). The absorption maxima of the Mann methyl viologen were found to be 604.5 m μ and 570 m μ in 0.1 M phosphate buffer pH 7.0 (Fig. 13). No extinction coefficient has been reported for methyl viologen. Methyl viologen is colorless in the oxidized form and blue in the reduced form. It is a one-equivalent redox indicator.

Benzyl viologen dichloride:



was obtained from Mann Research Laboratories, lot # R2829, and had an E'_0 of -0.314v. at pH 7.0 according to the suppliers. The reported E'_0 for benzyl viologen is -0.359v. at pH 7.0 (155), although it was not possible to obtain a sample with an E'_0 lower than -0.314v. The shape of the absorption curve of the Mann benzyl viologen fit very well the reported curve (156). The reported absorption maxima for benzyl viologen are $598\text{ m}\mu$ and $555\text{ m}\mu$ although the solvent is not given (156). The absorption maxima of the Mann benzyl viologen were found to be $597\text{ m}\mu$ and $555\text{ m}\mu$ in 0.1 M phosphate buffer pH 7.0 (Fig. 13). No extinction coefficient has been reported for benzyl viologen. Benzyl viologen is colorless in the oxidized form and purple in the reduced form. It is a one-equivalent redox indicator.

C. Microsomes

All microsomes used in this thesis were prepared from rabbit liver. New Zealand White rabbits weighing 4 to 6 pounds were used. Each rabbit received a dose of 0.13 gram phenobarbital per day, injected intraperitoneally for five days. The rabbits were then starved for 24 hours to reduce liver glycogen and were sacrificed by

FIG. 11a

REPORTED ABSORPTION SPECTRA FOR INDIGODISULFONATE
AND INDIGOTETRASULFONATE

Curve A: (solid line) Indigodisulfonate, 6.5×10^{-5} M in water.
Absorption maximum = 610 m μ .

Curve B: (dashed line) Indigotetrasulfonate, 1.32×10^{-4} M in water.
Absorption maximum = 590 m μ .

According to Holmes (150)

FIG. 11b

ABSORPTION SPECTRA OF INDIGO SULFONATES USED IN REDOX
EXPERIMENTS

Curve A: (solid line) National Aniline Indigodisulfonate, 8.2×10^{-4} M in 0.1 M phosphate buffer, pH 7.0. Absorption maximum = 615 m μ .

Curve B: (dashed line) K & K Indigotetrasulfonate, 9×10^{-4} M in 0.1 M phosphate buffer, pH 7.0. Absorption maximum = 600 m μ .

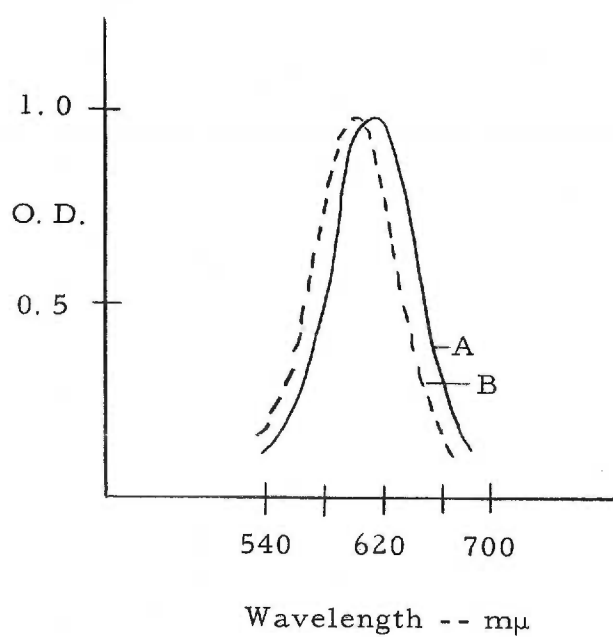
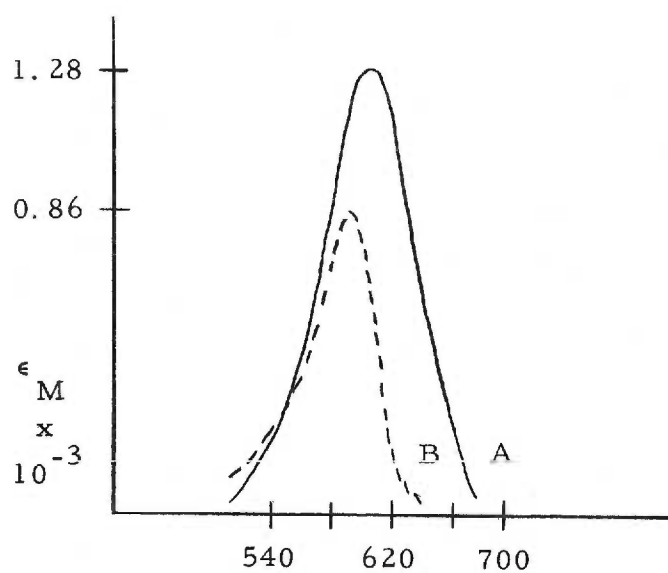


FIG. 12a

REPORTED ABSORPTION SPECTRUM FOR PHENOSAFRANINE

Same curve found for 1.16×10^{-5} M and 2.90×10^{-4} M phenosafranine in water. Absorption maximum = 520-522 m μ .

According to Michaelis and Granick (152)

FIG. 12b

ABSORPTION SPECTRUM OF PHENOSAFRANINE USED IN REDOX EXPERIMENTS

BDH phenosafranine, 2.2×10^{-5} M in 0.1 M phosphate buffer pH 7.0, absorption maximum = 520 m μ .

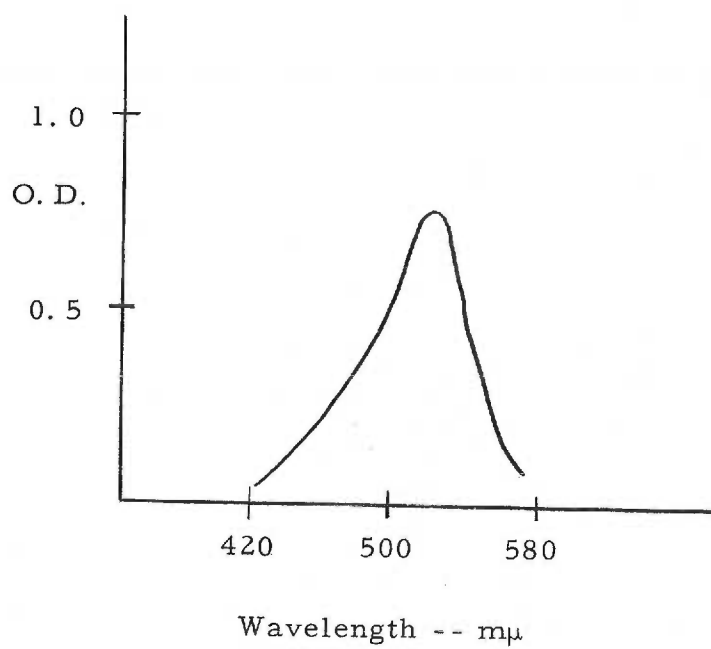
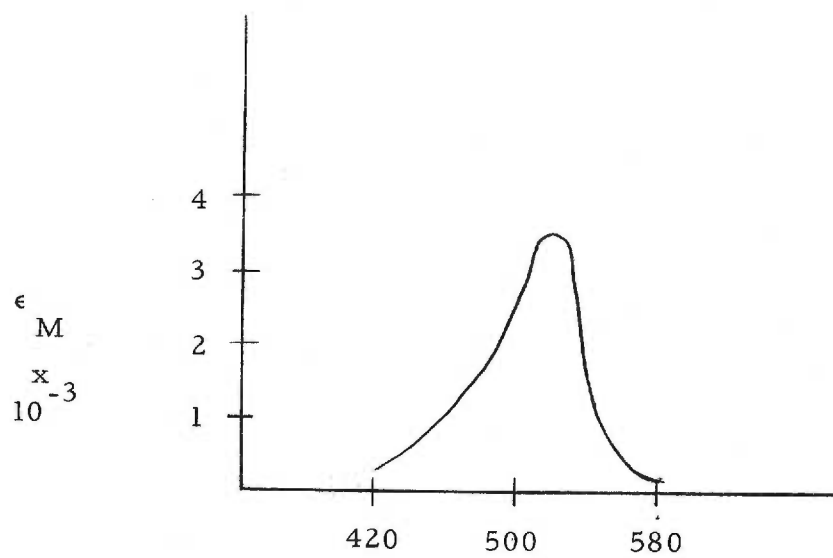


FIG. 13a

REPORTED ABSORPTION SPECTRA FOR METHYL VIOLOGEN AND BENZYL VIOLOGEN

Curve A: Benzyl Viologen, absorption maxima - 598 m μ and 555 m μ .

Curve B: Methyl Viologen, absorption maxima - 601 m μ and 570 m μ .

Information about concentration, pH, and solvent not given.

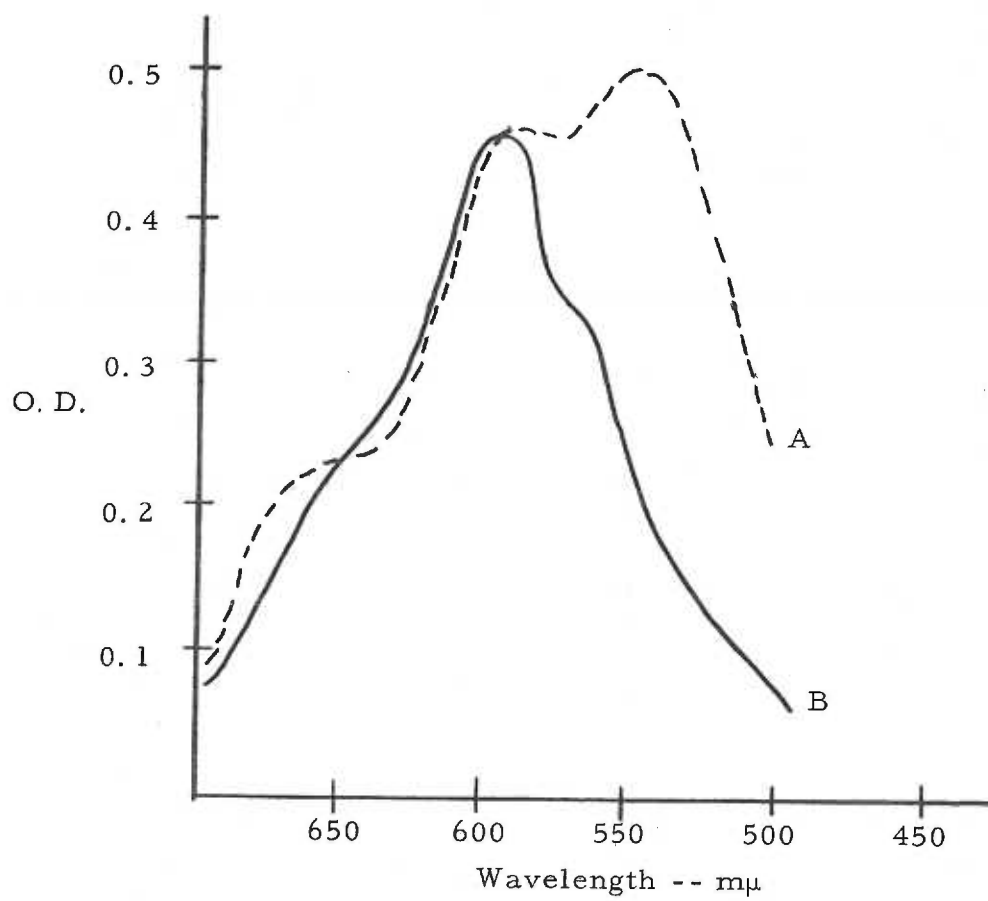
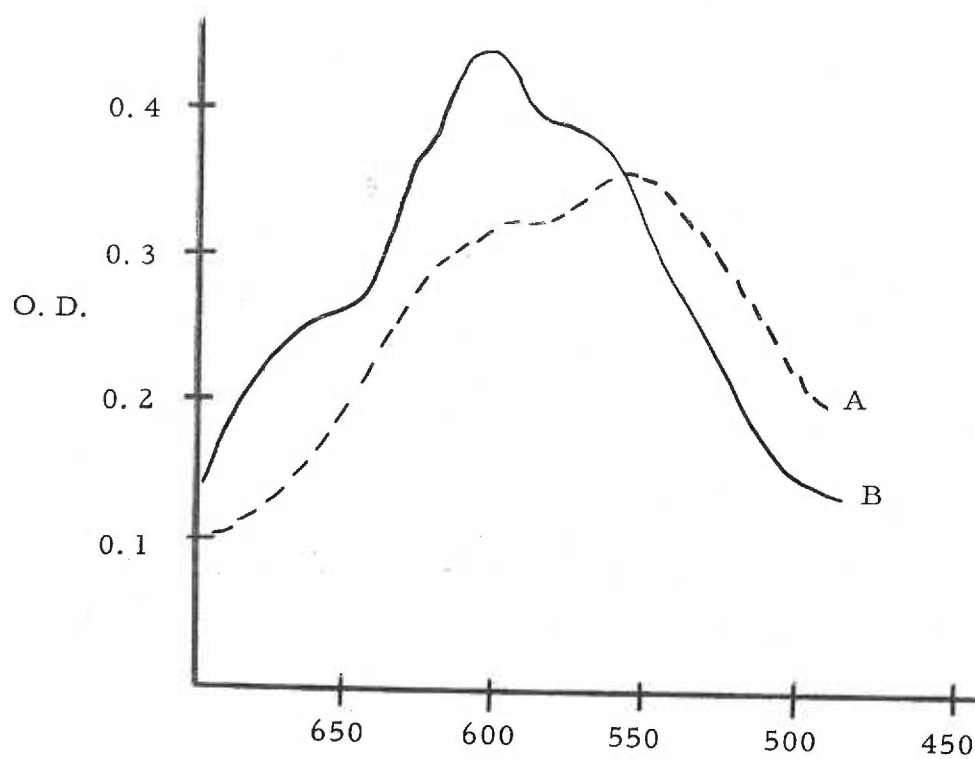
According to Michaelis and Hill (155)

FIG. 13b

ABSORPTION SPECTRA OF VIOLOGEN DYESTUFFS USED IN REDOX EXPERIMENTS

Curve A: Mann benzyl viologen, absorption maxima - 597 m μ and 555 m μ , 1.33×10^{-4} M; solvent, 0.1 M phosphate buffer, pH 7.0.

Curve B: Mann methyl viologen, absorption maxima - 604.5 m μ and 570 m μ , 0.99×10^{-4} M; solvent, 0.1 M phosphate buffer, pH 7.0.



producing air embolism. The livers were removed and placed in cold 0.25 M sucrose. All preparative steps were carried out at 4°C.

The livers were perfused immediately with 0.25 M sucrose, through the hepatic vein, to remove the hemoglobin. The tissue was then weighed, diced, and homogenized in a Potter-Elvehjem homogenizer with 3 volumes of 0.88 M sucrose (3 ml./gram liver). The supernatant obtained after centrifugation at 9000xg for 25 minutes, to remove mitochondria, nuclei, and cell debris, was diluted with 5 volumes of 0.04 M KCl. This was centrifuged at 59,000xg for 60 minutes. The sediment was then homogenized with 0.1 M phosphate buffer, pH 7.0, and centrifuged at 144,000xg for 60 minutes. The sediment was then suspended in 0.1 M phosphate buffer, pH 7.0, and frozen.

This microsome preparation, as described in Fig. 14, is a modification of the method of Mason et al. (2). All microsome preparations used consisted of a mixture of rough and smooth microsomes. The assistance of Annette Johnson and Nancy Avedovech in the preparation of microsomes is gratefully acknowledged.

The heme content of rabbit liver microsomes after phenobarbital induction is reported to be 4.38 ± 0.26 $\mu\text{moles/mg. protein}$. Cytochrome b_5 content is found to be 1.09 ± 0.05 $\mu\text{moles/mg. protein}$, cytochrome P-450 content is found to be 2.64 ± 0.26 $\mu\text{moles/mg. protein}$, and microsomal Fe_x content is found to be 2.17 ± 0.25

mμmoles/mg. protein. The copper content is found to be 0.44 ± 0.13 mμatoms/mg. protein and the total iron content is found to be 6.83 ± 0.33 mμatoms/mg. protein (49).

FIG. 14

SCHEMATIC REPRESENTATION OF RABBIT LIVER MICROSOME
PREPARATION

This preparation gives a mixture of rough and smooth microsomes.

After Mason et al. (2)

LIVER

PERFUSED WITH
0.25 M SUCROSE
WEIGHED
DICED
HOMOGENIZED
WITH 3 VOLUMES
0.88 M SUCROSE
CENTRIFUGED $9000 \times g$
25 MIN

SEDIMENT
DISCARD

SUPERNATANT
DILUTED WITH 5
VOLS. 0.04M KCL
CENTRIFUGED
 $59,000 \times g$ 60 MIN

SEDIMENT [MICROSOMES]
HOMOGENIZED WITH
0.1M $\text{PO}_4^{=}$ BUFFER, pH 7.0
CENTRIFUGED $144,000 \times g$
60 MIN

SUPERNATANT
DISCARD

SEDIMENT [MICROSOMES]
SUSPENDED IN 0.1M
 $\text{PO}_4^{=}$ BUFFER, pH 7.0
FROZEN

SUPERNATANT
DISCARD

2. Equipment

All pH determinations and titrations were carried out with a Radiometer TTT1 pH meter. A Beckman standard buffer solution pH 7.0 and a Matheson, Coleman and Bell standard buffer solution pH 4.0 were used to standardize the instrument.

Titration were carried out with an Agla micrometer syringe. The syringe had a capacity of 0.5 ml. and 0.01 ml. could be measured within 0.5 μ l..

Spectrophotometric measurements were made with a Cary model 14 recording spectrophotometer equipped with a model 1462 scattered transmission attachment and a model 1471200 light source. A Sylvania 620 watt DWY lamp was used. An RCA #6217 photomultiplier (range: 4000 \AA to 8000 \AA) was used as detector. A Zeiss PMQII spectrophotometer was used for NADPH, FMN, and some dyestuff concentration determinations.

Electron spin resonance spectroscopy was carried out with a Varian model V4500 EPR spectrometer with 100 kc field modulation and a Fieldial VFR 2200 magnetic field regulator. A circulator of the design of R. Sands and R. Hansen was used to control the incident microwave power (157).

A Cenco Hyvac vacuum pump (Type S-5-AF) was used for evacuations.

3. Procedures

A. Quantitative ESR

Electron spin resonance (ESR) is a technique for detecting unpaired electrons and for studying the interaction of these electrons with their surroundings (158). An electron is a spinning charge which has a magnetic moment. If the electron is placed in an external magnetic field, its magnetic moment can have two orientations, one parallel and one antiparallel to the magnetic field. The antiparallel orientation corresponds to the higher energy level (159). If energy is fed into the system, the gap between two energy levels is equal to the product of the frequency of the incident radiation (ν) and Planck's constant (h) (155):

$$\Delta E = h\nu$$

The energy gap is a function of the applied magnetic field, H :

$$h\nu = \Delta E = XH$$

X is a constant including the Bohr magneton (β) and the spectroscopic splitting factor (g) (154):

$$h\nu = g\beta H$$

In ESR, ν is the frequency of microwave radiation used as incident radiation and g is a measure of the contribution of the spin and orbital motion of the electron to its total angular momentum and is characteristic of each unpaired electron. For the completely free spin,

indigotetrasulfonic acid, and the initial technique of reducing and handling the dyestuff were based on the work of Strittmatter and Velick (54).

The development of the final procedure for determining the redox potential of microsomal Fe_x is given below. Reduction of microsomal Fe_x was found possible only with dyestuffs of lowest potential (methyl viologen and benzyl viologen). However, with each dyestuff tried it was necessary to establish whether any microsomal Fe_x reduction could be obtained. As lower potential dyestuffs were used, the effect of small amounts of oxygen became more pronounced and modification of the anaerobic technique became necessary with each dyestuff.

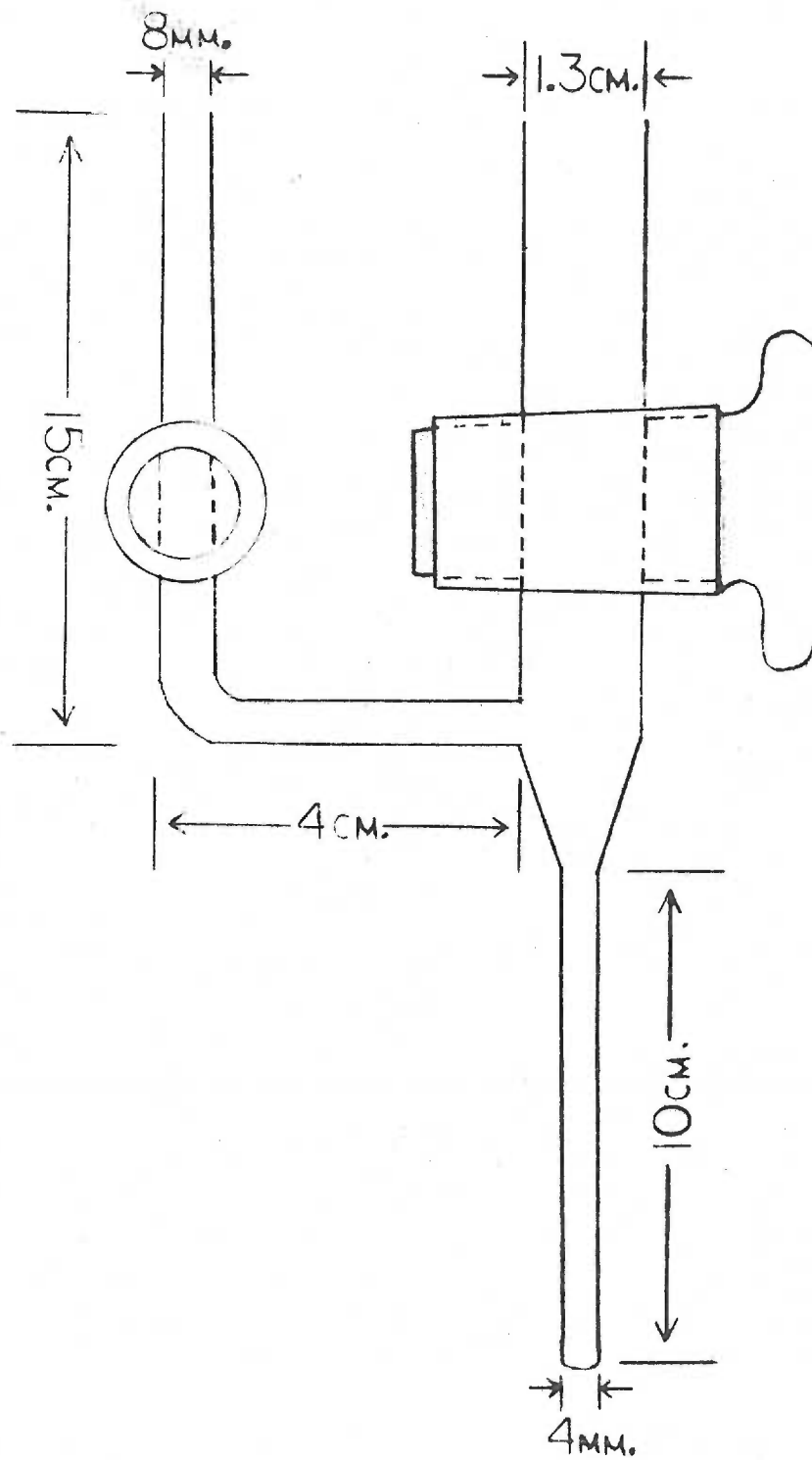
(1) Indigo Sulfonates

Microsomes (0.2 ml. of a 20 mg. protein/ml. preparation) were placed in an anerobic ESR tube (Fig. 15) with a three way stopcock attached to the side-arm and a serum stopper fitted over the large opening. A 5 ml. syringe, fitted with a long needle, was inserted through the stopper, the needle extending into the ESR tube. Palladium asbestos catalyst was placed in the syringe and the open end of the syringe barrel was closed with a serum stopper. The whole system was then evacuated and flushed with nitrogen which had been passed through vanadyl sulfate. After the last nitrogen flush,

FIG. 15

ANAEROBIC ESR TUBE USED IN REDOX POTENTIAL DETERMINATION OF MICROSOMAL Fe_x .

According to Beinert and Sands (164)



a stream of hydrogen was passed through the tube by using the three-way stopcock, and the serum stopper was removed from the top of the syringe. A solution of indigotetrasulfonate (2.5×10^{-3} M) was pipetted onto the catalyst and allowed to reduce. A Swinney filter adapter was placed between the syringe and the needle to remove the catalyst after reduction. Upon completion of dye reduction, the plunger was placed in the syringe and the reduced dye was added to the microsomes. Using this technique it was possible to obtain only about 50% reduced dyestuff in the ESR tube (Fig. 16). Curve A in Fig. 16 is the optical spectrum of reduced indigotetrasulfonate and microsomes. Curve B is the optical spectrum of the air oxidized mixture. This figure shows that only 50% reduction of dyestuff was obtained in the anaerobic ESR tube.

The next step was elimination of the threeway stopcock on the sidearm of the anaerobic ESR tube and use of hydrogen as the flush gas as well as for reduction. The hydrogen was passed over hot copper which is also an oxygen scavenger (165) before passage through the vanadyl sulfate gas train. A further anaerobic precaution was taken by purging the ESR tube with hydrogen overnight, the quartz ESR tube being heated by the copper furnace. By making these changes it was possible to obtain 80% reduced dyestuff when mixed with microsomes in the ESR tube. No microsomal Fe_x reduction was observed. (See Results, Fig. 23)

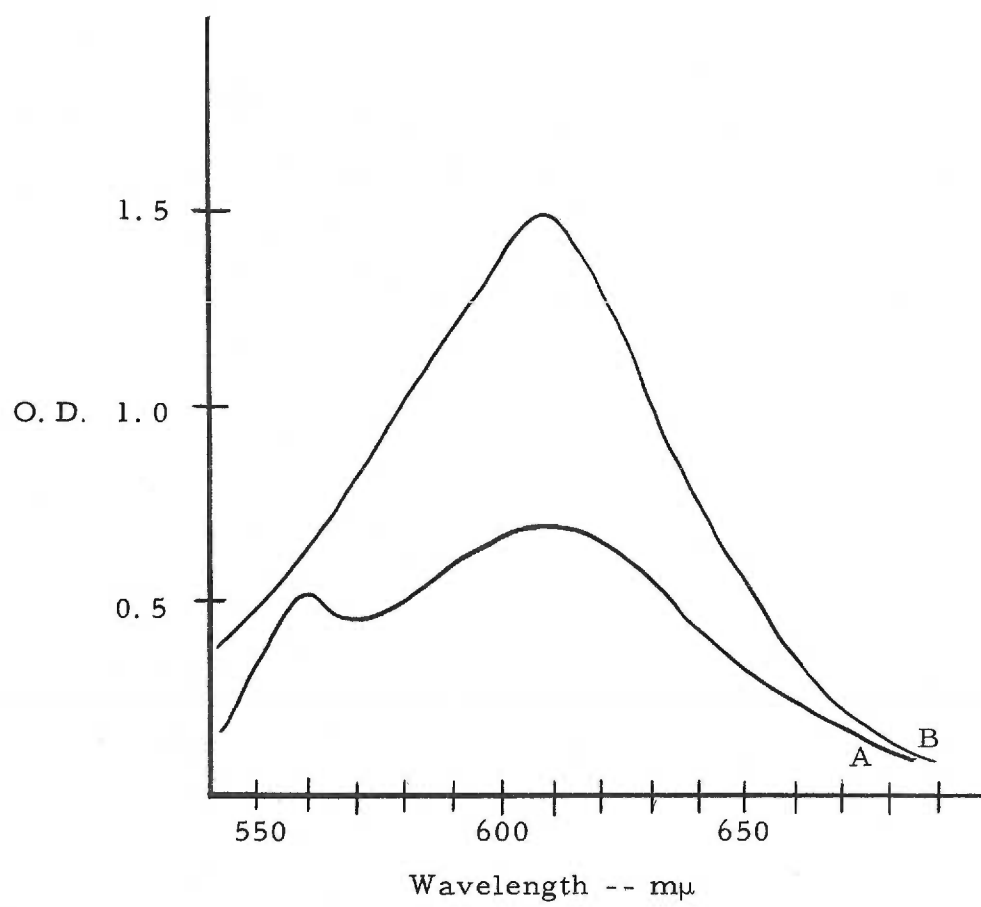
FIG. 16

50% REDUCED INDIGOTETRASULFONATE OBTAINED WITH
INITIAL ANAEROBIC TECHNIQUE

Absorption spectrum obtained from a mixture of microsomes (0.2 ml. of a 20 mg. protein/ml. preparation) and indigotetrasulfonate (2.5×10^{-3} M - before reduction).

Curve A is the reduced spectrum. Curve B is the air oxidized spectrum.

Note the peak at 558 m μ in Curve A. This corresponds to the α -peak of reduced cytochrome b₅ (54).



Cytochrome b_5 and dyestuff were measured spectrophotometrically at room temperature in the anaerobic ESR tube. A special cell holder designed to hold ESR tubes in the Cary scattered transmission attachment was used (Fig. 17). Microsomal Fe_x was observed at liquid nitrogen temperatures with the Varian ESR spectrometer.

The above procedure was also used with indigodisulfonate. No microsomal Fe_x reduction was obtained with this dyestuff either. (See Results, Fig. 24)

(2) Phenosafranine

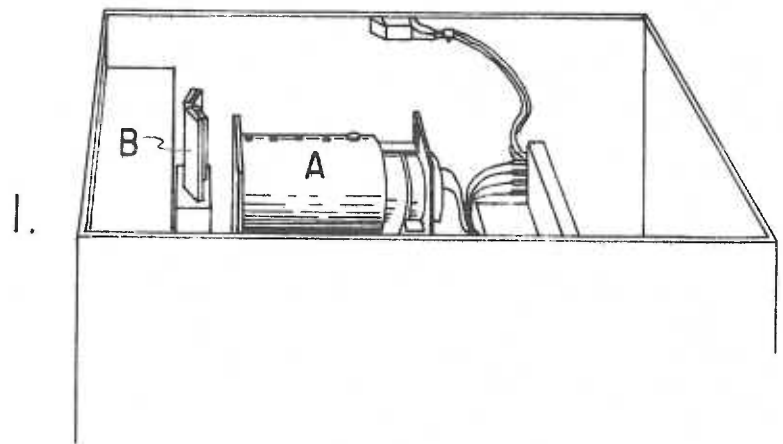
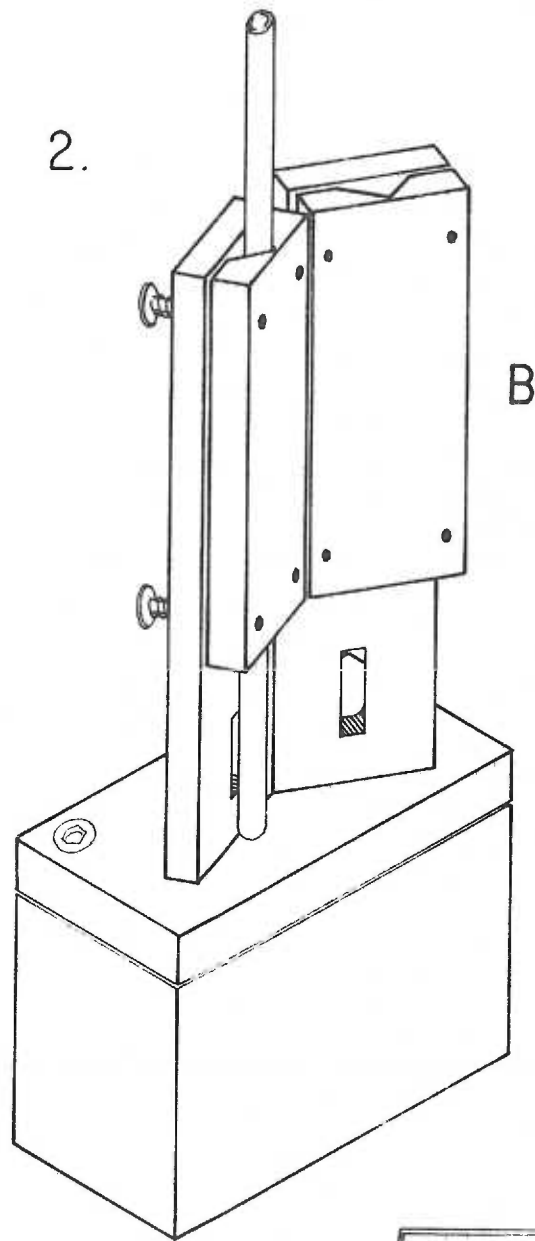
The procedure used with the indigo sulfonates was tried with phenosafranine. In this case the mixture of microsomes and reduced phenosafranine was titrated with potassium ferricyanide ($5 \times 10^{-4} M$), using an Agla micrometer syringe, through the same serum stopper used for the dyestuff addition. The initial phenosafranine concentration was $4.6 \times 10^{-3} M$. Even though about 60% of the reduced phenosafranine was oxidized upon mixing with the microsomes, there was some indication of reduction of microsomal Fe_x (see Results, Fig. 25).

In order to obtain a higher proportion of reduced microsomal Fe_x it was necessary to find a way of decreasing the amount of reduced phenosafranine oxidized upon mixing with the microsomes.

FIG. 17

ESR TUBE HOLDER FOR CARY SCATTERED TRANSMISSION
ATTACHMENT

- (1) Cary scattered transmission attachment.
 - A: large open-end photomultiplier
 - B: ESR tube holder
- (2) ESR tube holder (actual size).



This required modification of the anaerobic procedure. Previous anaerobic work with autoxidizable systems by Harbury (95), Ehrenberg (166, 167), and Minnaert (134) indicated that good results are obtained with a completely closed system. In such a system every operation must be carried out in an anaerobic environment, from reduction of the dyestuff to the observation of microsomal Fe_x .

To carry out the E'_0 determination of microsomal Fe_x in a closed system, it would be necessary to have a reduction chamber for the dye, a method of removing the catalyst from the reduced dye, an accurate buret for titration of the dye-microsome mixture, a way of moving the solutions into the sample cell, and a sample cell which could be used for both optical and ESR measurements.

A system which meets all the above requirements and still has as few joints and stopcocks as possible was constructed by Gunther Weiss from the author's design and is shown in Fig. 18. The procedure using this apparatus was to add 0.2 ml. of a microsome preparation (about 20 mg. protein/ml.) to the ESR tube and palladium asbestos catalyst to the reduction chamber. The whole apparatus, including the microsomes, was then evacuated and flushed with hydrogen ten times. Phenosafranine (1×10^{-3} M) was added to the reduction chamber against a hydrogen pressure and the reduction was carried out by bubbling hydrogen gas through the fritted disc at the bottom of the reduction chamber. Ferricyanide (4.9×10^{-3} M) was

FIG. 18

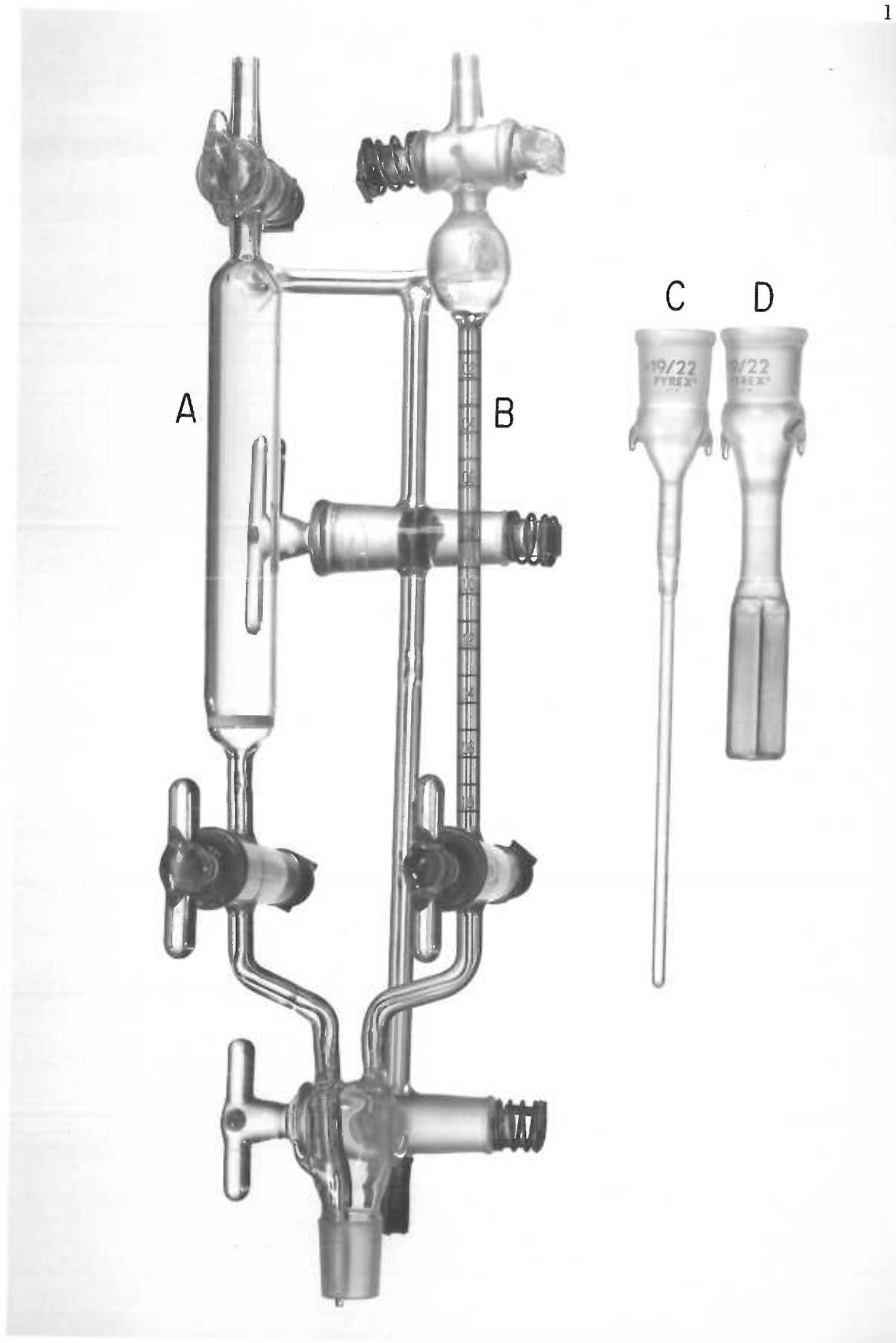
CLOSED SYSTEM USED FOR ANAEROBIC TITRATIONS

A: Reduction chamber

B: Buret

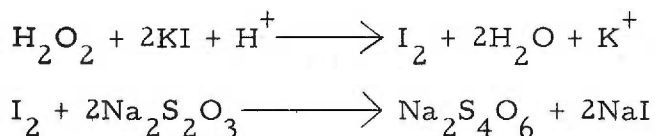
C: ESR attachment

D: Cuvette attachment



then added to the titration side of the apparatus and bubbled with hydrogen to remove dissolved oxygen. The reduced dye was added to the microsomes by changing the direction of the gas flow. This apparatus was also purged with hydrogen gas before use.

This technique did not appreciably decrease the amount of dye-stuff oxidation. One possible source of oxidizing equivalents was peroxidic oxygen in the microsomes. Peroxidic oxygen was estimated (see Results) in microsomes using the method of Skellon and Wills (168). This is a thiosulfate titration of iodine:



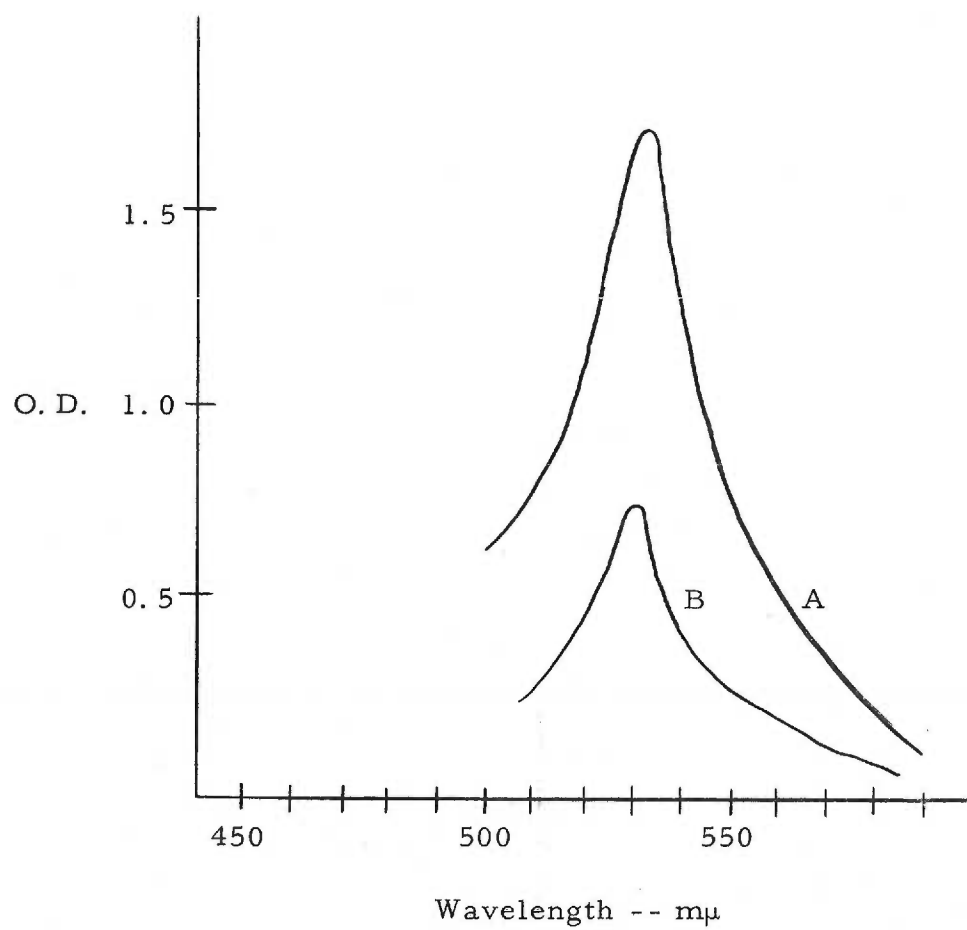
Another problem was that phenosafranine was being adsorbed onto the palladium asbestos catalyst during reduction (Fig. 19). Curve A of Fig. 19 shows the optical spectrum of a sample of phenosafranine before reduction with hydrogen and palladium asbestos. Curve B shows the optical spectrum of the same sample of phenosafranine after reduction and reoxidation by air. The decrease in absorption shows that a large amount of the dyestuff is adsorbed onto the asbestos during reduction.

The problem of dyestuff oxidation was solved in two ways. The initial concentration of phenosafranine was increased to 1×10^{-2} M and platinum asbestos was substituted for palladium asbestos as

FIG. 19

LOSS OF PHENOSAFRANINE UPON REDUCTION WITH
PALLADIUM ASBESTOS

Curve A was obtained before reduction. Curve B was obtained after reduction and reoxidation by air.
Initial dye concentration was 5×10^{-3} M.



catalyst. Platinum asbestos is a stronger catalyst than palladium asbestos and will reduce a dyestuff more quickly. The faster the phenosafranine was reduced the less opportunity there was for the dye to be adsorbed onto the asbestos.

These adjustments made it possible to add reduced phenosafranine to the microsomes and show that there was no reduction of microsomal Fe_x by this dyestuff (see Results, Fig. 26).

(3) Methyl Viologen

When the procedure used with phenosafranine was tried with methyl viologen, 40% reduction of microsomal Fe_x was observed as seen in Fig. 20. Curve A (5.5 cm.) in this figure shows the $g = 2.25$ ESR signal of microsomal Fe_x in the presence of hydrogen-reduced methyl viologen. Curve B (9.1 cm.) is the spectrum of the air oxidized sample and shows an increase of 40% in the signal height. The potential of methyl viologen is a bit lower than the potential of the hydrogen electrode at pH 7.0 and for this reason only partial reduction of dyestuff is possible using hydrogen gas and platinum asbestos. As discussed earlier, the viologen dyestuffs are colorless in the oxidized form and colored in the $1/2$ reduced form which is freely reversible and goes easily to the oxidized form. If the viologen dyes are reduced by an excess of sodium dithionite they will go to the colorless, fully reduced form which is stable and cannot be

FIG. 20

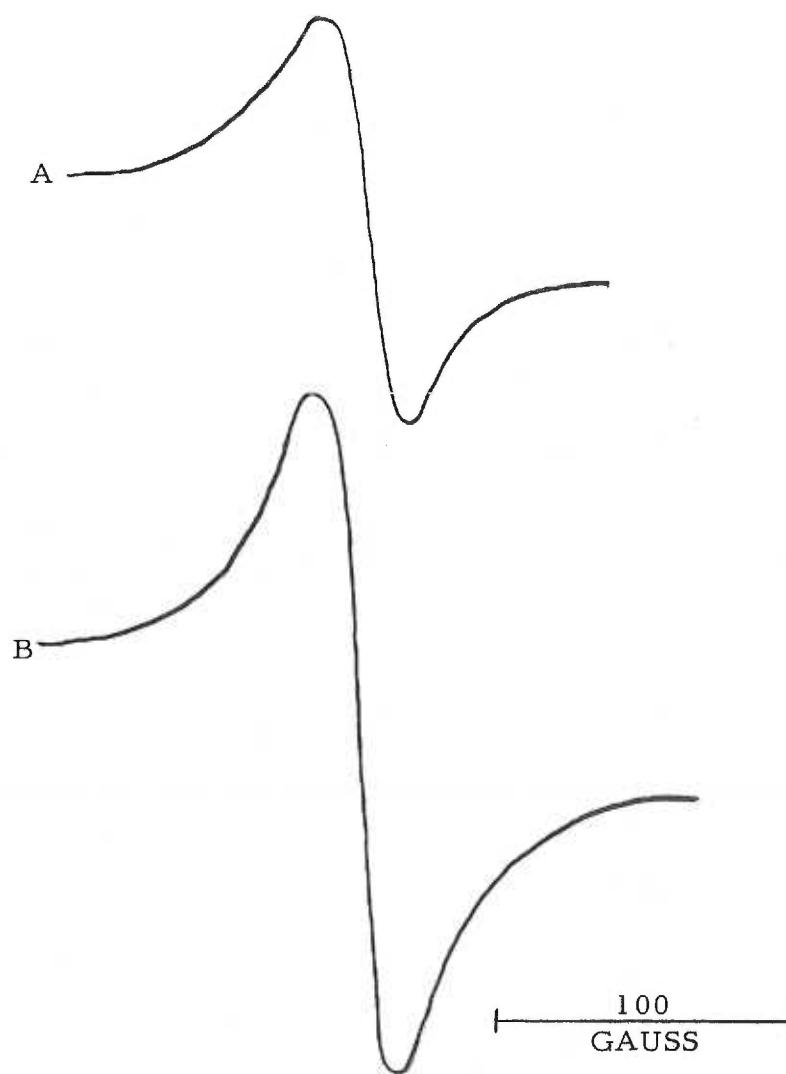
REDUCTION OF MICROSOMAL Fe_x BY HYDROGEN-REDUCED
METHYL VIOLOGEN

Curve A: The $g = 2.25$ ESR signal of microsomal Fe_x in the presence of reduced methyl viologen.

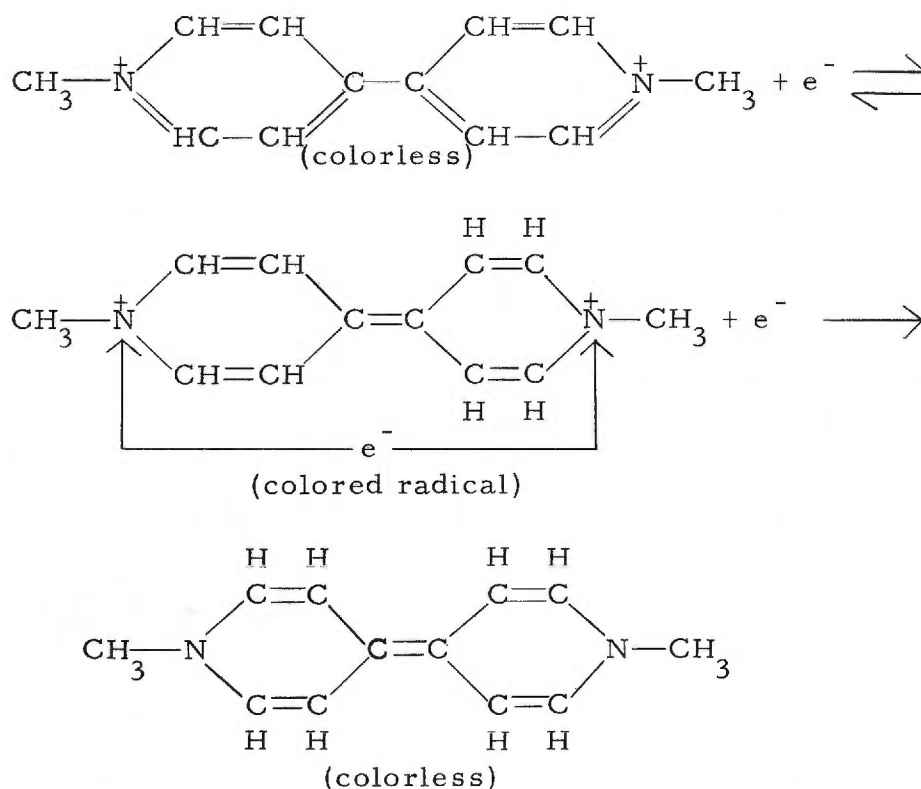
Curve B: The $g = 2.25$ ESR signal of microsomal Fe_x in the air oxidized sample.

Dyestuff concentration: 0.1 M (before reduction)
Used 0.3 ml. microsomes (38.1 mg. protein/ml.)

Obtained at -186°C .



reoxidized.



In order to obtain a greater amount of reduced methyl viologen it was necessary to use dithionite as the reducing agent, but because of the possibility of generating the fully reduced form it was necessary to know exactly how much dithionite was being used for reduction.

First it was necessary to determine how much dithionite could be added to the dye before the fully reduced methyl viologen began to form, as detected by loss of color. This was done by preparing a concentrated solution of methyl viologen (10^{-2} to 5×10^{-2} M) and adding a small aliquot (0.03 ml.) of the dye to the cuvette attachment of the anaerobic apparatus (Fig. 18). Phosphate buffer (0.1 M,

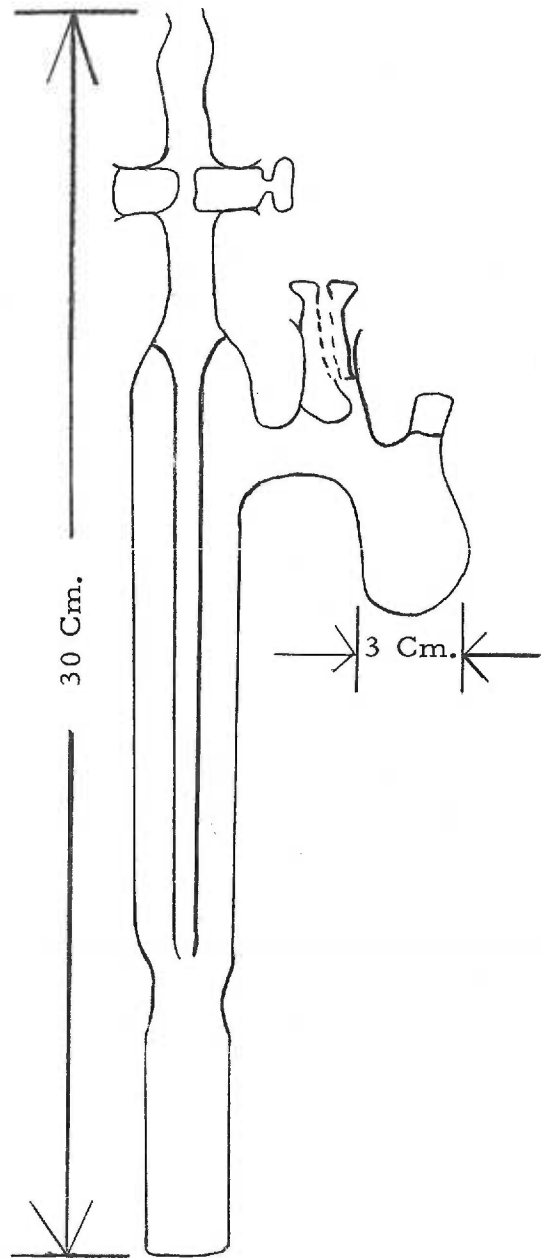
pH 7.0), glucose oxidase (1 mg.), and catalase (0.1 mg.) were added to the cuvette along with the dye to make 3 ml. total volume. The apparatus was then evacuated and flushed with hydrogen ten times, glucose (0.2 ml. of a 2M solution) was added to the dyestuff solution, and a standardized dithionite solution (2.3×10^{-3} M) was added to the titration side of the apparatus. The methyl viologen was titrated by dithionite in the Cary spectrophotometer. From the amount of dithionite necessary to give maximum color formation with the diluted dye sample, it was possible to extrapolate back to the concentrated dye sample and calculate how much dithionite would be necessary to produce a given ratio of oxidized to reduced methyl viologen.

The sodium dithionite was standardized by titration against FMN (169). A sample of FMN whose concentration was determined spectrophotometrically, using a millimolar extinction coefficient of $12.2 \text{ M}^{-1} \text{ cm}^{-1}$ at 450 m μ for FMN in 0.1 M phosphate buffer pH 7.0 (170), was placed in the cuvette of the Bois-Poltoratsky apparatus (Fig. 21) (171) and was evacuated and flushed with hydrogen. A weighed sample of dithionite was placed in 10 ml. of 0.1 M phosphate buffer, pH 7.0, which had been degassed with prepurified nitrogen. The Alga micrometer syringe with a 19 gauge needle was placed through a serum stopper on the dithionite degassing system and was flushed with prepurified nitrogen before the dithionite solution was taken up. The needle was removed from the syringe and a smaller

FIG. 21

BOIS-POLTORATSKY ANAEROBIC APPARATUS

According to Bois-Poltoratsky (171)



needle with a piece of polyethylene tubing was attached and the tubing was inserted into the Bois-Poltoratsky apparatus against a hydrogen pressure. The FMN was titrated by the dithionite in a dark room using an ultraviolet lamp. Disappearance of FMN fluorescence was used as end point. All standard dithionite solutions described in this thesis were prepared in this manner.

The next procedure used to obtain microsomal Fe_x reduction was to place a solution of concentrated methyl viologen in the reduction side of the apparatus and after bubbling with hydrogen, standard dithionite was added to give the desired ratio of oxidized to reduced dyestuff. The dyestuff was then added to the microsomes and microsomal Fe_x reduction was measured. The assumption was being made with this method that the ratio did not change significantly upon mixing with the microsomes because high dyestuff concentrations (around 10^{-1} M) were being used. This was unsatisfactory because the amount of reduced methyl viologen oxidizing equivalents in microsomes was not known. The extinction coefficient of methyl viologen is not reported in the literature. Since it was essential to ascertain the ratios of oxidized and reduced dyestuff in the presence of microsomes, it was necessary to determine the extinction coefficient of methyl viologen. This value then permitted direct spectrophotometric measurement of the dyestuff ratio in the presence of microsomes.

is valid only for the particular dye lot number used because the purity of the methyl viologen was not determined. The extinction coefficient determined is for the reduced minus oxidized difference spectrum of methyl viologen. This was done because in the final technique the same difference spectrum is taken for the mixture of methyl viologen and microsomes.

It was decided to go back to the original type of anaerobic ESR tube (Fig. 17) for microsomal Fe_x reduction because the large anaerobic apparatus (Fig. 18) would allow only one titration point per day. Dyestuff (0.5 ml.) was placed in a small flask covered with a serum stopper which had been tied down with copper wire. The dye was evacuated and flushed with hydrogen using a needle inserted through the stopper and then was bubbled with hydrogen. The dye was reduced with dithionite (4 to 5×10^{-2} M) to give a known ratio of oxidized to reduced dyestuff, and the dyestuff was taken up in a Hamilton gas-tight syringe which had been flushed with hydrogen. The anaerobic ESR tube was then evacuated and flushed with hydrogen, 0.1 ml. microsomes (20 mg. protein/ml.) added to the tube, and the reduced dye (0.2 ml.) added to the microsomes. All additions to the ESR tube were made against a hydrogen pressure.

The optical spectrum was recorded 15 minutes after the dyestuff addition and then the tubes were frozen in liquid nitrogen. After the ESR spectrum was taken the tubes were thawed and kept at

room temperature for 15 more minutes and the optical spectrum was again taken. The tubes were then frozen and the ESR spectrum was taken once again. The thawing and freezing procedure was then repeated once more to be absolutely certain equilibrium had been attained. The tubes were then thawed and opened to the air to allow the dyestuff and microsomal Fe_x to oxidize. The ESR and optical spectra of the oxidized tubes were then taken to determine the total amount of microsomal Fe_x present in each tube and to determine the microsomal contribution to the optical spectrum.

With methyl viologen it was found that maximum reduction of dye-reducible microsomal Fe_x was obtained for all ratios of oxidized and reduced dye except those which contain less than 10% reduced dye. For this reason it was necessary to use a dyestuff with a higher (more positive) potential than that of methyl viologen.

(4) Benzyl Viologen

The technique used for methyl viologen was also used with benzyl viologen; an extinction coefficient for the reduced minus oxidized dyestuff was determined. The limitations of this technique proved to be two-fold. First of all, the optical density of the dyestuff could not exceed the optical density limits of the Cary and secondly the non-cytochrome P-450 oxidizing equivalents of the microsomes had to be kept at a minimum. The maximum optical

density determinable with the Cary scattered transmission attachment was found to be about 4.3 using oxidized indigotetrasulfonate. Above this optical density Beer's law apparently no longer holds. This was corroborated by the Technical Service Department of Cary Instruments. To obtain these high optical densities, Kodak Wratten gelatin optical density filters were used as the spectrophotometric reference. To keep non-cytochrome P-450 microsomal oxidizing equivalents at a minimum, freshly prepared microsomes were divided into 1.5 ml. aliquots in serum stoppered test tubes, evacuated and flushed with hydrogen six times, and were frozen under hydrogen pressure. They were added anaerobically to the ESR tubes against a hydrogen pressure using an anaerobically prepared syringe.

By using the final technique with benzyl and methyl viologen it was possible to obtain a satisfactory titration curve (see Results, Fig. 27).

Since the dyestuff measurements were taken spectrophotometrically with ESR tubes as cuvettes, it was necessary to standardize the light path of each ESR tube with potassium chromate. Potassium chromate in 0.05 N KOH has a molar extinction coefficient of $4830 \text{ M}^{-1} \text{ cm}^{-1}$ at 371 m μ (172). Although the ESR tubes are cylindrical, a path length assumed equivalent to the thickness of a rectangle cuvette was obtained. The equivalent rectangular light path varied between 0.29 cm. and 0.33 cm., depending on the size of the

quartz tubing used for the ESR tube. Fig. 22 shows that with this assumption the optical properties of solutions in ESR tubes follow Beer's law. This figure shows that the optical density obtained with ESR tubes follows a straight line relationship with respect to dyestuff concentration.

The assumption that a cylindrical ESR tube can be used in the same manner as a rectangular cuvette is important to the results of the redox potential determination. The optical readings for this experiment were made with the Cary scattered transmission attachment which utilizes a large open-end photomultiplier placed directly behind the sample to collect the scattered light (see Fig. 17). The scattered transmission attachment is used with particulate systems, such as microsomes, to collect light which is scattered by the particles. If the curved surfaces of the ESR tube do cause more light scattering than a rectangular cuvette when both contain a particulate system, the large window of the photomultiplier should collect all the scattered light. Because the cylindrical ESR tubes follow Beer's law to the limits of the scattered transmission attachment (Fig. 22) the path length can be assumed to be equivalent to the thickness of a rectangular cuvette (173).

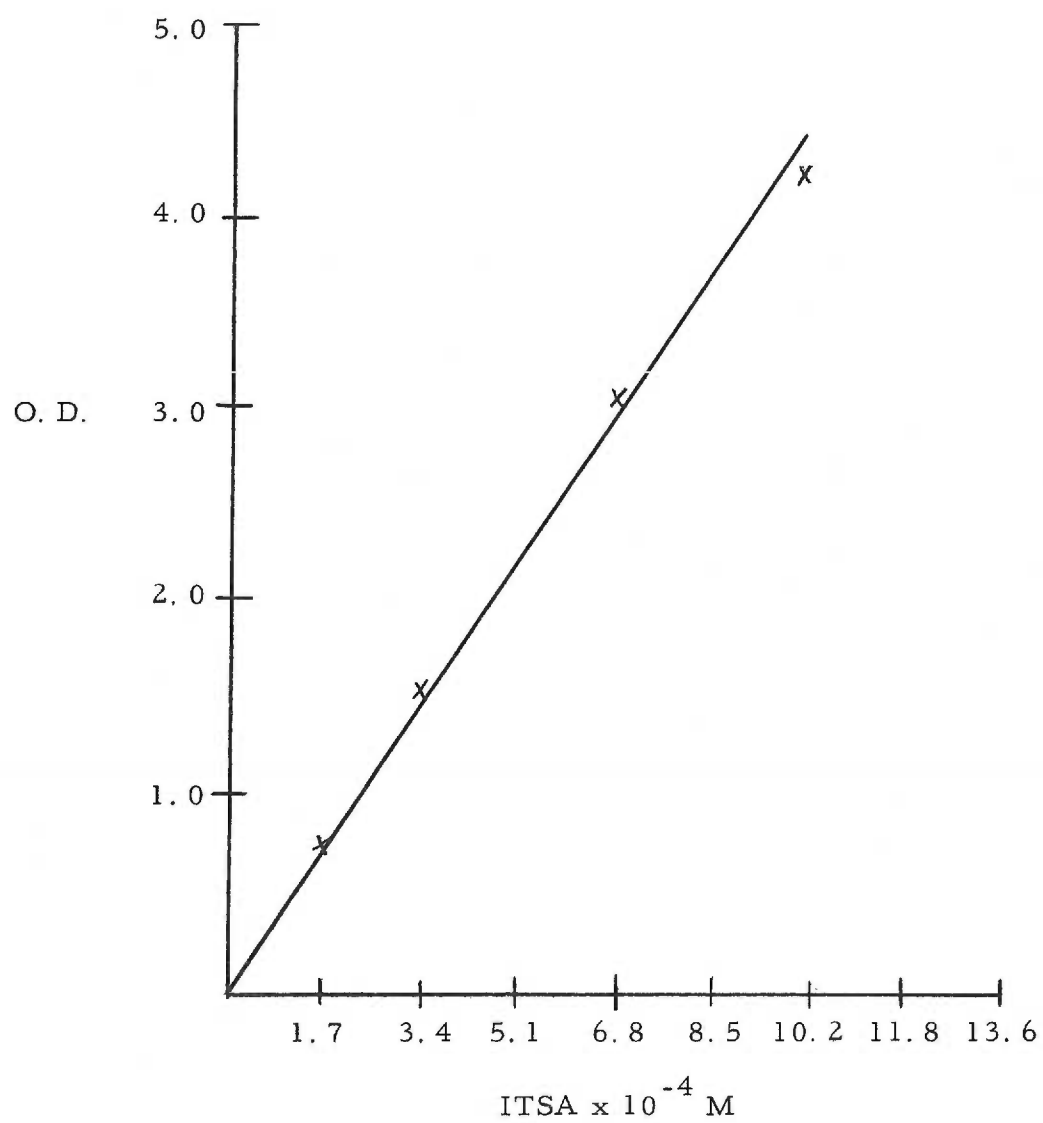
All ESR measurements of microsomal Fe_x were made at liquid nitrogen temperatures with the Varian V-4500 ESR spectrometer. A modulation amplitude of 15 gauss and a time constant of 1 second was

FIG. 22

BEER'S LAW RELATIONSHIP FOR SOLUTIONS IN CYLINDRICAL
ESR TUBES

The ordinate is optical density.

The abscissa is concentration of indigotetrasulfonate.



used in every case. The gain was adjusted according to the microsomal Fe_x concentration.

C. Stoichiometry of Cytochrome P-450 Reduction

The stoichiometry of reduction of cytochrome P-450 was examined spectrophotometrically by titrating microsomes with NADPH in the presence of CO. The anaerobic apparatus in Fig. 18 was used for this experiment, with the cuvette attachment. As described by Omura and Sato, the extinction coefficient of cytochrome P-450 at 450 m μ minus 490 m μ in the reduced-CO minus reduced difference spectrum is 91 mM⁻¹cm⁻¹ (70).

Microsomes (0.03 ml., 32.5 mg. protein/ml., 2.6 m μ moles cytochrome P-450/mg. protein), phosphate buffer 0.1 M pH 7.0 (2.7 ml.), glucose oxidase (0.5 to 1.0 mg.) and catalase (0.1 to 0.2 mg.) were added to the sample cuvette and the anaerobic apparatus was evacuated and flushed with hydrogen. Glucose (0.2 ml. of a 2 M solution) was then added to the sample and a standard solution of NADPH was added to the titration side of the apparatus. Finally the apparatus was evacuated one more time and it was then flushed with CO which had been passed through Fieser's reagent to remove the oxygen.

The titration was carried out in the Cary spectrophotometer with the scattering transmission attachment. The Cary was equipped

with a low range slide wire (0 to 0.2 O. D.) for these experiments. After each NADPH addition (0.01 ml.), the optical density at 450 m μ and at 490 m μ was recorded. After completion of the titration, the volume in the sample cuvette was measured. This was used to calculate the number of moles of reduced-CO cytochrome P-450 formed.

The standard solution of NADPH was prepared in the following way. Ten milliliters of 0.1 M phosphate buffer pH 7.0 was deoxygenated in ice by prepurified nitrogen. Solid NADPH was then added to the buffer. The solution was taken up in an anaerobic syringe as described for the dithionite standardization and the NADPH concentration was determined from the optical density at 340 m μ (ϵ mM = 6.22×10^6 cm²/mole) (174) recorded on the Zeiss. The solution in the syringe was then added to the anaerobic apparatus against a hydrogen pressure.

The reference cuvette for these experiments was a standard Thunberg cuvette containing the same amount of microsomes, buffer, glucose oxidase, glucose, and catalase as did the sample. Lubrol WX (an anhydrous condensation product of a long chain fatty alcohol and ethylene oxide obtained from I. C. I. Organics Inc.) was used for clarification of the reference although it was not used in the sample because it was found to inhibit P-450 reduction by NADPH. One milligram Lubrol per milligram protein was used. Sodium

D. Spin State Conversion

Microsomes were taken up in 0.1 M phosphate buffer, pH 7.4, and centrifuged for one hour at 40,000 rpm in a Spinco #40 rotor. The microsome pellet from one centrifuge tube was then taken up in a minimum amount of 0.005 M phosphate buffer, pH 6.8, and placed in a Radiometer vessel. One milligram Lubrol WX per milligram protein was added along with enough sodium fluoride to give 0.01 M F^- in a 3 ml. final volume. Enough citrate-phosphate buffer of a given pH was added to the Radiometer vessel to give 3 ml. final volume and the pH was recorded on the Radiometer. The solutions were stirred magnetically throughout the whole experiment. The titration was carried out by adding buffers of different pH to different microsome pellets, the volume of the buffer added being the same in each case (enough to give 3 ml. final volume). At various time intervals 0.2 ml. of the reaction mixture was removed from the Radiometer vessel, placed in an ESR tube, and frozen in liquid nitrogen. The pH and time were noted for each aliquot removed. All ESR tubes used had the same inside and outside diameters. A control ESR tube was prepared by taking up one microsomal pellet to 3 ml. with 0.005 M phosphate buffer, pH 6.8. The control also contained the same amounts of Lubrol and fluoride as did the titration samples.

The protein concentration at each pH was determined by the biuret procedure. The concentrations of the high and low spin forms of microsomal Fe_x were calculated as described earlier and were plotted against pH for each time interval.

E. Optical Rotatory Dispersion of Cytochrome P-450

ORD measurements were carried out on a cytochrome P-450 preparation from rabbit liver microsomes. This cytochrome P-450, prepared by the method of Miyake et al. (87), contained only small amounts of the other microsomal heme redox components. The concentration of cytochrome P-450 per milligram protein was not increased over that in microsomes in this preparation, but only a small amount of cytochrome b_5 was present in it (87).

The ORD measurements were carried out on a Cary model 60 recording spectropolarimeter in Dr. T. E. King's laboratory at Oregon State University. The cytochrome P-450 particles were frozen in liquid nitrogen and were transported to Corvallis in this manner. All optical spectra run in conjunction with the ORD spectra were taken on a Cary model 14 recording spectrophotometer. The assistance of Dr. F. C. Yong in carrying out the ORD measurements is gratefully acknowledged. Preparation of cytochrome P-450 particles by Mrs. Nancy Avedovech is also gratefully acknowledged.

The oxidized, reduced, and reduced-CO states of cytochrome

III. RESULTS

This section is divided into four parts. In the first part, results of the determination of the redox potential of liver cytochrome P-450 are given. In addition to presentation of the final redox potential curve, results of experiments leading up to the final choice of oxidation-reduction dyestuffs and other experimental conditions are given in order to clarify these choices. Furthermore, these results are consistent with and support the value of E'_o obtained for microsomal Fe_x .

The second part of this section discusses the determination of the stoichiometry of cytochrome P-450 reduction.

The third part reports results of experiments on the spin state conversion of microsomal Fe_x caused by change in pH. One of the properties of a Cu^{+2} -like ESR signal seen in microsomes at low pH is also presented here. Its relation to the spin state conversion studies is considered in the Discussion section.

The fourth part of this section contains results of optical rotatory dispersion measurements carried out on the cytochrome P-450 preparation described in the Experimental section.

1. Redox Potential Determination

The effect of reduced indigotetrasulfonic acid on reduction of microsomal Fe_x is shown in Fig. 23. Reduction of microsomal Fe_x was checked by observing changes in the signal height of the $g = 2.25$ peak of the microsomal Fe_x ESR signal (Fig. 29). In Fig. 23(b), Curve A (2.3 cm.) is the $g = 2.25$ peak of microsomal Fe_x in the presence of 70% reduced indigotetrasulfonate and Curve B (2.3 cm.) is the same peak of the air oxidized system. The signal height was unchanged by the reducing agent indicating that no reduction had taken place. Fig. 23(a) shows the optical spectra obtained from these samples. Curve A is the optical spectrum of 70% reduced indigotetrasulfonate and microsomes. Curve B is the absorption spectrum of the air oxidized system.

The effect of reduced indigodisulfonic acid on reduction of microsomal Fe_x is shown in Fig. 24. In Fig. 24(b), Curve A (2.3 cm.) is the $g = 2.25$ peak of microsomal Fe_x in the presence of 65% reduced indigodisulfonate and Curve B (2.3 cm.) is the same peak of the air oxidized system. The signal height was unchanged by the reducing agent indicating that no reduction had taken place. Fig. 24(a) shows the optical spectra obtained from these samples. Curve A is the optical spectrum of 65% reduced indigodisulfonate and microsomes. Curve B is the absorption spectrum of the air oxidized

system.

Indication of microsomal Fe_x reduction by 40% reduced phenosafranine is shown in Fig. 25. In Fig. 25(b), Curve A (4.4 cm.) is the $g = 2.25$ peak of microsomal Fe_x in the presence of 40% reduced phenosafranine and Curve B (5.2 cm.) is the same peak of the air oxidized system. The signal height increased 18% upon air oxidation indicating that reduction of microsomal Fe_x had taken place. Fig. 25(a) shows the optical spectra obtained from these samples. Curve A is the optical spectrum of 40% reduced phenosafranine and microsomes. Curve B is the absorption spectrum of the air oxidized system.

The proof that no reduction of microsomal Fe_x can be obtained with reduced phenosafranine is seen in Fig. 26. Curve A (12.3 cm.) is the $g = 2.25$ peak of microsomal Fe_x in the presence of 50% reduced phenosafranine and Curve B (12.0 cm.) is the same peak of the air oxidized system. The signal height is unchanged proving that no reduction of microsomal Fe_x is obtained with reduced phenosafranine.

An example of microsomal Fe_x reduction produced by hydrogen-reduced methyl viologen is shown in Fig. 20. Curve A (5.5 cm.) is the $g = 2.25$ peak of microsomal Fe_x in the presence of reduced methyl viologen. Curve B (9.1 cm.) is the air oxidized spectrum of the same sample. The final titration curve for the reduction of microsomal Fe_x with reduced methyl and benzyl viologen is shown in

It should be remembered that these values are for the reduced minus oxidized difference spectra of the dyestuffs as discussed in the Experimental section.

Peroxidic oxygen was estimated in two microsome preparations. Preparation I (42.7 mg. protein/ml.) contained $0.16 \pm 17\%$ μ moles peroxide/mg. protein and preparation II (53.7 mg. protein/ml.) contained $0.13 \pm 27\%$ μ moles peroxide/mg. protein. This concentration could alter the ratio of oxidized and reduced dyestuff added to microsomes.

FIG. 23

EFFECT OF REDUCED INDIGOTETRASULFONATE ON
MICROSOMAL Fe_x

(a) Optical Spectra

Curve A: Reduced indigotetrasulfonate and microsomes.

Curve B: Air oxidized indigotetrasulfonate and microsomes.
Obtained at room temperature.

(b) ESR Spectra

Curve A: $g = 2.25$ peak of microsomal Fe_x in the presence of
reduced indigotetrasulfonate.

Curve B: $g = 2.25$ peak of microsomal Fe_x after air oxidation.
Obtained at -178°C .

Initial indigotetrasulfonate concentration: 2×10^{-4} M (before
reduction). 0.1 ml. microsomes used (56 mg. protein/ml.).

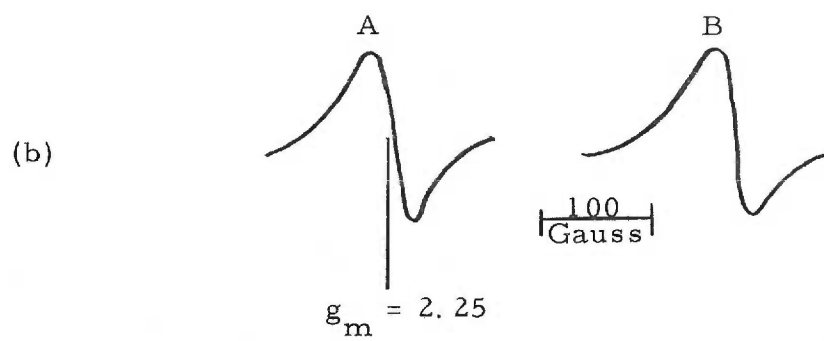
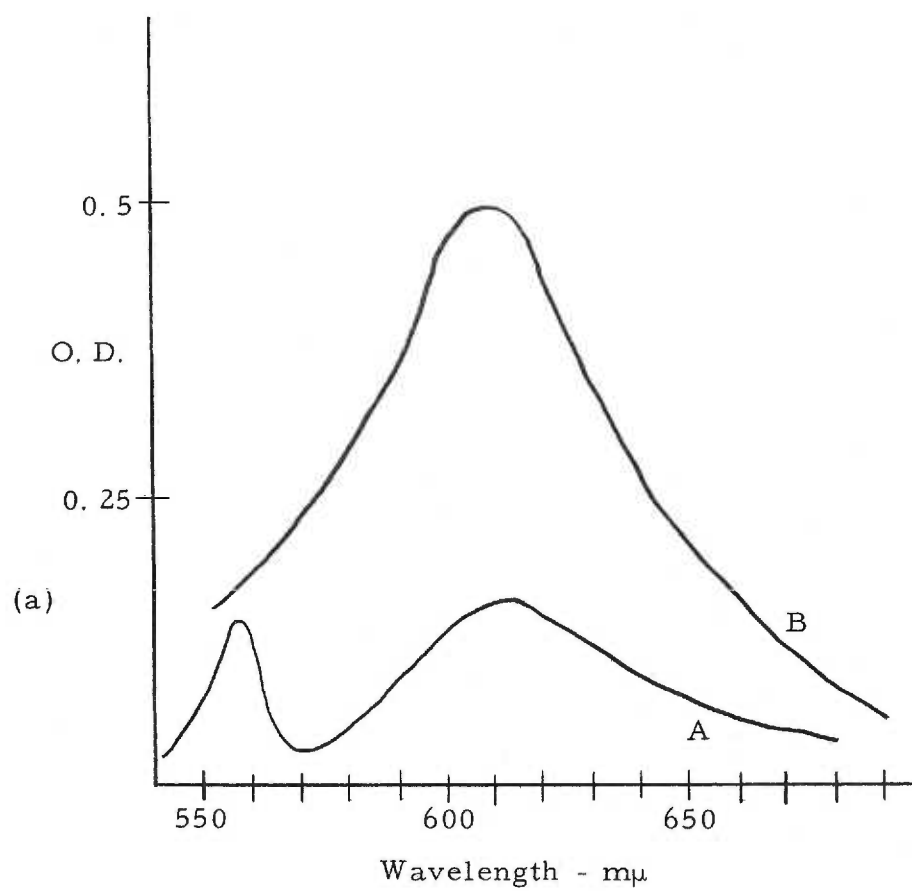


FIG. 24

EFFECT OF REDUCED INDIGODISULFONATE ON MICROSOMAL Fe_x

(a) Optical Spectra

Curve A: Reduced indigodisulfonate and microsomes.

Curve B: Air oxidized indigodisulfonate and microsomes.

Obtained at room temperature.

(b) ESR Spectra

Curve A: $g = 2.25$ peak of microsomal Fe_x in the presence of reduced indigodisulfonate.

Curve B: $g = 2.25$ peak of microsomal Fe_x after air oxidation. Obtained at -178°C .

Initial indigodisulfonate concentration: 2.4×10^{-3} M (before reduction). 0.1 ml. microsomes used (56 mg. protein/ml.).

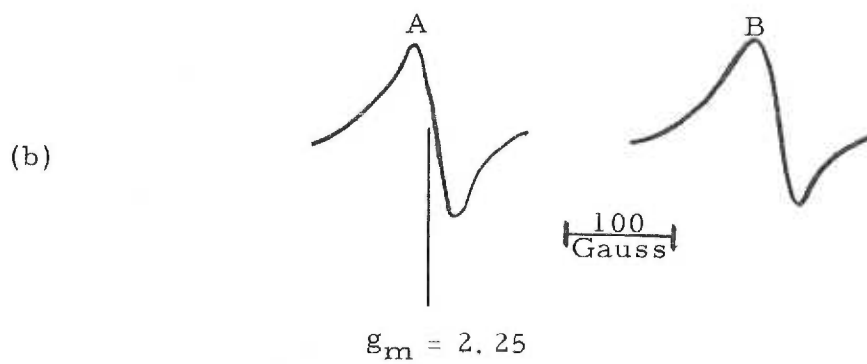
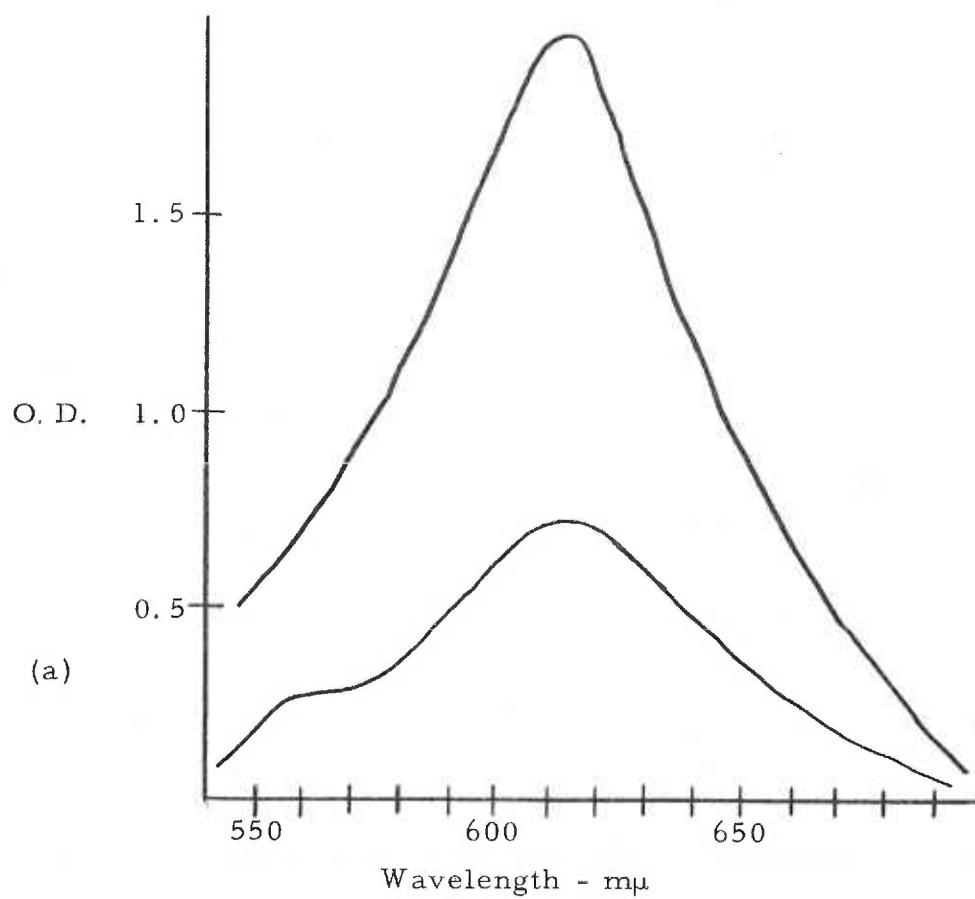


FIG. 25

INDICATION OF MICROSOMAL Fe_x REDUCTION BY REDUCED
PHENOSAFRANINE

Optical Spectra

Curve A: Reduced phenosafranine and microsomes.

Curve B: Air oxidized phenosafranine and microsomes.

Obtained at room temperature.

ESR Spectra

Curve A: $g = 2.25$ peak of microsomal Fe_x in the presence of reduced phenosafranine.

Curve B: $g = 2.25$ peak of microsomal Fe_x after air oxidation.

Obtained at -176°C .

Initial phenosafranine concentration: 4.6×10^{-3} M (before reduction).
0.1 ml. microsomes used (33 mg. protein/ml.).

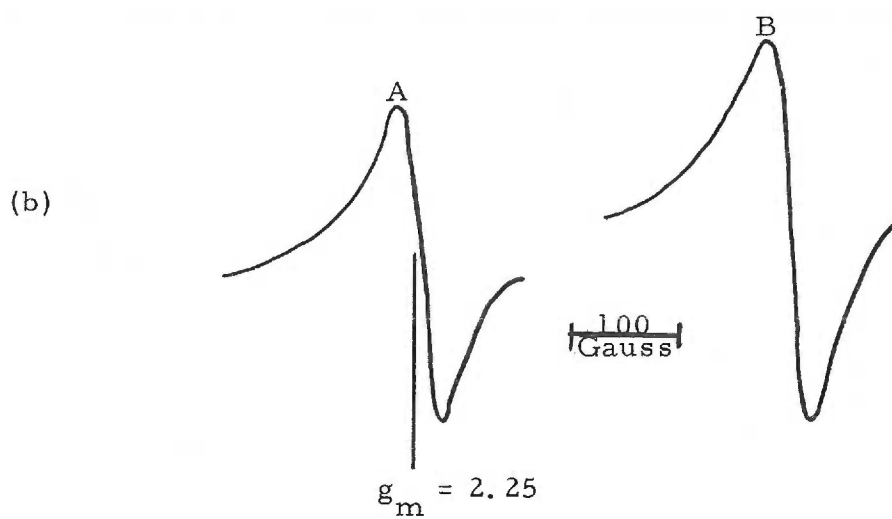
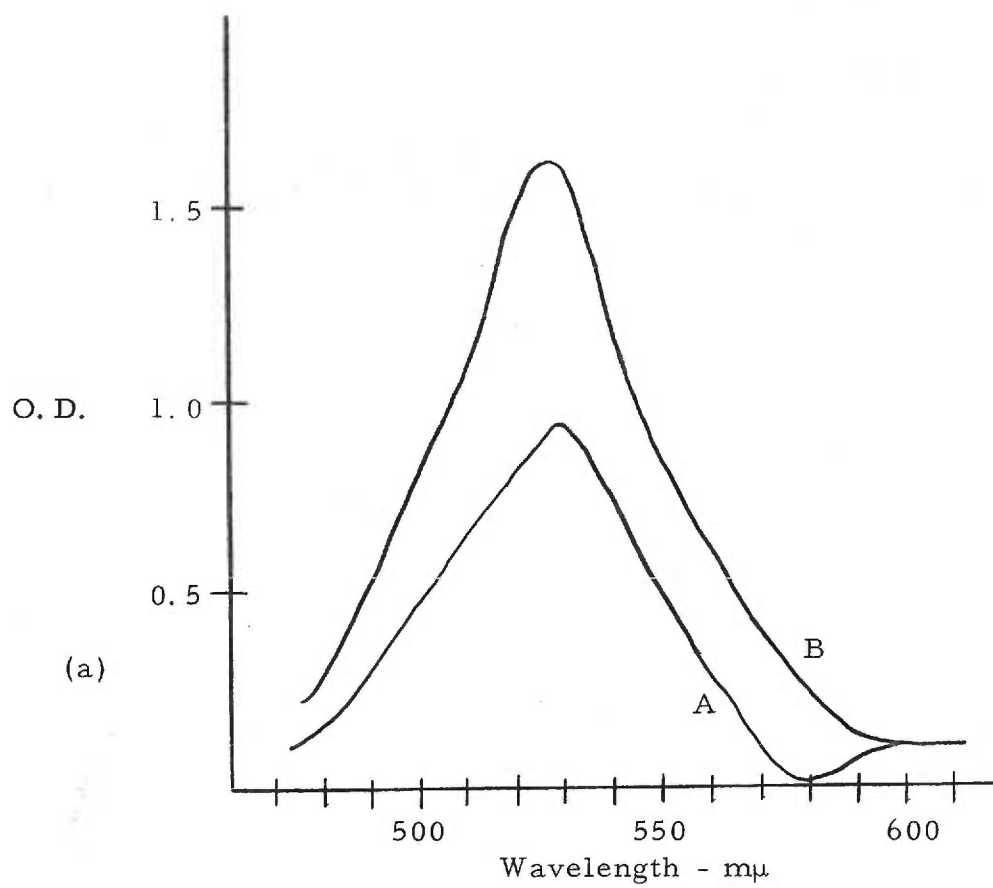


FIG. 26

PROOF THAT REDUCTION OF MICROSOMAL Fe_x BY REDUCED
PHENOSAFRANINE DOES NOT OCCUR

Curve A: $g = 2.25$ peak of microsomal Fe_x in presence of 50%
reduced phenosafranine.

Curve B: $g = 2.25$ peak of microsomal Fe_x in presence of air oxi-
dized phenosafranine.

Obtained at -178°C .

Initial phenosafranine concentration: 10^{-2} M (before reduction).
0.3 ml. microsomes used (35.5 mg. protein/ml.).

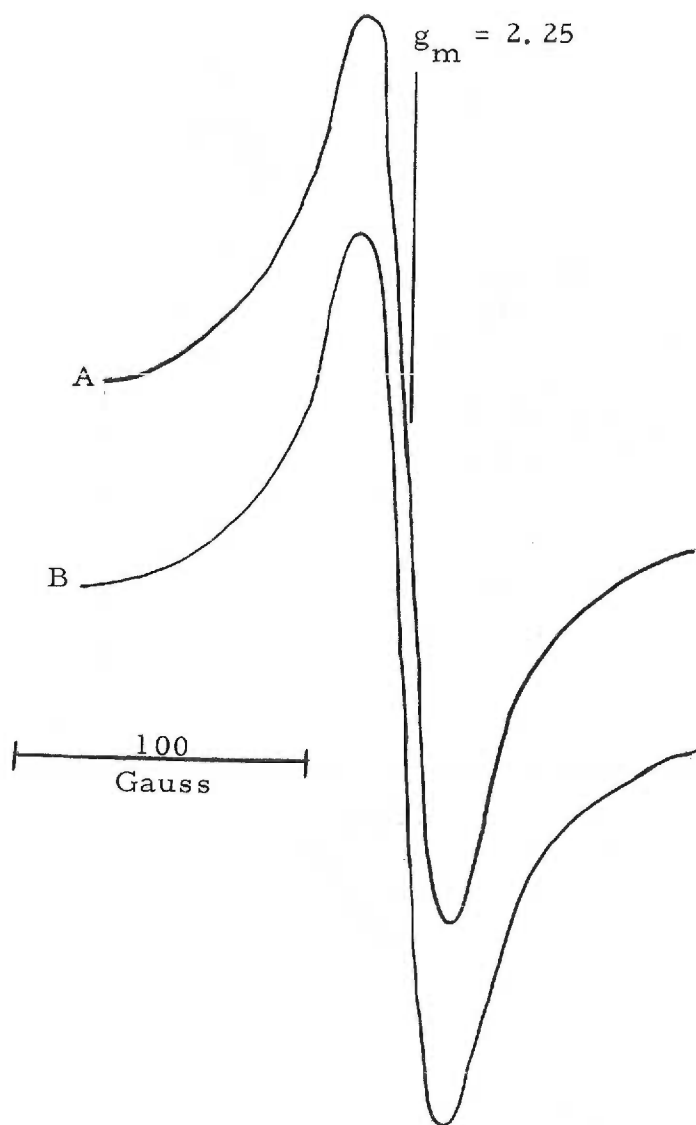


FIG. 27

REDOX TITRATION CURVE OBTAINED FOR MICROSOMAL Fe_x

This curve was obtained by using reduced methyl viologen and reduced benzyl viologen. The ordinate is potential (E) expressed in millivolts, the abscissa is per cent reduction of the $g = 2.25$ ESR peak of microsomal Fe_x .

- (x) represents points obtained with reduced benzyl viologen.
- (o) represents points obtained with reduced methyl viologen.

The microsome preparation used to obtain this curve contained 18 mg. protein/ml. and 2.22 μmoles cytochrome P-450/mg. protein.

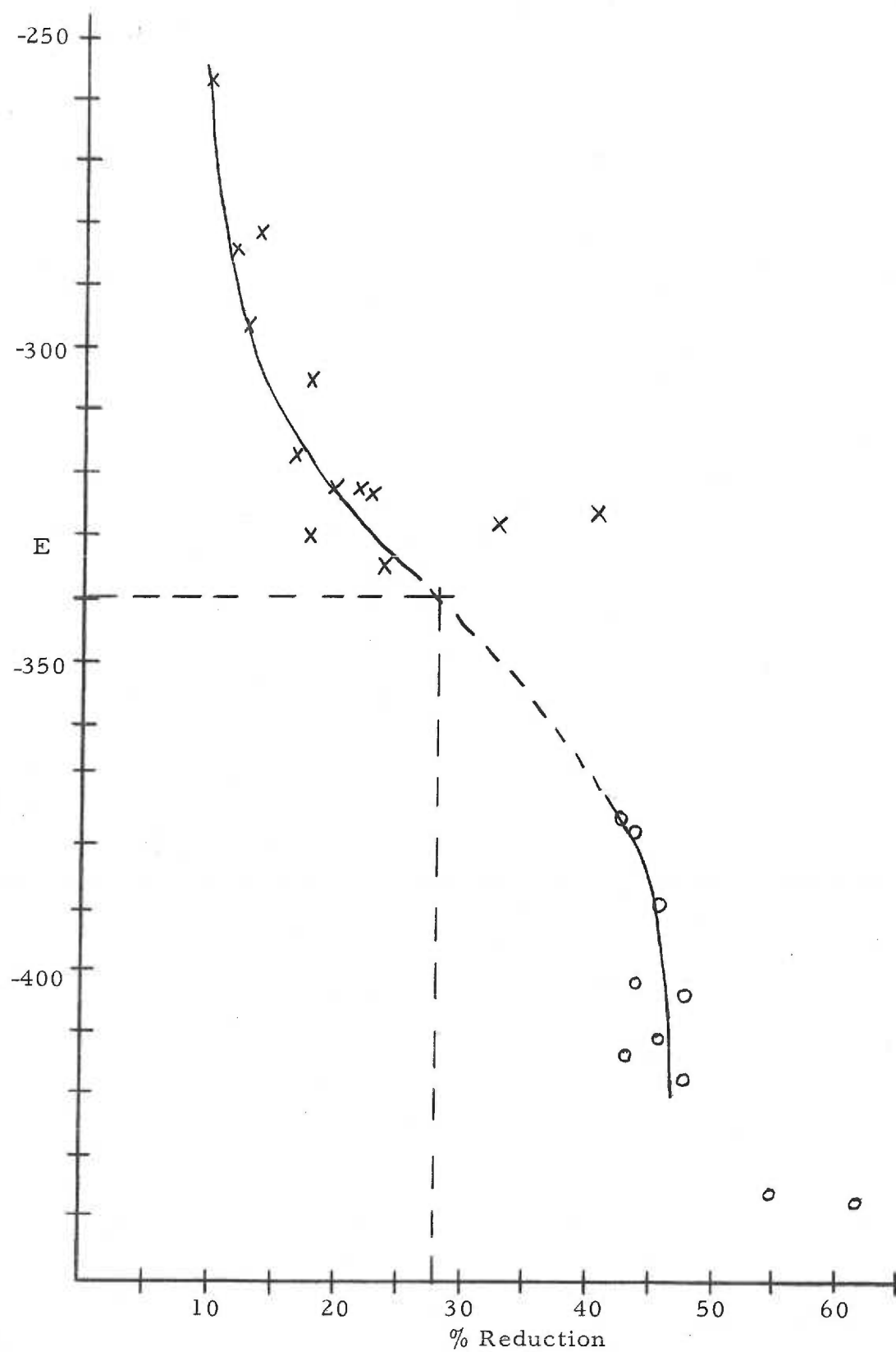


TABLE 6

MAXIMUM PER CENT REDUCTION OF MICROSOMAL Fe^{2+} BY
REDUCED METHYL VIOLOGEN IN VARIOUS MICROSOMAL
PREPARATIONS

Microsome Preparation	Protein Concentration	Maximum % Microsomal Fe _x Reduction
1 (Book 9 pg. 29)	39 mg. protein/ml.	52
2 (Book 10 pg. 38)	36.2 mg. protein/ml.	49
3 (Book 10 pg. 97)	22.5 mg. protein/ml.	52
4 (Book 11 pg. 31)	21.5 mg. protein/ml.	56
5 (Book 11 pg. 47)	18 mg. protein/ml.	47

2. Stoichiometry of Cytochrome P-450 Reduction

A typical curve obtained from the NADPH titration of microsomal cytochrome P-450 in the presence of CO is shown in Fig. 28. The amount of the CO complex of reduced cytochrome P-450 formed is plotted against the amount of NADPH added. The number of equivalents required to reduce cytochrome P-450 is obtained from the slope of the middle of the sigmoid titration curve (see Discussion). This value is found to be 1.4 in Fig. 30, remembering that each mole of NADPH represents two reducing equivalents. In Table 7 a list of many titrations is seen. In this table it will be noted that the n -values for cytochrome P-450 range between one and two. Because of this range, the example in Fig. 28 is presented to show the shape of the titration curve and not to indicate that the n -value of cytochrome P-450 is 1.4. The n -value of cytochrome P-450, as seen in Table 7, is less than two. The redox titration curve (Fig. 27) shows that the n -value of cytochrome P-450 is one (see Discussion).

FIG. 28

NADPH TITRATION CURVE OF CYTOCHROME P-450 IN THE
PRESENCE OF CO

Microsome preparation: 32.5 mg. protein/ml. , 2.6 μ moles
cytochrome P-450/mg. protein.

NADPH: 1.2×10^{-5} M.

The titration was carried out at room temperature.

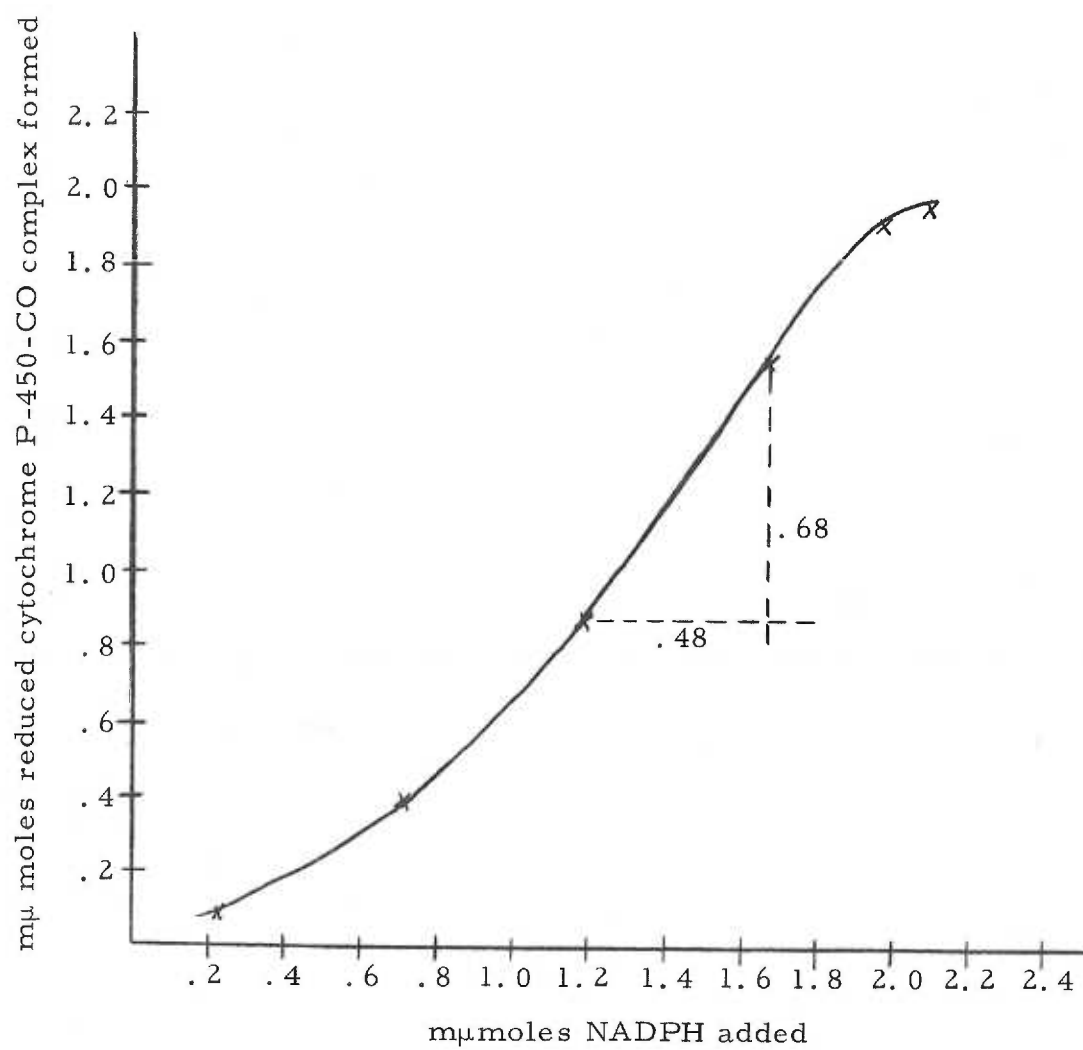


TABLE 7

RESULTS OF NADPH TITRATION OF CYTOCHROME P-450 IN THE
PRESENCE OF CO.

The n-value is the number of NADPH equivalents required for reduction of one molecule of cytochrome P-450. This value is obtained from the middle of the titration curve as seen in Fig. 28.

Experiment	Microsome Protein		Cytochrome P-450 Concentration	NADPH		n-value
	Concentration			Concentration		
1. Book 4 page 73	23 mg. protein/ml.		2.2 μ moles/ mg. protein	3.5×10^{-5} M		2.0
2. Book 4 page 79	51.6 mg. protein/ml.		2.8 μ moles/ mg. protein	4.7×10^{-5} M		1.4
3. Book 4 page 83	51.6 mg. protein/ml.		2.8 μ moles/ mg. protein	2.4×10^{-5} M		1.0
4. Book 4 page 85	51.6 mg. protein/ml.		2.8 μ moles/ mg. protein	2.2×10^{-5} M		1.0
5. Book 4 page 86	51.6 mg. protein/ml.		2.8 μ moles/ mg. protein	1.9×10^{-5} M		1.1
6. Book 8 page 33	37.4 mg. protein/ml.		2.7 μ moles/ mg. protein	2.4×10^{-5} M		1.9
7. Book 8 page 36	37.4 mg. protein/ml.		2.7 μ moles/ mg. protein	1.9×10^{-5} M		1.6
8. Book 8 page 44	27.9 mg. protein/ml.		2.4 μ moles/ mg. protein	2.2×10^{-5} M		1.5
9. Book 8 page 46	27.9 mg. protein/ml.		2.4 μ moles/ mg. protein	1.7×10^{-5} M		1.5

Experiment	Microsome Protein		Cytochrome P-450 Concentration	NADPH Concentration	n-value
	Concentration				
10. Book 8 page 59	33 mg. protein/ml.		3.3 mμmoles/ mg. protein	2.2×10^{-5} M	1.6
11. Book 8 page 61	33 mg. protein/ml.		3.3 mμmoles/ mg. protein	1.7×10^{-5} M	1.9
12. Book 8 page 68	20 mg. protein/ml.		3.1 mμmoles/ mg. protein	2.0×10^{-5} M	1.7
13. Book 8 page 72	32.5 mg. protein/ml.		2.6 mμmoles/ mg. protein	1.2×10^{-5} M	1.4

3. Spin State Conversion

The ESR spectrum of the low spin, microsomal hemoprotein, microsomal Fe_x is seen in Fig. 29. "Because the true g-values of magnetically anisotropic substances are difficult to obtain from overlapping signals of randomly oriented samples (frozen solutions), the following designations are used to mark field positions: g_m is a position, in terms of g-value, of maximal absorption: while s_m refers to positions, calculated as g-values, of maxima or minima in the spectrum plotted as a derivative curve" (86).

The effect of pH on the disappearance of the $g_m = 2.25$ component of the low spin microsomal Fe_x ESR spectrum is seen in Fig. 31. The different curves in this figure represent aliquots of the same microsome sample at different pH's. The aliquots were centrifuged and the pellets obtained were diluted to 3 ml. with acidic buffers (see Experimental). For this reason, the protein concentration varies somewhat from sample to sample, but the amount of spin/mg. protein is the same for each sample. All samples were frozen in liquid nitrogen five minutes after addition of the acidic buffers.

As the pH of a microsome suspension is lowered, a new ESR signal at $s_m = 6.1$ appears (86). A signal at this position has been attributed to high spin ferric hemoproteins (68) and in microsomes

has been identified as the high spin signal of microsomal Fe_x (86). The ESR spectrum of high spin microsomal Fe_x , as formed by acid treatment of microsomes, is shown in Fig. 30. The effect of pH on the appearance of the $s_m = 6.1$ signal of microsomal Fe_x is seen in Fig. 32. These curves were obtained from the same samples used to obtain the curves in Fig. 31.

Fig. 33 shows the amount of high and low spin microsomal Fe_x plotted as a function of pH for samples treated with acidic buffers for five minutes at room temperature. Because the microsome samples used at different pH's contained different amounts of protein (although the same amount of spin/mg. protein), a direct plot of signal height against pH was not used. The maximum high spin signal (pH 4.5 - 3 minutes) was integrated and compared to the integrated metmyoglobin fluoride signal (see Experimental). This value was taken to represent the maximum amount of ESR detectable high spin microsomal Fe_x per milligram protein. The signal height at other pH's were then compared with this value to obtain the per cent high spin compound. The same was done with the $s_m = 2.25$ low spin signal, the low spin microsomal Fe_x signal being compared with the Cu^{+2} standard signal. As seen in Fig. 33, 50% formation of the high spin form was observed at pH 4.85 for the samples treated for five minutes, while 50% loss of the low spin form was observed at pH 4.90.

Fig. 34 shows the amount of high and low spin microsomal Fe_x

plotted as a function of pH for samples treated with acidic buffers for one hour. It is seen from this figure that 50% formation of high spin was observed at pH 4.9, while 50% loss of low spin was observed at pH 5.3. Also note that the total amount of ESR detectable spin at pH 5.7 has decreased about 20%. This 20% appears to be loss of low spin form which is not detected as high spin form.

An ESR signal at $g = 2.06$ has been observed during acid treatment of microsomes (86). This signal has the characteristics of a Cu^{+2} ESR signal (86). The effect of p-chloromercuriphenylsulfonate (PCMS) on this signal is shown in Fig. 35. Curve A shows the $g = 2.06$ signal in microsomes at pH 5.1 after treatment with acidic buffers for 3 minutes in the absence of PCMS. Curve B shows that the signal has essentially disappeared after one hour in the absence of PCMS. Curve C shows the same signal in a microsome sample at pH 4.9 after treatment with acidic buffers for 3 minutes in the presence of PCMS. Curve D shows that the signal remains after one hour in the presence of PCMS.

FIG. 29

TYPICAL ESR SPECTRUM OF LOW SPIN MICROSOMAL Fe_x

pH 6.8, Temperature: -178°C , 30.8 mg. protein/ml. 2.18
m μ moles microsomal Fe_x /mg. protein.

FIG. 30

TYPICAL ESR SPECTRUM OF HIGH SPIN MICROSOMAL Fe_x

pH 4.5, Temperature: -178°C , 21.7 mg. protein/ml., 2.18
m μ moles microsomal Fe_x /mg. protein.

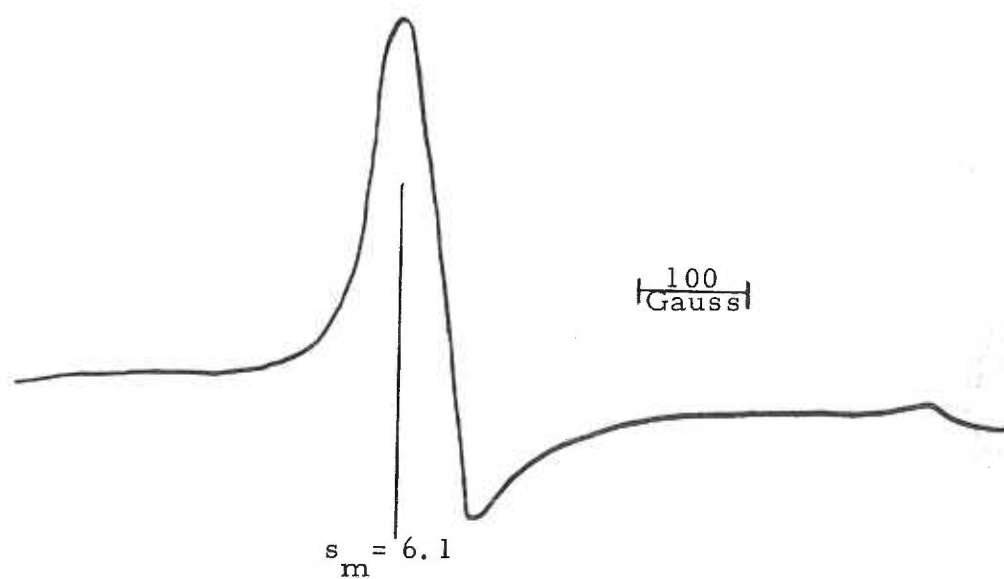
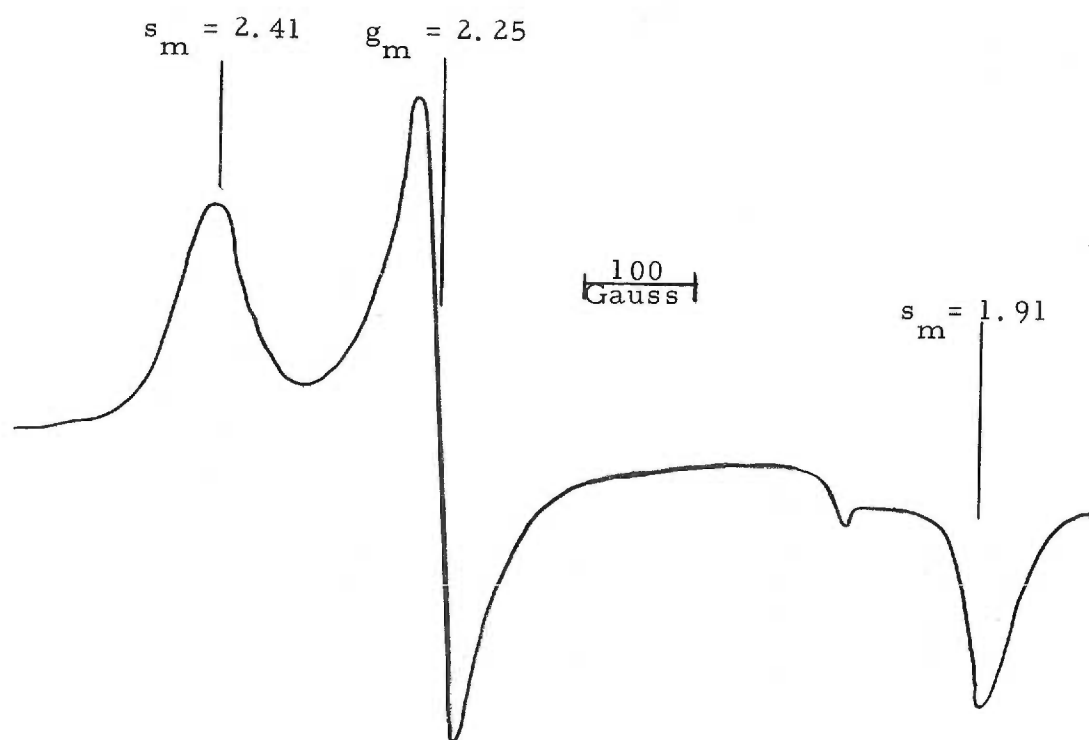


FIG. 31

EFFECT OF pH ON THE $g = 2.25$ COMPONENT OF THE LOW SPIN
MICROSOMAL Fe_x ESR SPECTRUM

All were taken at $-178^{\circ}C$, from samples frozen after five minutes treatment with acidic buffers of different pH's.

All contain 2.18 μ moles microsomal Fe_x /mg. protein.

- (A) pH 6.8, 30.8 mg. protein/ml.
- (B) pH 5.75, 21.8 mg. protein/ml.
- (C) pH 5.6, 24.6 mg. protein/ml.
- (D) pH 5.3, 20.2 mg. protein/ml.
- (E) pH 5.2, 21.8 mg. protein/ml.
- (F) pH 5.0, 20.2 mg. protein/ml.
- (G) pH 4.75, 20.3 mg. protein/ml.
- (H) pH 4.7, 21.8 mg. protein/ml.
- (I) pH 4.6, 16.4 mg. protein/ml.
- (J) pH 4.6, 18.3 mg. protein/ml.
- (K) pH 4.5, 21.7 mg. protein/ml.
- (L) pH 4.3, 17.9 mg. protein/ml.

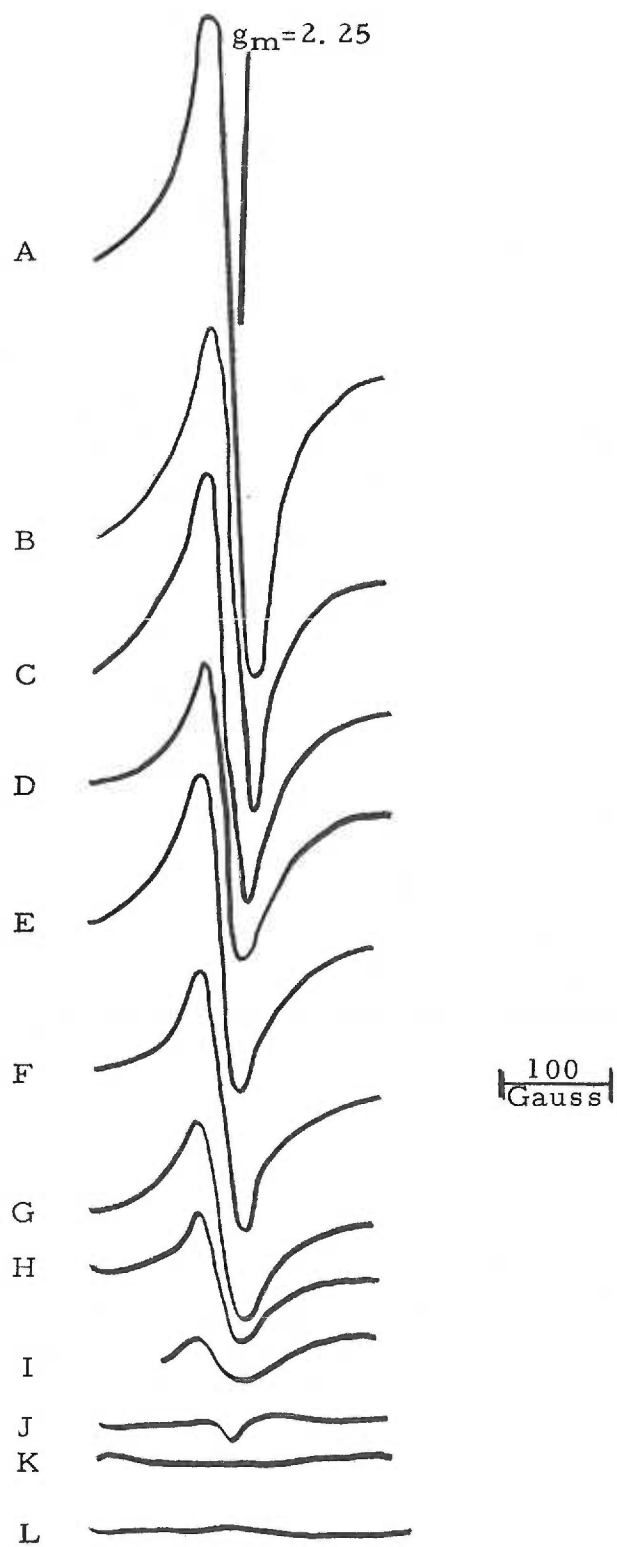


FIG. 32

EFFECT OF pH ON THE $g = 6.1$ COMPONENT OF THE HIGH SPIN
MICROSOMAL Fe_x ESR SPECTRUM

All were taken at -178°C , from samples frozen after five minutes treatment with acidic buffers of different pH's.

All contain 2.12 μmoles microsomal Fe_x /mg. protein.

- (A) pH 4.3, 17.9 mg. protein/ml.
- (B) pH 4.5, 21.7 mg. protein/ml.
- (C) pH 4.6, 18.3 mg. protein/ml.
- (D) pH 4.6, 16.4 mg. protein/ml.
- (E) pH 4.7, 21.8 mg. protein/ml.
- (F) pH 4.75, 20.3 mg. protein/ml.
- (G) pH 5.0, 20.2 mg. protein/ml.
- (H) pH 5.2, 21.8 mg. protein/ml.
- (I) pH 5.3, 20.2 mg. protein/ml.
- (J) pH 5.6, 24.6 mg. protein/ml.
- (K) pH 5.75, 21.8 mg. protein/ml.
- (L) pH 6.8, 30.8 mg. protein/ml.

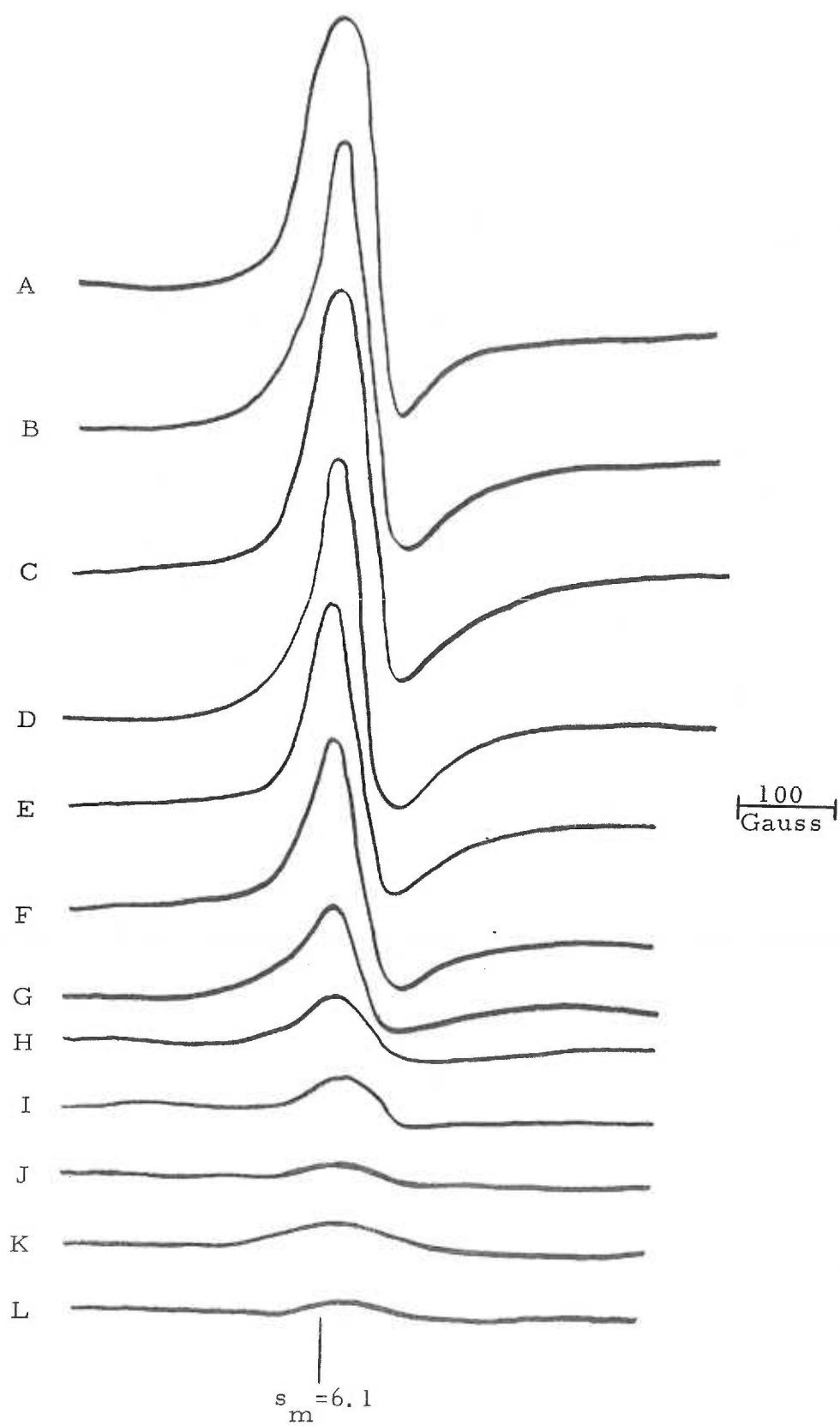


FIG. 33

pH EFFECT ON HIGH AND LOW SPIN MICROSOMAL Fe_x - 5
MINUTE SAMPLES

The values plotted here are for the same samples shown in Figs. 31 and 32. The dashed lines represent the points at which 50% high spin was observed and 50% low spin loss was observed.

These samples were treated with acidic buffers for five minutes at room temperature before they were frozen and the ESR spectra were taken.

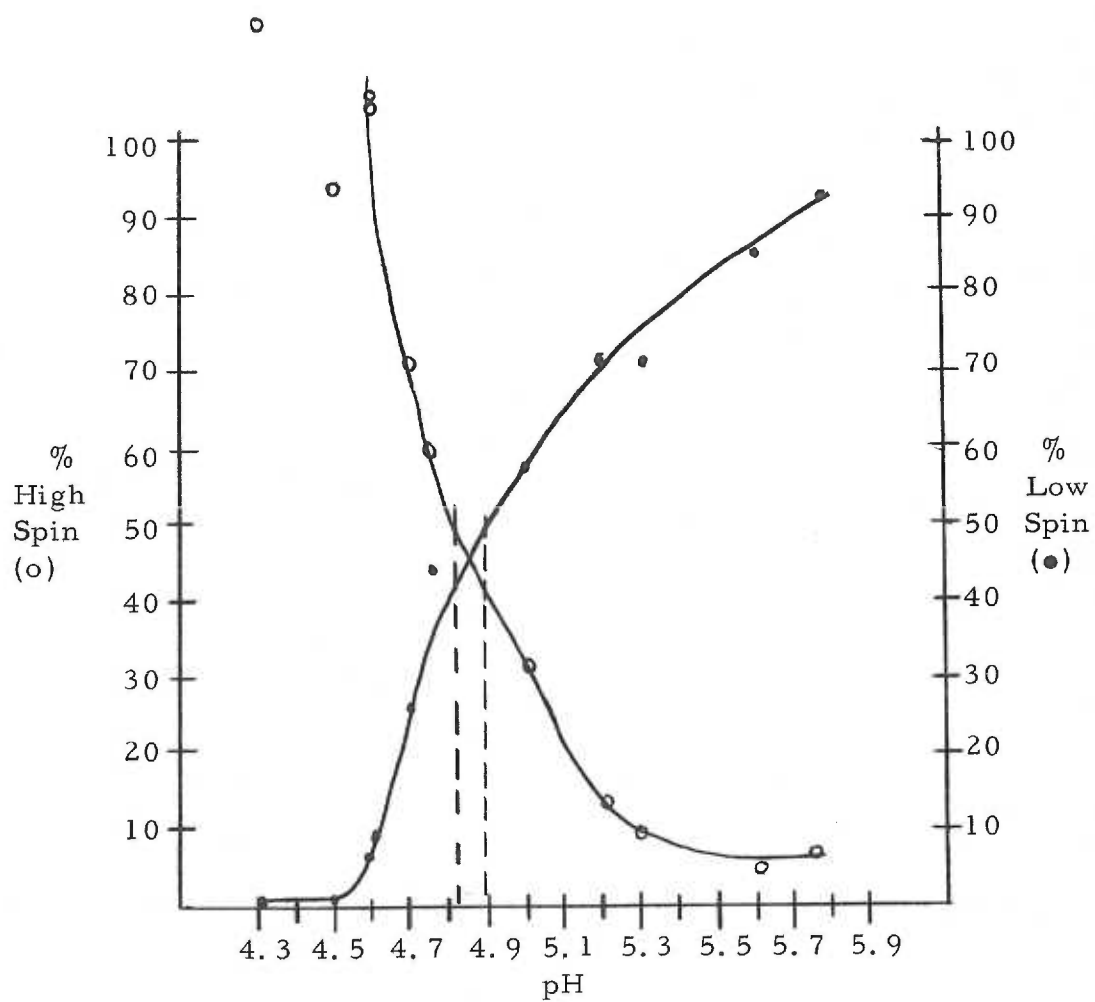


FIG. 34

pH EFFECT ON HIGH AND LOW SPIN MICROSOMAL Fe_x -
1 HOUR SAMPLES

The values plotted here are for the same samples as in Fig. 33. The dashed lines represent the points at which 50% high spin was observed and 50% low spin loss was observed.

These samples were treated with acidic buffers for one hour at room temperature before they were frozen and the ESR spectra were taken.

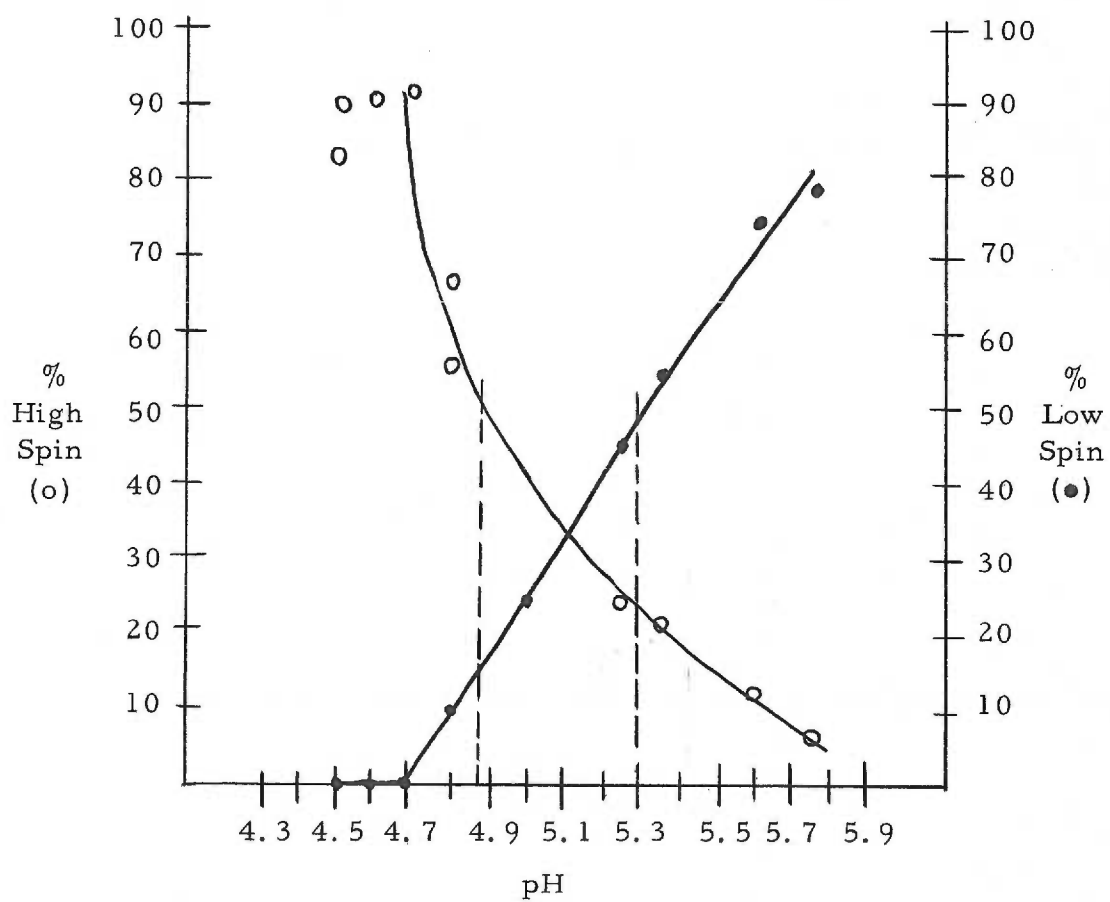
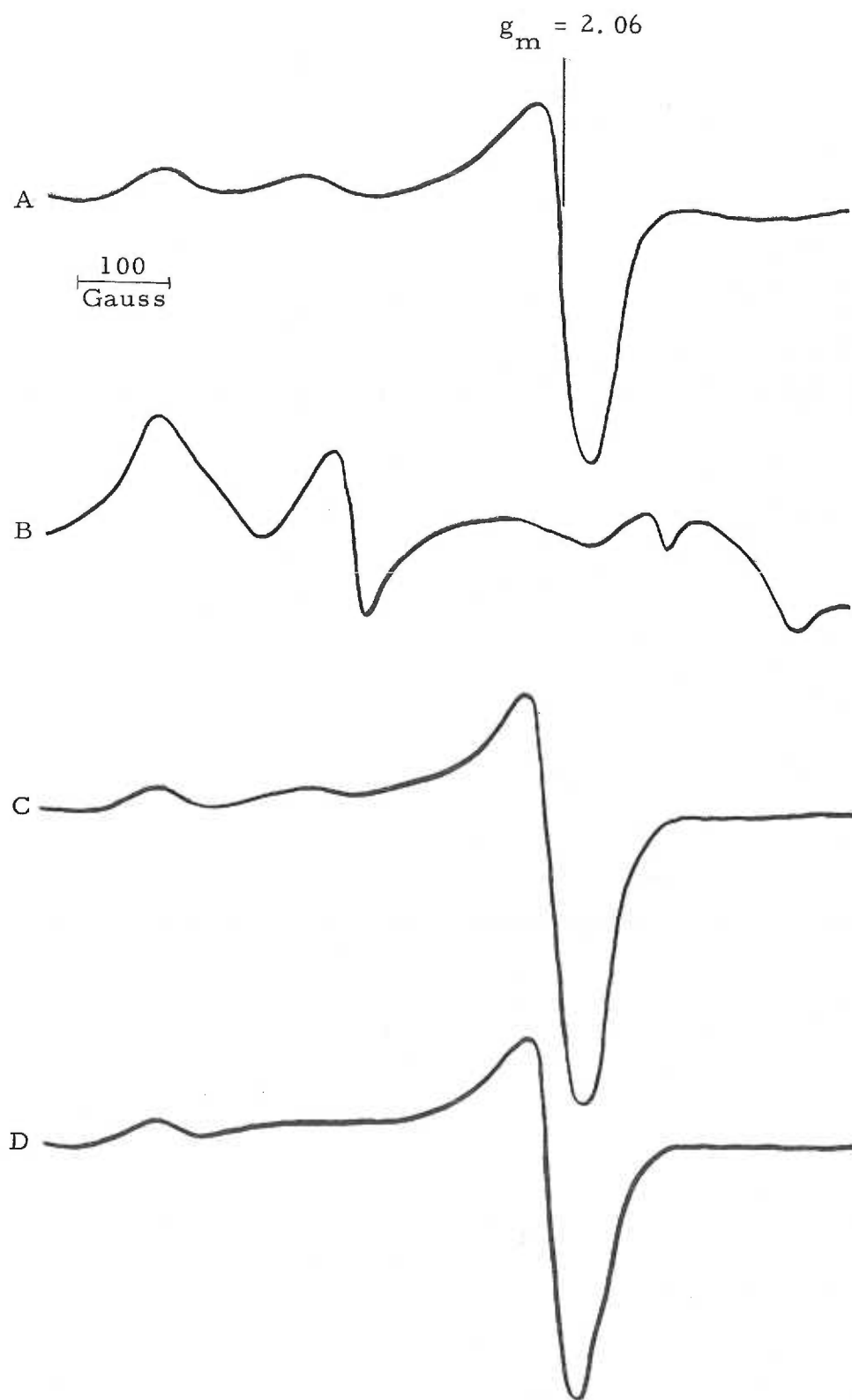


FIG. 35

PCMS EFFECT ON $g_m = 2.06$ ESR SIGNAL IN ACID TREATED
MICROSOMES

- Curve A: pH 5.1, 21.6 mg. protein/ml., -180°C , gain factor is 20,
3 min. after acid addition. No PCMS.
- Curve B: pH 5.1, 21.6 mg. protein/ml., -180°C , gain factor is 200,
1 hour after acid addition. No PCMS.
- Curve C: pH 4.9, 24.8 mg. protein/ml., -180°C , gain factor is 5,
3 min. after acid addition. 10 mM PCMS.
- Curve D: pH 4.9, 24.8 mg. protein/ml., -180°C , gain factor is 5,
1 hour after acid addition. 10 mM PCMS.



4. Optical Rotatory Dispersion

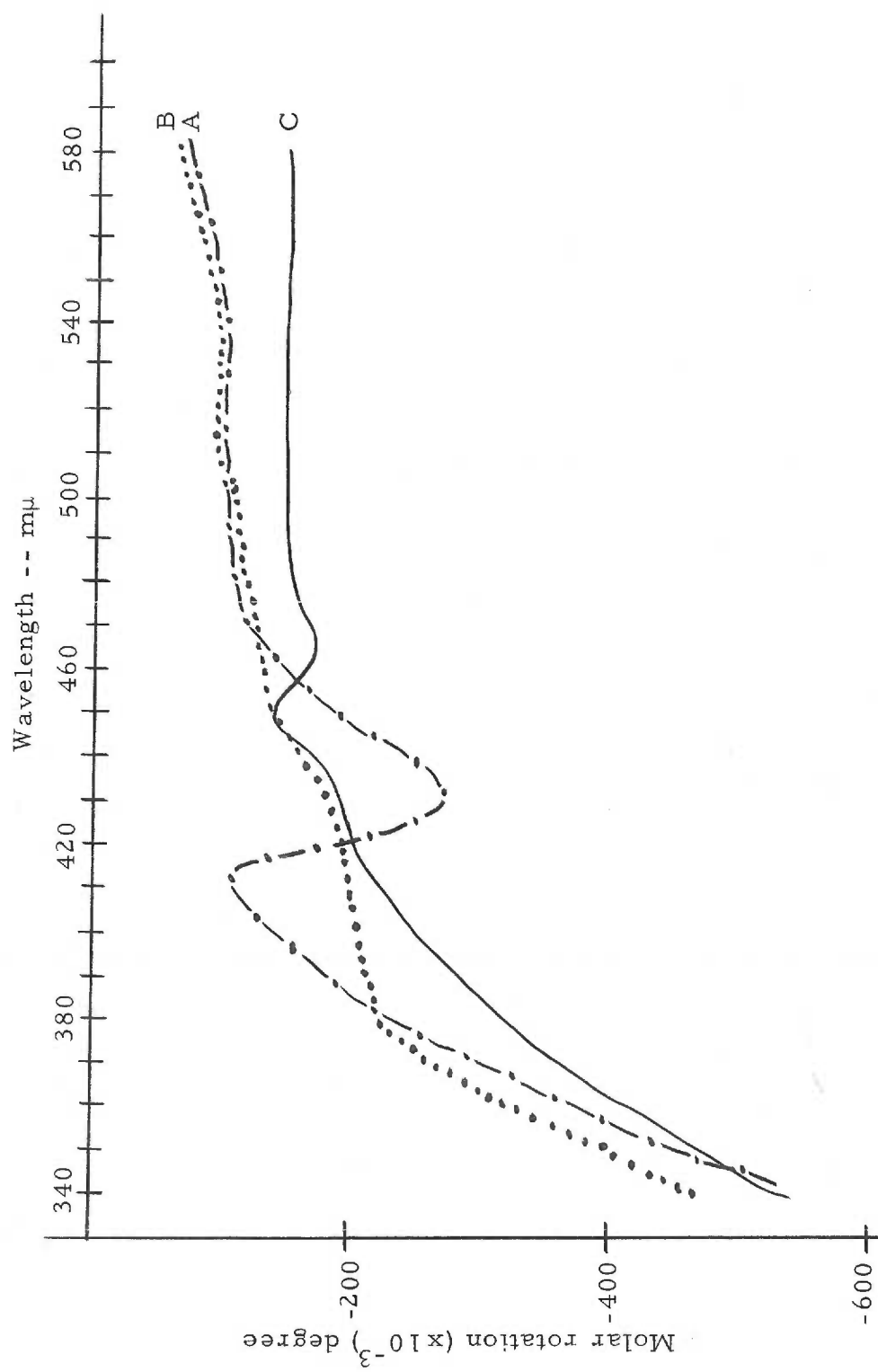
The optical rotatory dispersion curves of the cytochrome P-450 preparation are seen in Fig. 36. The oxidized form of cytochrome P-450 (curve A) shows a negative Cotton effect with a minimum at 432 m μ and a maximum at 410 m μ . The inflection point of this Cotton effect is close to the absorption maximum of the optical spectrum of oxidized cytochrome P-450 (415 m μ) (87). Upon dithionite reduction of cytochrome P-450 this Cotton effect essentially disappears with only a broad rotation in the Soret region observed (curve B). The addition of CO to reduced cytochrome P-450 gives a new negative Cotton effect with a minimum at 465 m μ and a maximum at 447 m μ (curve C). The inflection point of this Cotton effect is close to the absorption maximum of the reduced-CO form of cytochrome P-450 which is 450 m μ .

The abscissa in Fig. 36 is wavelength, while the ordinate is molar rotation expressed in the units of degrees per mole of heme per liter per decimeter (175).

FIG. 36

OPTICAL ROTATORY DISPERSION CURVES OF CYTOCHROME
P-450

- Curve A: (-, - - - -) Oxidized cytochrome P-450, 2.5 mg. protein/
ml., 6.3 μ M cytochrome P-450.
- Curve B: (. . . .) Reduced cytochrome P-450, 2.4 mg. protein/
ml., 7.2 μ M cytochrome P-450.
- Curve C: (_____) Reduced cytochrome P-450 - CO, 2.4 mg.
protein/ml., 6.0 μ M cytochrome P-450.



IV. DISCUSSION

This section is divided into five parts. In the first four parts, discussion of results presented in the previous section is given. In the fifth part an attempt is made to integrate the results in a general way.

1. Redox Potential Determination

The points obtained from the redox titration of microsomal Fe_x (Fig. 27) have been subjected to statistical analysis. Because of the potential gap in the titration curve, which could not be experimentally overcome, it was necessary to carry out a statistical analysis of the points to ascertain what sort of line should be drawn through them. A linear correlation was done by computing the Pearson r for the points (176):

$$r = \frac{N\sum XY - (\sum X)(\sum Y)}{\sqrt{[N\sum X^2 - (\sum X)^2] [N\sum Y^2 - (\sum Y)^2]}}$$

where X is the per cent reduction of microsomal Fe_x and Y is the potential (E) calculated from the ratio of oxidized and reduced dye-stuff. A value of $r = 0.936$ was obtained. This indicates that the data are not very far from being linear, a Pearson r of 1.000 representing a perfect linear relationship (176). A nonlinear correlation

was done by computing the eta (η) coefficient for the points (176):

$$\eta_{yx} = \sqrt{\frac{\sum[(\sum y')^2 f_x] - \left\{ [\sum(\sum y')]^2 / N \right\}}{\sum f_y'^2 - [(\sum f_y')^2 / N]}}$$

The potential (E) from -0.257v. to -0.417v. was divided into 3 millivolt increments, y' being the increment number. The per cent reduction of microsomal Fe_x was also divided into increments, each increment being equal to 1% reduction. f_x is the number of observed points of per cent reduction of microsomal Fe_x found in each per cent reduction increment. f is the number of observed points of per cent reduction of microsomal Fe_x found in each potential increment. N is the number of observations of per cent reduction of microsomal Fe_x . A value of $\eta = 0.987$ was obtained. "If the data are curvilinear, eta is larger than r ; the discrepancy between the two is related to the size of the departure from linearity" (176). Therefore, a curved line through the data is necessary.

The standard redox potential titration curve for a reversible oxidation-reduction system is sigmoid in nature, the curve for a one-electron process having a steeper slope than the curve for a two-electron process (22). A sigmoid curve, such as the one for a one-electron process, is not too far from being linear. Because there was no reason to suspect unusual redox properties for microsomal Fe_x , a standard redox potential curve was drawn through

the data.

The points in Fig. 27 cover a potential range of 160 millivolts. For a two-electron reduction, the potential difference between 1% reduction and 99% reduction is 120 millivolts as calculated from the Peters equation. Considering these facts and knowledge of the stoichiometry of cytochrome P-450 reduction by NADPH, a redox potential curve representing a one-electron reduction can be drawn through the points. This type of curve seems to best fit the data in Fig. 27.

For a one-electron process a potential difference of 160 millivolts represents dye-reducible microsomal Fe_x reduction of 4-5% to 95-96% as calculated from the Peters equation. Therefore 50-51% of the low spin ESR signal is dye reducible. In order to draw a symmetrical redox potential curve through the points in Fig. 27, covering 160 millivolts, it is necessary to assume that the first 7-8% of the low spin ESR signal represents a species with a more positive redox potential than the 42-44% dye-reducible microsomal Fe_x indicated by the titration curve. The 7-8% low spin signal which is not part of the titratable microsomal Fe_x may represent low spin cytochrome P-420. Low spin cytochrome P-420 has been previously observed (49) and the reported redox potential for cytochrome P-420 (-0.02v. at pH 7.0) is far more positive than the range of the titration curve. Also, all microsome preparations contain some

cytochrome P-420, although its spin state is not known. For these reasons it is assumed that 7-8% of the low spin ESR signal represents low spin cytochrome P-420 and is not being titrated by the dye-stuffs in the same manner as microsomal Fe_x .

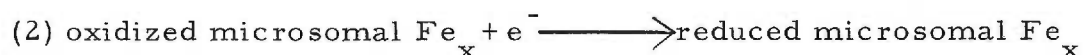
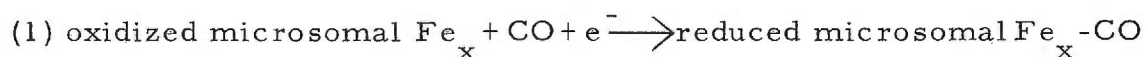
The question of whether a symmetrical titration curve should be drawn through the points is an important one which affects the determination of the E'_o . Why should the 160 millivolts represent 5% to 95% reduction of microsomal Fe_x ? If we assume that the highest potential point (-0.257v.) represents 1% dye-reducible microsomal Fe_x reduction, the lowest potential point on the curve (-0.417v.) must represent about 80% dye-reducible microsomal Fe_x reduction as calculated from the Peters equation. This is clearly not possible from the slope of the line drawn through the points at the lower end of the titration curve. In fact, at both ends of the potential range, the points represent nearly vertical lines. For this reason, a symmetrical curve covering the 160 millivolts best fits the array of points.

If only 50-51% of the low spin ESR signal is reduced by dye-stuffs, there remains 49-50% of the low spin signal to be accounted for. It is possible that the 49-50% of the low spin ESR signal not reduced by dyestuffs is a different type of microsomal Fe_x with a redox potential below -0.42v.. However, the physiological meaning of a biological molecule with a redox potential this low is not clear. The

lowest known potential of a biological molecule is that of ferredoxin, a non-heme iron protein with a redox potential of -0.43v. at pH 7.0. The function of this protein is to reduce NADP to NADPH in photosynthetic reactions (177). Microsomal Fe_x , on the other hand, is reduced by NADPH (5). A more likely explanation for the non-reducible microsomal Fe_x is that it is in an environment which is not accessible to the reduced dyestuffs. As indicated in Table 6, only about 50% of the microsomal Fe_x is reducible by methyl viologen (the lowest potential dyestuff used) in a number of different microsome preparations. In the phospholipid-protein environment of the microsomes, the remaining microsomal Fe_x may not be accessible to the dyes.

The presence of CO has a profound effect on the reduction of microsomal Fe_x . It has been demonstrated that 30% microsomal Fe_x is reduced by NADH in the absence of CO, but complete reduction is found in the presence of CO (5). Dyestuffs, such as indigo-tetrasulfonate, show no reduction of microsomal Fe_x in the absence of CO (see Fig. 23), but in the presence of CO, reduction is observed (see Results). The CO may be changing the equilibrium conditions by removing small amounts of reduced microsomal Fe_x to the reduced-CO form. This means that the reduced-CO/oxidized equilibrium has a more positive redox potential than the reduced/oxidized equilibrium. That is, the E'_0 for reaction (1) is more positive than

that for reaction (2):

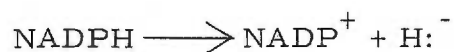


If the points on the titration curve represent 4% to 96% reduced microsomal Fe_x and 42% of the microsomal Fe_x is dye-reducible, the average E'_O is found to be -0.338v. at pH 7.0. This is an average of 21 points, has a range of -0.291v. to -0.373v. and a standard deviation of 0.016v.. If the points on the titration curve represent 5% to 95% reduced microsomal Fe_x and 44% of the microsomal Fe_x is dye-reducible, the average E'_O is found to be -0.339v. at pH 7.0. This is an average of 21 points, has a range of -0.296v. to -0.374v. and a standard deviation of 0.016v.. The E'_O of microsomal Fe_x as determined from the titration curve (Fig. 27) is about -0.34v..

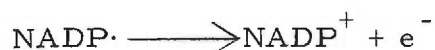
The reduction of cytochrome P-450 is catalyzed by NADPH cytochrome c reductase. This reductase contains two FAD molecules which alternate between FADH_2 and $\text{FADH}\cdot$ during catalysis (65) and has an unknown redox potential. The E'_O of $\text{FADH}_2 \rightleftharpoons \text{FAD}$ is -0.219v. at pH 7.0 in 0.1 M phosphate buffer (22). This value is the average of two one-electron steps, one of lower potential than the average E'_O and one of higher potential. For this reason it is possible that the potential of the $\text{FADH}_2 \rightleftharpoons \text{FADH}\cdot$ equilibrium of NADPH cytochrome c reductase is low enough to meet the energy

requirements of cytochrome P-450 reduction. It is not known if both FAD molecules of this reductase are involved in cytochrome P-450 reduction.

The redox potential of the NADPH system, as measured potentiometrically in 0.1 M tris (hydroxymethyl) aminomethane-HCl buffer, is -0.317v. at pH 7.0 (140). How can NADPH reduce cytochrome P-450 which has a redox potential of -0.338v. \pm 0.016v. at pH 7.0 even if the energy requirements of NADPH cytochrome c reductase do fit those of cytochrome P-450? First of all, the E'_o of the $\text{NADPH} \rightleftharpoons \text{NADP}^+$ equilibrium may be different in its microsomal environment than in a tris buffer solution. If the E'_o is lower in the microsomal environment, reduction could be attained. A further possibility is that the oxidation of NADPH involves two one-electron steps. Formally, oxidation of NADPH by NADPH cytochrome c reductase involves the transfer of a hydride ion (a hydrogen nucleus with two electrons) to the reductase. This reaction may proceed via an actual hydride ion transfer (178):



or by a two-step reaction involving transfer of a hydrogen atom preceded or succeeded by the transfer of an electron (178):



If the latter is the case, the redox potential of the NADPH system

represents the average of two redox potentials; one of lower potential than the reported E'_0 and one of higher potential. In this case, a mechanism can be imagined whereby the two FAD molecules of NADPH cytochrome c reductase have different redox potentials, the one with the lower potential is reduced by the lower potential step of NADPH oxidation; and this FADH_2 molecule reduces cytochrome P-450.

If NADPH oxidation does involve hydride ion transfer, the energy requirements of cytochrome P-450 reduction may be met by a change in the redox properties of NADPH in its microsomal environment. Another possibility is that the redox potential of cytochrome P-450 is raised by combination of this heme protein with substrate during the mixed-function oxidations. As seen in the Introduction, evidence has been accumulated which indicates that substrate binds to cytochrome P-450. It is possible, although not necessary, that binding of substrate to cytochrome P-450 changes the electronic nature of the heme, thereby raising the redox potential. Gillette and coworkers have recently demonstrated that type I substrates increase the rate of microsomal cytochrome P-450 reduction by NADPH while type II substrates decrease this rate (83). This result could be interpreted in terms of an increased redox potential, although other interpretations, such as a change in conformation upon binding of substrate, seem equally valid.

The redox potential found for microsomal Fe_x implies that a low potential will be found for the reductase step involved in microsomal Fe_x reduction. If adrenal mitochondrial cytochrome P-450 has the same properties as liver cytochrome P-450, it is expected that the redox potential of +0.164v. at pH 7.4 reported for adrenodoxin (90), the non-heme iron protein which transfers electrons between flavoprotein and P-450, is not correct.

The redox potential found for microsomal Fe_x is the lowest reported potential for any heme protein (the same as purified cytochrome b). It is, however, well within the physiological potential range. The meaning of this low potential in structural terms is very important. It indicates that a strong electron donor is a ligand on microsomal Fe_x (28). The proposal has been made that microsomal Fe_x is the sulfide of cytochrome P-420 (49) (Fig. 37). This is quite possible because the sulfide group would be a good electron donor. In the case of ferredoxin, iron is complexed by labile sulfide (liberated as H_2S by acid) and cysteine sulfhydryls and the redox potential is very low (177). Whatever the microsomal Fe_x ligand system may be, it can be expected to be strongly electron donating in nature.

Microsomal Fe_x is involved in mixed-function oxidation reactions. If, in these reactions, molecular oxygen is reduced by a series of one electron steps, the E'_0 for the first reaction:

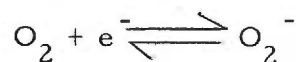
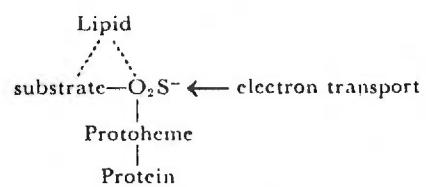
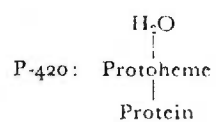
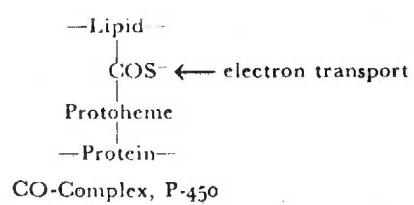


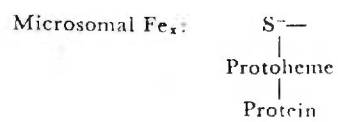
FIG. 37

THE PROPOSED LIGAND SYSTEM OF MICROSOMAL Fe_x AND THE
RELATIONSHIP BETWEEN MICROSOMAL Fe_x AND P-450^x

According to Mason et al. (49)



Enzyme-Substrate-TPNH-Acceptor Complex



should be more positive than -0.34v. at pH 7.0. George has calculated this potential from thermodynamic data to be -0.45v. at pH 7.0 (179). The thermodynamic characteristics of the microsomal mixed-function oxidation system must raise the potential of this reaction to above -0.34v. , if it is the first step and microsomal Fe_x is the oxygen activating enzyme.

Because the dyestuff concentrations were determined at room temperature and the microsomal Fe_x concentrations at liquid nitrogen temperature, the possibility of equilibrium changes taking place at these very different temperatures must be considered. It has been suggested that cytochrome P-450 is high spin at room temperature and is low spin at liquid nitrogen temperature (180). Recently, it has been shown that the optical spectrum of cytochrome P-450 represents a low spin heme protein at both room and liquid nitrogen temperatures (181). This indicates that microsomal Fe_x does not change over the temperature range and that the equilibrium positions measured are constant with respect to temperature. While this thesis work was in progress, the preparation of cytochrome P-450 particles was achieved (87). These particles contain very small amounts of cytochrome b_5 and would have allowed spectrophotometric observation of cytochrome P-450 and dyestuff at room temperature. However, because of the amount of energy invested in experimentation on the intact microsome system, it was decided not to use

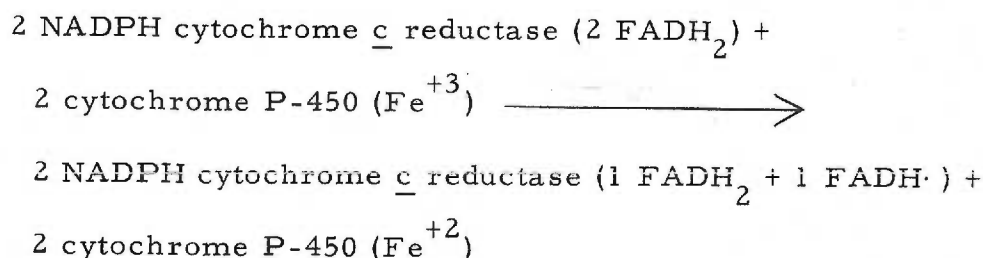
cytochrome P-450 particles for the redox potential determination. A further consideration was that redox potentials of cytochromes change at various stages of purification (Table 3) and intact microsomes presented cytochrome P-450 in its most native environment.

It is possible that only one reductase FAD molecule is responsible for cytochrome P-450 reduction and the other FAD molecule has the responsibility of reducing some other electron acceptor. This could explain why the n -values found are somewhat greater than one. It has been suggested by Ullrich et al. that there is a "divergence" of NADPH reducing equivalents in microsomes to an as yet uncharacterized electron acceptor (182). They base this argument on the fact that cytochrome b_5 is reduced by NADPH. If some of the NADPH reducing equivalents are diverted to another electron acceptor, the sigmoid nature of the NADPH titration curve can be explained. Only in the middle of the titration are NADPH reducing equivalents being substantially used for cytochrome P-450 reduction. Some of the first NADPH reducing equivalents are being used for cytochrome P-450 reduction, but other electron acceptors may also be reduced by these equivalents. At the center of the titration curve it is still possible that some NADPH reducing equivalents are being used for reduction of components other than cytochrome P-450 and therefore the n -value appears greater than one.

The change in stoichiometry of cytochrome P-450 reduction at higher NADPH concentrations may be due to a NADP^+ inhibition of the reaction. The NADP^+ inhibition of oxidative demethylation of aminopyrine in rat liver microsomes has been reported and is found to be competitive with respect to NADPH (183). However this

inhibition has not been directly related to reduction of cytochrome P-450. The NADP^+ inhibition of NADPH cytochrome c reductase has also been reported (63). The possibility of a second, more complex, stoichiometry for cytochrome P-450 reduction as represented by the upper portion of the titration curve can not be excluded.

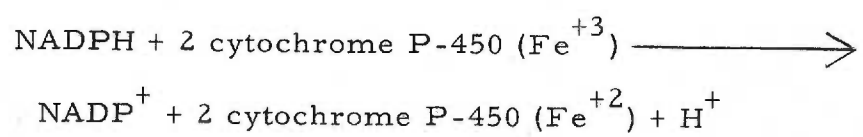
If only one of the reductase FAD molecules is responsible for cytochrome P-450 reduction, the stoichiometry is:



This stoichiometry would apply if other reactions requiring NADPH reducing equivalents are going on simultaneously with cytochrome P-450 reduction.

The stoichiometry obtained from the redox potential curve in Fig. 27 indicates a one-electron reduction of cytochrome P-450. For a one-electron reduction, the difference in potential between 25% reduction and 75% reduction should be 0.058v. as calculated from the Peters equation. For a two-electron reduction, this difference should be 0.028v.. The potential difference between 25% reduction and 75% reduction of microsomal Fe_x is 0.053v. (-0.315v. to -0.368v.). This clearly indicates that cytochrome P-450 reduction is a one-electron process.

Whatever the mechanism of NADPH cytochrome c reductase during cytochrome P-450 reduction, the overall stoichiometry of cytochrome P-450 reduction is:



3. Spin State Conversion

The purpose of the experiments on the spin state conversion of microsomal Fe_x as a function of pH was to examine more closely the results obtained by Murakami and Mason (86). They observed this conversion as a function of pH and concluded that the low and high spin forms represent the same heme group but different ligand systems. They used 6N HCl to obtain the conversion of spin state. The difficulty with using acid is that it is impossible to obtain instantaneous mixing of the system. For this reason a homogeneous conversion mixture is not obtained and the true pH characteristics of the spin state conversion are not revealed. By using acidic buffers the conversion is homogeneous throughout the microsome sample.

The results in Fig. 33 show that after exposure to acidic conditions for five minutes the pH at which 50% of the low spin microsomal Fe_x disappears (pH 4.9) and the pH at which 50% of the high spin microsomal Fe_x appears (pH 4.85) are the same. This indicates that the apparent pK of the conversion is 4.9 and that ionization of the same group is responsible for the loss of low spin and for the formation of high spin; whether this group is a ligand of the heme moiety or involved in some aspect of protein conformation.

The results in Fig. 34 show that after one hour the midpoint for formation of high spin microsomal Fe_x is the same as after 5

minutes (pH 4.9) but the midpoint for the loss of low spin has increased to pH 5.3. It is also found that the total amount of detectable spin at one hour is about 20% less than at five minutes. The results suggest (a) the low spin form is less stable to hydrogen ions than the high spin form and decomposition of the low spin form takes place with time or, (b) there is an ESR undetectable intermediate in the conversion which is slowly formed at pH's above the apparent pK of the reaction. Such an ESR-undetectable form has been reported for the spin state conversion of microsomal Fe_x caused by PCMS (86).

The results in Fig. 35 show that the Cu^{+2} -like ESR signal at $g = 2.06$ is greatly affected by PCMS. Copper has been detected in microsomes by analytical procedures (2), however it has been ruled out as an integral part of the cytochrome P-450 complex because the copper concentration is not increased by phenobarbital treatment of rabbits in the same way as cytochrome P-450 concentration (49). If this ESR signal is due to copper, as has been indicated (86), the PCMS results can be explained in the following manner. At neutral pH the copper is in the cuprous state or in an ESR undetectable cupric form. Upon treatment with acidic buffers the copper is autoxidized or it is released from its environment. In the presence of PCMS the protein sulfhydryl groups are bound and cannot reduce the copper after this change has taken place. In the absence of PCMS the

sulfhydryl groups can reduce the copper and the ESR signal disappears. Protein sulfhydryl groups have been found to be capable of reducing cupric copper (161, 184). These results do not clarify the nature of copper in native microsomes, but they do give some insight into the nature of the spin state conversion.

It is not possible to state whether the spin state conversion represents the titration of some ligand on the heme group by hydrogen ions or titration of the protein conformation which then changes the electronic structure of the iron. The copper results indicate that some conformational change is taking place. The best explanation of the acid titration results is that the conformation responsible for the low spin form of microsomal Fe_x is pH dependent and can be altered by acid causing rearrangement of the electronic structure of the heme and therefore appearance of the high spin form. This conversion appears to involve an ESR undetectable intermediate.

4. Optical Rotatory Dispersion

The ORD curves obtained for cytochrome P-450 show a change in symmetry at the heme chromophore with change in oxidation state. Optical rotation is observed when a sample transmits the two circularly polarized components of a beam of plane polarized light with unequal velocity (185). If there is an unequal absorption of the left and right circularly polarized light in addition to the unequal velocity of transmission of circularly polarized light, a Cotton effect will result (185).

The Cotton effect observed for oxidized cytochrome P-450 has a maximum at 410 m μ which corresponds closely to the Soret band of the absolute absorption spectrum of the cytochrome P-450 preparation (89). This Cotton effect appears to be simple and is superimposed on the protein backbone rotation. It reflects an asymmetric structure of the heme chromophore in the oxidized state.

Upon reduction, the oxidized Cotton effect disappears although there is some indication of asymmetry around 400 m μ superimposed on the protein backbone rotation. The disappearance of this Cotton effect reflects a loss of asymmetry and implies that cytochrome P-450 changes conformation upon dithionite reduction. This loss of asymmetry probably results from the formation of similar ligand systems on both sides of the cytochrome P-450 heme plane, although

it is possible that the asymmetric perturbation of the reduced cytochrome P-450 heme chromophore is much weaker than that of the oxidized one (175). The appearance of a Cotton effect upon addition of CO to the reduced form indicates that a ligand has been added to the iron (CO) which again gives an asymmetric chromophore.

These results show that the conformation immediately around the cytochrome P-450 heme, which affects the electronic nature of the chromophore, is dependent on the oxidation state of the heme. Such a conformational change has been suggested for cytochrome P-450 involved in mixed-function oxidation (86). If the results obtained with dithionite reduction can be extrapolated to cytochrome P-450 reduction by NADPH in the microsomes, a conformational change must be considered as part of the mechanism of microsomal mixed-function oxidations involving cytochrome P-450. It should be pointed out that reduction of cytochrome P-450 in these particles by NADPH in the presence of microsomal NADPH cytochrome c reductase has not yet been satisfactorily achieved (181).

Recent experiments on ORD of cytochrome P-450 in the presence of aniline, which is hydroxylated by cytochrome P-450 and is believed to complex with cytochrome P-450 (186), show very little change of the oxidized cytochrome P-450 Cotton effect. These studies have not yet been carried out on the reduced form of the enzyme (181).

Mixed-function oxidations require the reaction of cytochrome P-450 with substrate, oxygen, and two electrons. If these interactions all take place at a locus, the cytochrome P-450 heme group; a change in conformation during the process is not unexpected.

5. Integration of Results

If there is one underlying property of cytochrome P-450 which is reflected by the results presented in this thesis, it is that cytochrome P-450 has a very specific environment in the microsomes.

The redox potential determination shows cytochrome P-450 to have the lowest redox potential of any known heme protein. The greater the donor power of the ligand system attached to the fifth and sixth coordination positions of the iron, the more negative the redox potential of a heme protein. At least one of the ligands bonded to the heme iron must be furnished by the protein portion of the molecule. This ligand may be a sulfhydryl group of cysteine, an imidazole nitrogen of histidine, or some other nucleophilic amino acid residue, all of which would be electron donating. The other group bonded to the iron atom may be furnished by the protein in the form of one of the above amino acid residues. It may also be furnished by the protein or phospholipid of the microsomal membrane. A further possibility is that there is a small molecule or no ligand attached to the sixth coordination position of the cytochrome P-450 heme. However, because of the low redox potential of cytochrome P-450, it is expected that strongly electron donating ligands will be found bonded to both coordination positions of the cytochrome P-450 heme.

The results of the spin state conversion experiments indicate that this ligand system can be easily changed by a relatively small change in pH. The ORD results show that the symmetry of the environment around the heme is dependent on the oxidation state of cytochrome P-450 and some conformational change is involved in the mechanism of mixed-function oxidation. The change in symmetry upon reduction of cytochrome P-450 may be due to a change in the ligand system of the heme.

Some aspect of the special environment of cytochrome P-450 in microsomes is reflected in every property of the molecule, and this environment must be understood before the mechanism by which cytochrome P-450 functions in mixed-function oxidations can be clarified.

V. SUMMARY

The standard oxidation-reduction potential (E'_o) of microsomal Fe_x is $-0.338v. \pm 0.016v.$ at pH 7.0. This is the lowest reported redox potential for any unpurified heme protein. This low redox potential indicates that the ligand system of microsomal Fe_x is strongly electron donating, although it is impossible to identify this ligand system at the present time.

The stoichiometry of the reduction of cytochrome P-450 by NADPH in the presence of CO is found to be close to 2 moles cytochrome P-450 reduced per mole of NADPH. This same stoichiometry is found from the redox potential titration curve.

The conversion of microsomal Fe_x from the low spin form to the high spin form as function of pH indicates that the conformation responsible for the low spin form is pH dependent and can be altered by acid treatment causing rearrangement of the electronic structure of the heme and therefore appearance of the high spin form. This conversion appears to involve an ESR indetectable intermediate.

The optical rotatory dispersion of cytochrome P-450 shows a change in symmetry of the heme chromophore with change in oxidation state. This implies that a conformational change is an integral part of microsomal mixed-function oxidations involving cytochrome P-450.